4-2008

The Development of a Progressive Failure Model of a Fiber-Rein forced Composite Lamina

Michael Maletta
Grand Valley State University

The Development of a Progressive Failure Model of a Fiber-Reinforced Composite Lamina

A thesis by

Michael Maletta, M.S.E.
presented April 2008

In partial fulfillment of the requirements for the
Master of Science in Engineering degree
(Mechanical)

Advisor: Dr. Pramod Chaphalkar

Padnos School of Engineering & Computing
Grand Valley State University

The Development of a Progressive Failure Model of a Fiber-Reinforced Composite Lamina

A
Padnos College of Engineering and Computing
M.S.E Thesis Presentation
by
Michael Maletta

ABSTRACT

Void formation is a common problem in many composite material manufacturing processes. Composites fail when micro-cracks, which usually originate at voids, propagate through the material. The mechanical properties of a lamina depend not only on the constituent properties, but also on the tow packing configuration, void content and void distribution. This paper develops a method to determine the mechanical properties of a tow and lamina and develops a progressive failure model to predict the strength of a lamina with varying void content, void distribution and tow packing configuration, using finite element analysis.

The strength a lamina with various tow packing configurations, void content and void distribution were investigated utilizing the progressive failure model. The tow packing configuration can affect the strength of a lamina by approximately 25 percent. Voids located near the gaps between the tows severely affect the strength of the lamina. The transverse stiffness of tows in a lamina also significantly affects the failure strength and strain of the lamina.

GRAND VALLEY
STATE UNIVERSITY

ACKNOWLEDGEMENTS

I would like to thank my family and friends for supporting me through my life. Especially, my loving wife, Anne, for believing in me and putting up with the long hours I have spent working on my computer.

I would like to express my sincere gratitude to Dr. Pramod Chaphalkar for his guidance and support throughout the duration my graduate education and especially during this project. I am grateful for the time he took to explain the topic of composite materials and finite element analysis. I would also like to thank Dr. Anyalebechi and Dr. Pung for taking the time to review my thesis presentation and paper.

TABLE OF CONTENTS

LIST OF TABLES

LIST OF FIGURES

1 INTRODUCTION

Composite materials have been popular in many industries, such as aerospace, military, aquatic, and recreation, since the 1940's. Historically, the concept of fiber reinforcement is very old. There are biblical references to straw-reinforced clay bricks in ancient Egypt. Iron rods were used to reinforce masonry in the nineteenth century, leading to the development of steel-reinforced concrete.

Composite materials are macroscopic combinations of two or more distinct materials that have readily discernible interfaces between them, that is, they do not dissolve or merge completely into one another [1]. A composite material's mechanical performance and properties are designed to be superior to those of the constituent materials acting independently. In the case of fiber-reinforced composites, one phase is comprised of fibers and the other phase is the matrix. The fibers form a discontinuous phase that is dispersed throughout the matrix and function as the primary load- carrying members. The fibers have excellent mechanical and thermal properties but need some mechanism, which enable them to adhere together as one object during exposure to loads. The matrix phase, also known as the resin, is usually made of a polymer and serves as the method to adhere the fibers together [2]. As well as bonding the fibers together, the matrix provides protection and support for the sensitive fibers and local stress transfer from one fiber to another [3].

The attraction to composite materials is the great combination of high strength and lightweight. Composite materials can be used in areas where conventional materials would not optimally perform. Composite materials also have the flexibility that can

significantly decrease the number of components required by reducing the number of fasteners, weldments, joints, and as a result a lesser assembly time. Some other advantages of composite materials include low coefficient of thermal expansion (CTE), good vibrational damping, and resistance to temperature extremes, corrosion and wear. Two-phase composite materials are generally classified into three broad categories depending on the type, geometry, and orientation of the reinforcement phase: particulate composite, discontinuous or short-fiber composites, and continuous composites. Particulate composites consist of particles of various sizes and shapes. The particles are randomly dispersed within the matrix. Discontinuous or short-fiber composites contain short fibers or whiskers as reinforcement. The short fibers, which are usually quite long compared with the diameter, can be either all oriented along one direction or randomly dispersed. Continuous fiber composites contain long continuous fibers that run from one edge of the composite to the other. The fibers can be parallel (unidirectional), can be oriented at right angles to each other (cross-ply or woven), or can be oriented along several directions (multidirectional). Continuous fiber composites are the most efficient in terms of stiffness and strength, see Figure 1-1 [4].

Fiber-reinforced composites can be further classified into broad categories based on the type of matrix used: polymer-matrix composites (PMC), metal-matrix composites (MMC), ceramic-matrix composites (CMC), and carbon matrix composites. Table 1-1 displays some common matrix and reinforcement combinations for a given composite type.

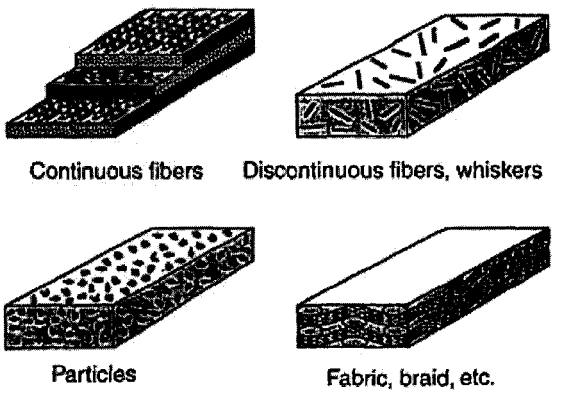

Figure 1-1: Common forms of fiber reinforcement: continuous fibers, whiskers, particulate, and braid [5].

Table 1-1: Common matrix and reinforcement material combinations [6].

Composite Type	Reinforcement	Matrix
Polymer	Carbon (graphite)	Polyester, epoxy, PEEK
	S-glass/E-glass	Polyimide, epoxy
	Kevlar (Aramid)	Thermoplastics
	Boron	PEEK, polysulfone, epoxy, etc.
Metal	Boron	Aiuminum
	Borsic	Magnesium
	Carbon (graphite)	Titanium
	Silicon carbide/Alumina	Copper
Ceramic	Silicon carbide	Silicon carbide
	Alumina	Alumina
	Silicon nitride	Glass-ceramic, Silicon nitride
Carbon	Carbon	Carbon

1.1 Area of Investigation

The scope of this project encompasses continuous uni-directional fiber-reinforced polymer-based composites. The primary focus is on a single ply or lamina and the manufacturing processes that can result in void formation within the matrix of the lamina. An investigation will be conducted to determine how voids affect the mechanical properties of laminae.

2 LITERATURE REVIEW

This chapter discusses the results of published studies of the effects of voids on the mechanical properties of various types of composite materials, void characteristics, void content measurement, common composite manufacturing processes, carbon tows, and progressive failure models. The behavior of fiber-resin composite systems with voids under various loading types has been widely studied, discussed below. The void content has an effect on composite interlaminar strength, transverse Young's modulus, Poisson's ratio, shear modulus, and interlaminar fracture toughness. These, in turn, can have considerable effects on the tensile and compressive strengths, shear strength, impact resistance, fatigue life, and stiffness of the composite materials. Voids may also provide paths by which air may reach fibers, resulting in either oxidation of the fibers or degradation of the fiber matrix interface [7]. However, there is no general agreement on the magnitude of the effect of voids on the mechanical properties of composites [8]. Some work has been documented on the development of progressive failure models for composite laminates. However, very little has been done on the progressive failure of lamina with various void content and tow/fiber configurations.

2.1 Manufacturing Processes and How They Affect Void Formation

For most fiber-resin composite systems, void content is dependent on manufacturing techniques and curing procedures. The fabrication process is one of the most important steps in the application of composite materials. An assortment of manufacturing methods are available for composites, they include autoclave molding,

filament winding, pultrusion, resin transfer molding (RTM), and vacuum-assisted resin transfer molding (VARTM) [9].

Void formation in composite laminates occurs whenever volatile polymerization by-products (primarily water) are unable to escape from the laminate during the cure process. It is normally assumed that voids are eliminated when the manufacturer's suggested cure schedule is closely followed. However, adherence to the manufacturer's cure cycle does not always guarantee void free composites [7]. Porosity is dependent on variables such as temperature, temperature rates and pressure applied during the process. The proper resin temperature will produce the correct resin viscosity, allowing the resin to fully wet each of the fibers. The appropriate applied pressure pushes any air bubbles to the surface of the lamina [10]. A common problem in the manufacture of polymer composites is the formation of defects such as voids, resin-rich regions, delaminations, foreign inclusions, crimped and distorted fibers. Voids are arguably the largest problem because they are difficult to avoid and are detrimental to mechanical properties [8]. Completely eliminating voids from composites produced by a full-scale production facility may not be possible for all fiber-resin composite materials [11].

One composite manufacturing process: the preformed stack of composite plies is placed in a pre-heated metal die mold and the cure pressure is applied to the die. The temperature is increased at a steady rate until an optimum temperature is reached. The temperature and pressure are held constant for a specified length of time. Figure 2-1 displays how the cure pressure affects the formation of voids within the composite. As apparent, the void content increases at the low and high ends of the cure pressure range. Many manufacturing issues contribute to the formation of voids in composites, including

the formation of unstable byproducts produced during the cure reaction of the polymeric matrix, the use of high viscosity resin combined with closely packed fibers that are not completely wetted by resin, the entrapment of air, and fabrication accidents such as a leaking vacuum bag or poor vacuum source [8]. At lower pressures, the void content probably increases because the required pressure to remove the volatiles and air pockets is lacking. At higher pressures, the volatiles and air pockets are most likely trapped within the laminate [11]. The ideal cure pressure, which minimizes the void content, appears to be between 1.5 and 5 MPa.

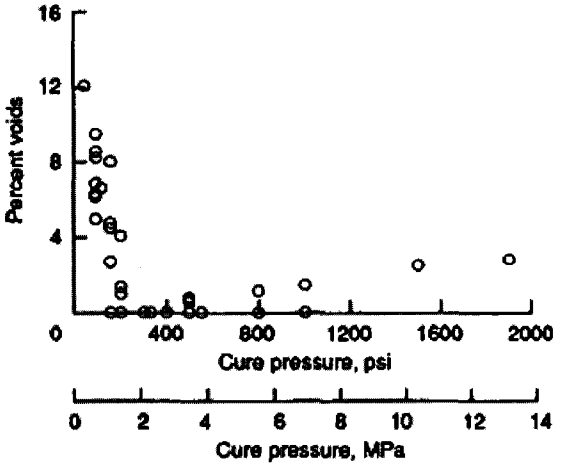

Figure 2-1: Composite void content as a function of cure pressure [11].

Liquid composite molding (LCM) is another manufacturing process where it is found that voids exist not only between fiber tows (macro voids), but also inside fiber tows (micro voids) [12]. Resin transfer molding (RTM) is a common form of LCM. Poorly wetted fibers are often the issue in LCM and pultrusion processes. The unwetted fibers have no load carrying capacity in the transverse direction while in longitudinal direction fibers are still effective. Fibers are often used in tows in LCM processes.

Resin Transfer Molding is a process in which a liquid thermoset resin is injected into a mold cavity containing dry fabric preform. Due to relatively low injection pressure applied in processing, it permits the use of lower cost mold [13].

Vacuum-assisted resin transfer molding (VARTM) is a manufacturing process in many composite material applications where void content is critical. It is critical that the manufacturer ensures good resin flow and complete wetout of the reinforcement under vacuum pressure. Vacuum integrity is extremely critical because any leaks will introduce air into the laminate, causing a loss of compaction and increased void content. It is recommended that full vacuum be maintained for a minimum of 24 hours at 22°C/72°F to allow the system to cure to a stable condition [14].

Material type has an impact how carefully a laminate must be processed. For instance, carbon fiber has much higher requirements with regard to processing accuracy. Alignment inaccuracies and void content have a much higher impact on the mechanical properties of a carbon laminate than they do on glass laminate properties. According to Wind energy consultant Dayton Griffin of Global Energy Concepts LLC, "blades tend to be thick and long, and the evacuation channels aren't great, leading to higher void content." That is, as blade manufacturers move from hand lay-up to the more efficient vacuum infusion processes, incorporating carbon becomes more difficult [10].

2.2 Fiber and Tow Characteristics

Konev et al [15] investigated the Modulus of Elasticity of carbon tow with VMN-4 fibers. The following specific modulus of elasticity were found for the tows 270-324

GPa before heat treatment and 360-560 GPa after heat treatment at 3000 degrees Celsius. All samples had a linear density of 350 tex, mass in grams per kilometer.

A microscopic study revealed that fibers within a tow are arranged in bundles looking like cylinders with an elliptical cross section. Binetruy et al [16] modeled the tows in their study as cylindrical fibers bundled with a rectangular cross section. According to Daniel and Ishai, fibers in composites with fiber volume ratios, above 60%, tend to nest in near hexagonal packing [6].

Figure 2-2 displays the cross-section of a graphite/epoxy composite showing the tow cross-section and the tow packing. The tows are flat and have an elliptical shape, the packing of the tows looks to be a cross between square packed and hexagon packed.

Figure 2-2: Cross-section of a graphite/epoxy lamina, displaying the tow cross-section and packing [17].

According to Volume 21 of the ASM Handbook [5] the diameter of carbon fibers typically ranges from 8 to 10 μm. Usually the larger the tow size the lower the cost per pound.

Table 2-1 and Table 2-2 display fiber bundle dimensions for unidirectional tapes and prepregs and towpreg form parameters, such as resin content and tow width. The width of a tow ranges from 1600 to 6400 μm.

Table 2-1: Fiber bundle dimensions of unidirectional tapes and prepregs [5].

Material	Yield/tow		Filament size	
	m/kg	yd/lb	μm	μin.
Graphite (1000 to 12,000 filaments per tow)	300–1200	150–600	5–10	200–390
Fiberglass (2450–12,240 filaments per tow)	490–2400	245–1200	4–13	160–510
Aramid (800–3200 filaments per tow)	2000–7850	980–3900	12	470

Table 2-2: Towpreg form parameters [5].

Parameter	Typical range
Strand weight per length, g/m (lb/yd)	0.74–1.48 (0.00150–0.0030)
Resin content, %	28–45
Tow width, cm (in.)	0.16–0.64 (0.06–0.25)
Package size, kg (lb)	0.25–4.5 (0.5–10)

2.3 Measurement of Void Content

Determination of the void content of a composite is not an easy task. Most voids are internal and cannot be visually detected by the human eye. Even if all where detectable by eye, counting voids would be a time consuming and inefficient task. Two vastly different methods are employed to measure the void content within a composite: nondestructive and destructive techniques.

Two ultrasonic nondestructive procedures are utilized to determine defects within the composite. The two procedures are black-white C-scan and amplitude scan. One technique of the black-white C-scan is double through transmission, Figure 2-3. In this technique an ultrasonic signal is sent through the specimen and reflected off a plate and sent back through the specimen, defects present in the composite specimen cause transmission loss. Usually, three independent scans of each plate are performed to measure the absorption coefficient of the selected areas with approximately uniform porosity level. The average value of these measurements is the absorption coefficient of the samples. The ultrasonic absorption coefficient is defined as a ratio of the measured transmission loss and the plate thickness [8].

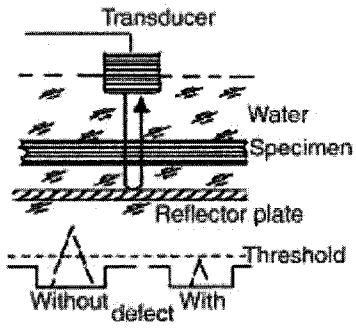

Figure 2-3: Ultrasonic C-scan double through transmission technique [8].

The imbedded defects in the composite material cause variations in ultrasonic attenuation. Areas of low attenuation, thus the presence of defects, show up as white areas in the black-white C-scan, Figure 2-4*(a)*, and as low signal levels in the amplitude scan, Figure 2-4*(b)*.

The destructive technique for measuring the void content of a composite is calculated from the measured fiber content, density values and the following equation [11]:

$$V_v = 1 - D_c\left(\frac{W_f}{D_f} + \frac{W_r}{D_r}\right) \tag{2.1}$$

where V_v = void volume fraction, D_c = composite density, D_f = fiber density, D_r = resin density, W_f = fiber weight fraction, and W_r = resin weight fraction.

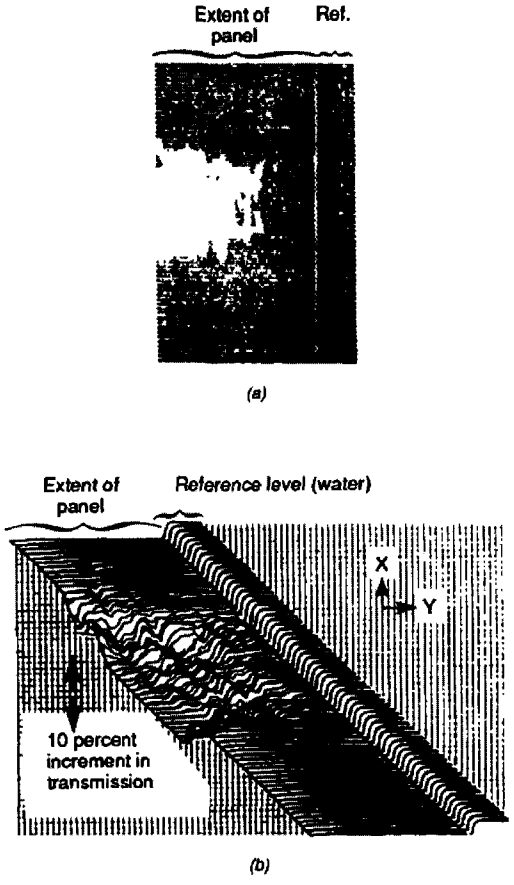

Figure 2-4: Diagram of (a) ultrasonic black-white C-scan and (b) amplitude scan of same composite panel showing variation in ultrasound due to attenuation by voids and fiber content variations in typical graphite-polymide composite [11].

Fiber density values are obtained from the material's vendor. Test specimens are cut from a composite laminate and various standardized destructive tests are preformed to determine the remaining variables in the equation above. The composite density and resin density measurements are made by a water immersion technique in agreement with ASTM D-792. The acid digestion technique (ASTM D-3171) is used to measure the fiber content, where the matrix is digested in hot nitric acid. This procedure determines the weight fractions of both the fiber and matrix; the difference between the sum of these two values and the total weight of the specimen is the void weight fraction.

A correlation can be established between the void content determined by acid digestion (ASTM D-3171) and the absorption coefficients measured in the ultrasonic C-scan [4]. The results of this correlation can be seen in Figure 2-5 and as expected the lower absorption levels correspond to lower void contents. A linear correlation between porosity and absorption coefficient can be observed for laminates with a void content range between 0 to 3.5%. Thus, greater void content causes increased ultrasonic attenuation levels.

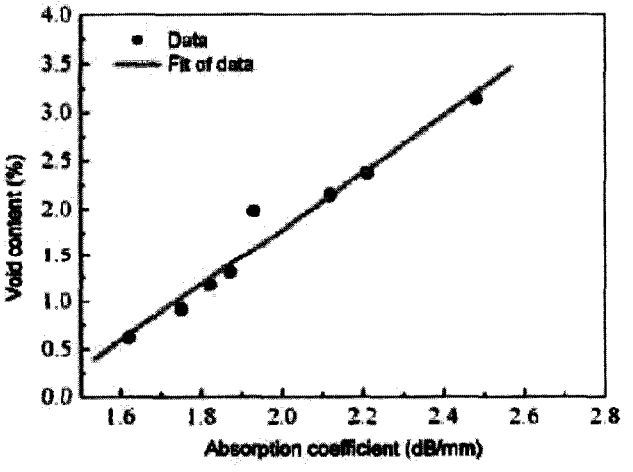

Figure 2-5: Correlation between void contents and absorption coefficient [4].

All of the void content measurement techniques above represent an average value over the given volume. They do not provide any information on the shape, size, and distribution of the voids, other inspection techniques are used to determine these parameters.

2.4 Void Characteristics

Depending on the type of manufacturing processes and the processing and material conditions, voids differ in shape, size, and location [12]. Metallographic samples are taken from the composite laminate to determine the void size, distribution and shape. The samples are mounted, polished and photographed at various high magnification levels. A magnification of 200x allows the assessment of voids as small as the radius of a single fiber of 7 μm. Typical photomicrographs are displaying the fiber end view of a composite are seen in Figure 2-6 and the fiber side view in Figure 2-7. The voids are represented by the dark spots, holes between the fibers. The voids in Figure 2-6*(c)* can be seen as circular in shape and Figure 2-7*(c)* shows the voids as long slits. From these figures, it can be deduced that the voids are cylindrical in shape and located between the plies. Another observation is that the voids seem to be randomly distributed within the composite, not uniformly distributed as many studies assume.

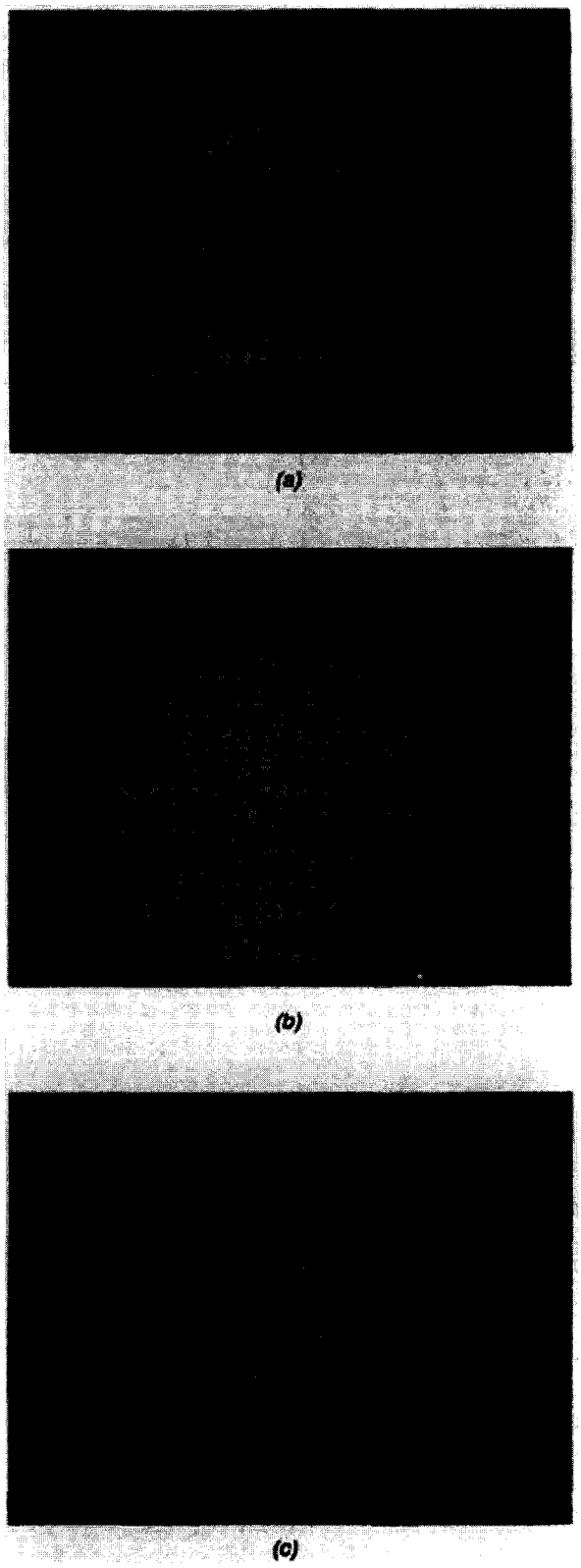

Figure 2-6: Photomicrographs showing the fiber end view of a composite with (a) 1.25, (b) 3.9, (c) 12.1 volume % voids [11].

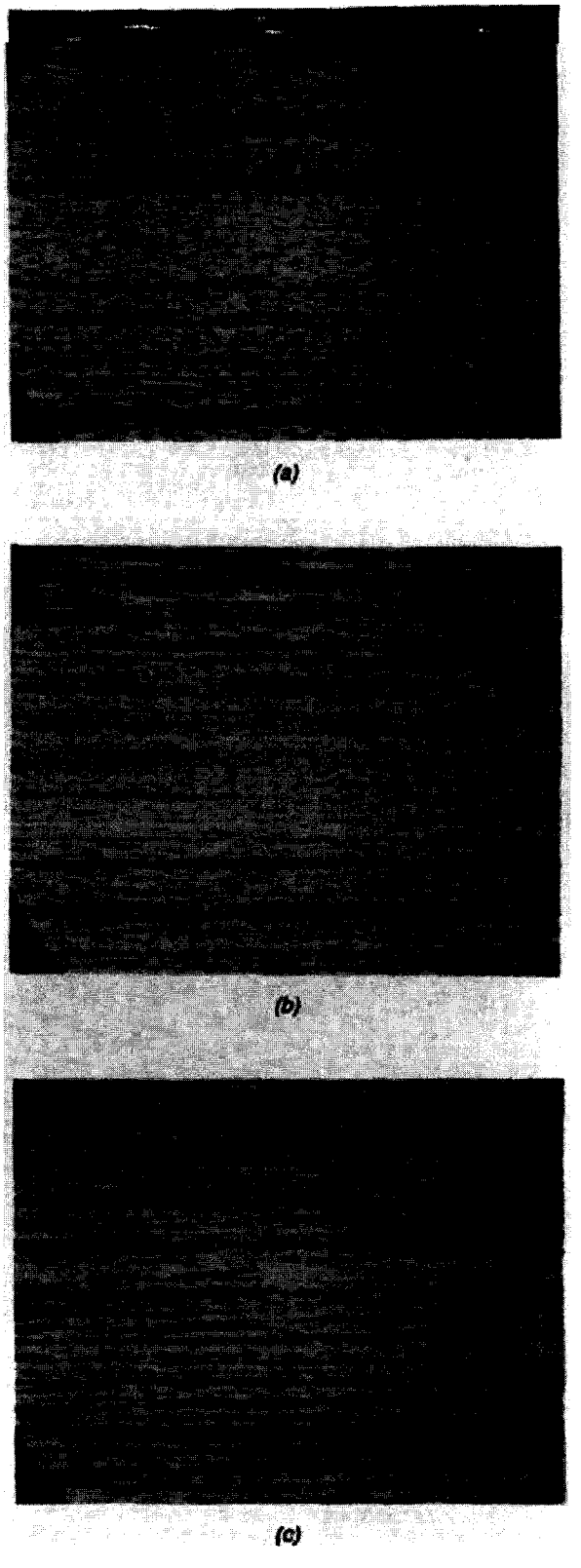

Figure 2-7: Photomicrographs showing the fiber side view of a composite with (a) 1.25, (b) 3.9, (c) 12.1 volume % voids [11].

Current opinion is that there are three possible configurations for voids in composites: spherical, elliptical and cylindrical. Previous studies showed that in thermoset laminates, voids tend to be small and spherical at low void contents (less than 1.5%) and tend to be bigger and cylindrical at higher percentages [10].

The photomicrographs in Figure 2-6 and Figure 2-7 display what appears to be macro voids, the small size or larger than the fibers, and many appear to occur between plies. Voids can also occur at sizes smaller than fibers and within fiber tows, these are known as micro voids. Fiber tows are a bundle of thousands of fiber filaments with a fiber content of usually greater than 70 percent.

From Hamidi et al [18], the average void sizes in an E-glass/epoxy composite range from 66.7 to 41.1 μm. Voids are seen at three different locations within molded composites: areas rich in matrix away from fibers (matrix voids), areas rich in preform (intra-tow voids), and transitional areas between the matrix and tows.

2.5 Effect of Voids Mechanical Properties and Strength

Bowles and Frimpong [11] studied the effect of voids on the interlaminar shear strength (ILSS) of polyimide matrix composite system. The Hercules AS graphite fiber/PMR-15 composite was chosen for the study because void-free composites and composites with varying void contents can be readily produced by using standard specified cure cycles and varying the processing parameters. Each test specimen was cut from unidirectional prepreg sheets that were made by drum-winding graphite fibers and impregnating the fibers with the required amount of PMR-15 polyimide. Transverse and longitudinal fiber directions were used in the specimens to see if the resin flow during

impregnation had any effect on the reproducibility of mechanical properties. The interlaminar shear tests were made at room temperature in accordance with ASTM D-2344 by using a three-point loading fixture. Figure 2-8 displays the ILSS data for composite with 60% fiber volume fraction with void contents determined from four different types of data: measured, spherical void predictions, cylindrical void predictions, and ICAN predictions. ICAN (Integrated Composite Analyzer) is a computer program developed by Lewis Research Center for predicting composite ply properties.

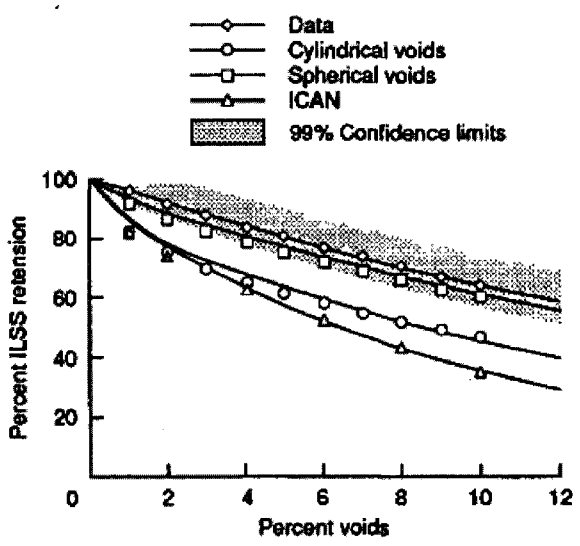

Figure 2-8: ILSS as a function of void content for 60% fiber volume fraction AS/PMR-15 unidirectional composites [11].

It can be seen that the spherical void prediction more closely represents the measured data, even though the photomicrographs displayed cylindrical voids. While the cylindrical prediction and ICAN data show lower ILSS values, cylindrical void shape could be used for a more conservative prediction. All data measurement types display the same trend; as the percent of voids increase the ILSS decreases.

Zhan-Sheng Guo et al [8] worked toward establishing the acceptable level of defects in a composite component, a critical issue in design. An overly conservative acceptance criterion causes many parts that could perform satisfactorily to be unnecessarily discarded, increasing manufacturing cost. However, an excessively liberal acceptance criterion can result in in-service failure of some components. Both situations can be avoided by a judicious choice, based on a reliable failure criterion, of acceptable level of defects in the part. Interlaminar shear strength tests (ASTM D2344), flexure strength test (ASTM D790), and tensile strength tests (ASTM D3039) were performed on 10 specimens a piece. The tensile strength tests were performed on specimens with the dimensions of 180 x 12 x 2 mm and in an Instron mechanical testing machine with a test speed of 0.5 mm/min. They also established a fracture criterion that correlates fracture stress with void content, or in this case ultrasonic attenuation. They investigated interlaminar shear strength, flexural strength, and tensile strength. The resulting failure criterion for the strength of composite laminates containing voids is:

$$\sigma_f = H(\alpha)^m \tag{2.2}$$

where σ_f is the fracture stress, H is the laminate toughness, α is the ultrasonic absorption coefficient in decibels per millimeter, and m is the slope parameter. Equation (2.2) provides a good fit to experimental results for specimens with voids. However, it predicts infinite fracture stress for void-free laminates [8]. Therefore, for low void contents, the fracture criterion assumes that fracture occurs according to classical fracture

mechanisms. Figure 2-9 displays a plot of the experimental tensile strength of laminates with various void contents (absorption coefficient). A best fit curve and equation are applied to the data. The best fit curve closely fits the experimental data.

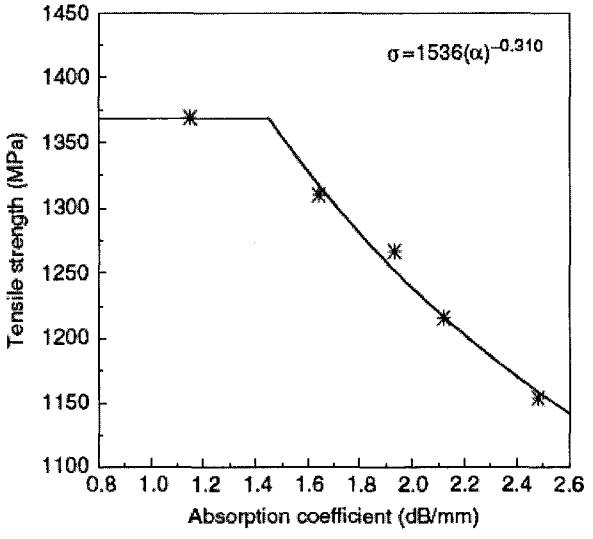

Figure 2-9: Tensile strength vs. ultrasonic absorption coefficient [8].

It can be seen that for low void contents the tensile strength is constant and at an absorption coefficient of approximately *1.45 dB/mm*, the tensile strength begins to decrease logarithmically. This point of slope change is the critical point, where the void content begins to affect the laminate strength. The corresponding critical void content is *1.10 percent* with a toughness of 1536 MPa and slope parameter of 0.310. This critical value establishes an acceptance criterion for nondestructive inspection of composite laminates.

Yinan Wu et al [12] developed a model to estimate elastic properties of polymer composites with voids of various sizes and locations based on a multi level

homogenization procedure incorporated with the composite cylinder and Mori-Tanakan micromechanics models [12]. The geometric model used in this method assumed cylindrical voids imbedded in a concentric cylindrical annulus of the matrix. The elastic properties examined were the axial and transverse Young's modulus and axial and transverse shear modulus. Three cases were considered voids in composites reinforced by fiber filaments: (1) voids much smaller than fibers; (2) voids much larger than fibers; and (3) voids surround fibers when fibers are poorly wetted. Four cases were considered for fiber tow reinforced composites: (1) micro voids smaller than fibers; (2) micro voids larger than fibers; (3) macro voids smaller than tows; and (4) macro voids larger than tows. Schematics for all seven cases is displayed in Figure 2-10.

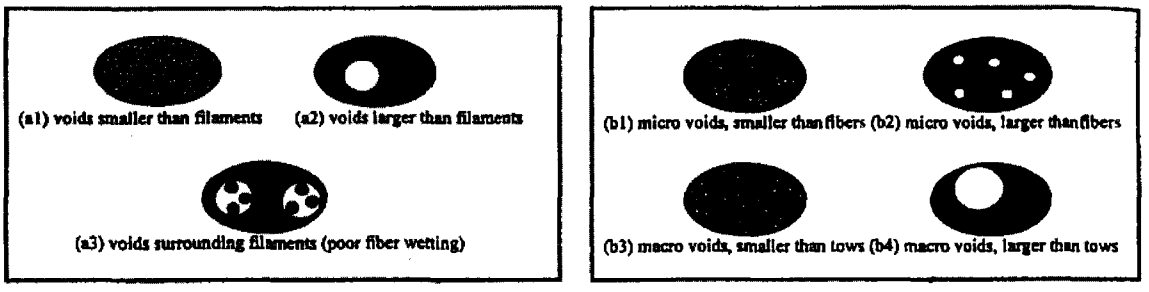

Figure 2-10: Schematics of voids (a) in fiber filament composite, (b) in fiber tow reinforced composite [12].

In the case of composites reinforced by fiber filaments with small voids, the content of voids has a great influence over axial shear modulus, transverse Young's and shear moduli. In these three cases, the voids have a detrimental effect on these properties. The axial Young's modulus is unaffected by the void content. It is linearly increasing with apparent fiber fraction and also uniformly decreasing with the increase of porosity. This illustrates that the law of mixtures is still a good approximation for axial Young's

modulus. Next, a comparison of the effect void size for small voids, large voids, and poor fiber wetting at the same porosity was presented. The results showed that small voids and poor fiber wetting has a larger detrimental effect on the axial shear modulus, transverse Young's and shear moduli than the large voids. This appears to be different from general observations that composites with large voids degrade more in strength than with small voids. The difference is understandable since the strength is determined by local stress level which is intensified more by large voids while elastic properties are determined in an average sense [12].

For the case of composites reinforced by fiber tows, voids can be found inside fiber tows (micro voids) or between tows (macro voids). In the study, the macro and micro voids were considered separately so the individual effects could be illustrated, even though in actual composites they may coexist. A true volumetric fraction of fibers in tows was set at 80 percent and porosity of 5 percent was used. The study showed that overall, the presence of large voids appears to have a relatively small effect on the elastic properties of the composite, while small voids in or between fiber tows have a huge negative effect on the elastic moduli except for axial Young's modulus. Small voids have the tendency to erode the binding between the tows or between the fiber filaments inside tows. At higher fiber fractions the small voids between the tows has a very severe effect on the transverse Young's modulus and shear modulus and axial shear modulus.

Yinan Wu et al also conducted a finite element analysis for a rectangular composite coupon with small voids and under unidirectional tension. Much like the case that this paper presents. The model contained inclusions, aligned glass fibers, and voids. Using symmetry, only a quarter of the coupon was modeled and the model was divided into 200

identical unit cells. A superelement was built for the unit cell and the transverse Young's modulus of the composite was obtained from the result of average displacements at the ends of the tensile coupon. The finite element value was 2.303×10^3 MPa and the predicted value from the multi level homogenization procedure was 2.376×10^3 MPa, an error of 3.16%.

B. D. Harper et al [7] conducted a study to investigate the effects of voids upon the hygral and mechanical properties of AS4/3502 graphite/epoxy. Uniaxial tensile specimens with void contents ranging between 0.2% and 6% by volume were used to determine the effect of voids upon the axial and transverse Young's moduli, axial shear modulus, and axial Poisson's ratio. All specimens were tested using an MTS closed loop hydraulic test system, the elastic moduli were determined from evaluating the slope of the stress-strain curve. Poisson's ratio was determined by computing the slope of the axial strain vs. transverse strain plots. As the expected the axial elastic Young's modulus and Poisson's ratio remains constant among the various void contents. However, the transverse Young's modulus and shear modulus varied a great deal between high and low void content specimens.

The effects of voids upon the diffusion of moisture into the test specimens were also investigated. The presence of moisture within graphite/epoxy materials will degrade their physical and mechanical properties. In most cases, the amount of degradation has been found to depend primarily upon the total amount of moisture absorbed. In the study 4 ply specimens with 1% and 5% void contents were exposed to an environment of 24°C and

100% humidity. The results showed that the 5% void content specimen had a higher rate of absorption and larger total amount of moisture absorbed.

2.6 Progressive Failure

Composite failure is not predictable with a higher reliability compared to metallic structures due to the large number of material parameters and structural elements that contribute to the composite load redistribution and load carrying capability. Fracture initiation is associated with defects such as voids, machining irregularities, stress concentrating design features, damage from impacts with tools or other objects resulting in discrete source damage, and non-uniform material properties stemming, for example, from improper heat treatment. After a crack initiates it can grow and progressively lower the residual strength of a structure to the point where it can no longer support design loads making global failure imminent [9].

The macroscopic failure is usually preceded by an accumulation of the different types of microscopic damage and occurred by the coalescence of the small-scale damage into macroscopic cracks. Damage progression in a fiber-reinforced composite structure will usually initiate by matrix cracking due to tensile stress transverse to the fiber direction and/or additional new failures are initiated in different parts of the structure as a result of local stress redistribution [9].

Pal and Bhattacharyya [19] conducted a progressive failure analysis on a cross-ply laminate plate to assess the macroscopic failure criteria using the finite element method. In the laminates the failure is must more complex than isotropic material. The weakest ply in the laminate fails first and this failure causes a redistribution of stresses within the

remaining lamina of the laminate. The first ply failure does not necessarily imply the total failure of the laminate but it is only the beginning of a progressive failure process. If the stresses of the weakest lamina exceed the allowable strength of the lamina, the lamina fails which is called the first-ply failure. Each lamina is treated as homogeneous and orthotropic in which the fibers are oriented arbitrarily. Hence, each layer is exactly the same and the variations, such as voids, that occur in real lamina are neglected.

The methodology for this analysis is as follows the stresses and strains are calculated for all layers, these stresses are then compared with the material allowable strength and then failure load is determined. If the failure load of a lamina is detected, the lamina properties are changed so that the affected stiffness of the failed lamina is discounted completely. Displacements and stresses are recalculated and the stresses for the remaining lamina are checked against the failure criteria to compute the failure load of the second weakest lamina. The process continues ply-by-ply until the ultimate failure load of a laminate is achieved.

Graphite/epoxy unidirectional laminae were used in arbitrary orientations to form a symmetric cross-ply laminate. The maximum ultimate failure load occurs at an angular fiber orientation of 60 degrees with a value of approximately 29 MPa x 0.001. The ultimate failure load increases with increase in the angle of fiber orientation and number of layer in the laminate.

2.7 Conclusion

It is a normal occurrence for voids to be created during the manufacture of composite lamina. Composite material failure tests yield varying results, presumably due to void contents and variations in fiber packing. Micro-cracks initiate at defects such as voids, machining irregularities and stress concentrating design features. Voids create more significant issues than other defects because they occur internally and when the micro-cracks finally reach the surface and become visible it is too late, the material has failed.

Most examinations on the effect of voids on the mechanical properties of fiber-reinforced polymer composites are experimental. Very little work has been completed to develop finite element models to predict the deterioration of the strength of fiber-reinforced polymer composites due to voids. The work that has been completed on the progressive failure of composites usually focus on a macroscopic level, looking at the failure of each ply in a laminate. They do not take into account the effect of voids and fiber packing configurations on the failure of each lamina.

An investigation should be completed to look into how voids affect the failure of fiber-reinforced lamina using the finite element method. How do the micro-cracks propagate through the matrix? Does the fiber or tow arrangement affect the crack propagation? An attempt to answer these question and others will be made in this paper.

3 MODEL AND METHOD

3.1 Objectives and Scope

There are many different types of composite materials: polymer matrix, ceramic matrix, metal matrix, and structural composites as discussed in chapter 1. This project focuses on polymer matrix lamina with fiber reinforcement in the form of fiber filament bundles called tows. The objective of this project is threefold; one is to create the tow and lamina geometry, with or without voids and with various fiber/tow configurations utilizing an ANSYS Parametric Design Language (APDL) program. The second objective is use the created geometries to calculate the mechanical properties of fiber reinforced polymer composite lamina with various void contents and fiber/tow packing configurations using finite element analysis. The third objective is to develop a progressive failure model of the fiber reinforced lamina to predict the strength of composite lamina with varying void contents and determine the mode of failure for various fiber/tow packing configurations using finite element analysis.

3.2 Assumptions and Limitations

The following assumptions were made in the completion of this work:

1) Fiber filaments inside the tows are packed in a hexagon configuration.
2) Tows are packed in the following configurations:
    a. Square arrangement
    b. Hexagon arrangement

3) The gaps between all tows are equal length.
4) Matrix cracks do not propagate through the tows. All cracks propagate through the matrix and around the tows.
5) The tows are treated as homogenous solids when modeled in the repeating unit of tows inside a lamina, the reason cracks to not propagate through the tows.
6) The interphase/interface between the fibers/tows and matrix is neglected.

3.3 Model Loading

The most critical loading of a unidirectional composite is transverse loading. This type of loading results in high stress and strain concentrations in the matrix and interface/interphase [6]. Thus, the choice of loading for the progressive failure analysis was along the transverse z-axis. The orientations of the axes with respect to the lamina geometry are shown Figure 3-1. The x-axis lies along the fiber direction, the y-axis lies along the thickness of the lamina and the z-axis the width. The ability to complete the progressive failure analysis with loading in the y-axis and z-axis was achieved. However, for practical purposes the analysis was only carried out in the z direction. Transverse tensile physical testing is normally conducted along the width of the lamina, not the thickness. The test coupon is cut from somewhere inside of the lamina plate.

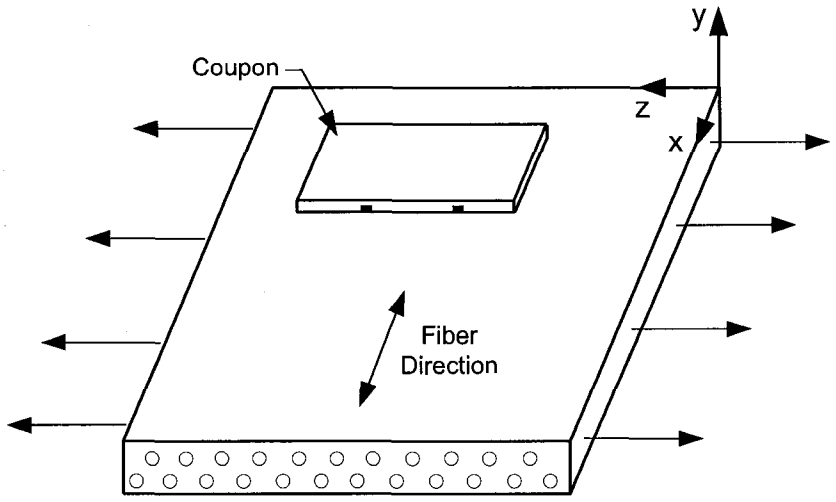

Figure 3-1: Transverse tensile test lamina with test coupon, loading and axis orientation displayed.

The ASTM Standard Test Method for Tensile Properties of Polymer Matrix Composites Materials (D3039) was utilized as the testing method for the progressive failure model. The tensile test was performed at a constant cross-speed of approximately 0.5 mm per minute, at room temperature, in the transverse direction.

3.4 Model Geometry

3.4.1 Tow Geometry

An APDL program was utilized to create the geometry of the fiber inside a tow; a tow is a bundle of fibers with a very high fiber volume fraction, usually between 70 and 80 percent. An idealized elliptical shaped tow is utilized for geometric model. The ellipse is comprised of the major radius, a, and minor radius, b, displayed in Figure 3-2. The flatness ratio of the ellipse is defined as the ratio of the minor radius to major radius.

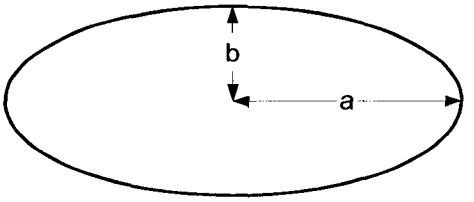

Figure 3-2: Typical Elliptical Tow Cross Section.

The fibers inside a tow are usually packed in a hexagon pattern to achieve the high fiber volume fraction, Figure 3-3.

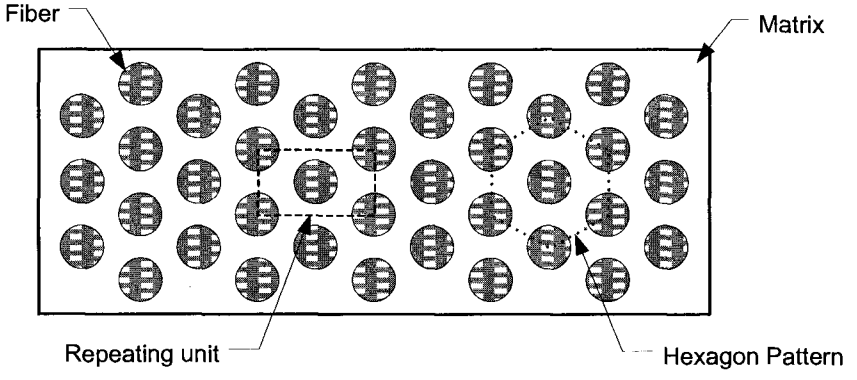

Figure 3-3: A elliptical tow cross section with a hexagonal packing and repeating unit displayed.

The repeating unit is the simplest model that can be formed to represent the cross section and is very useful for element modeling and analysis. Figure 3-4 displays the hexagonal unit cell that was used in the model of the tow.

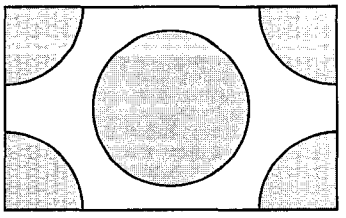

Figure 3-4: Hexagonal repeating unit of fiber inside a tow.

3.4.2 Lamina Geometry

Two tow packing configurations were used in the determination of the lamina geometry, square and hexagon. The square and hexagon tow packing configuration in a lamina can be seen in Figure 3-5.

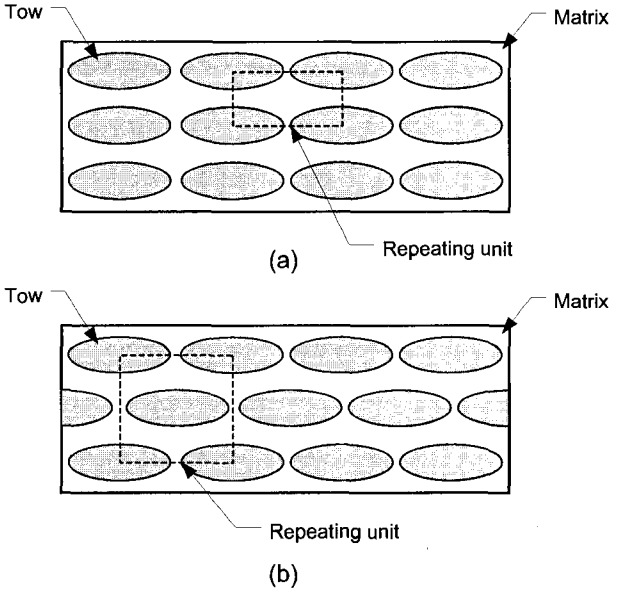

Figure 3-5: Tow packing configurations in a lamina with repeating units (a) square and (b) hexagon.

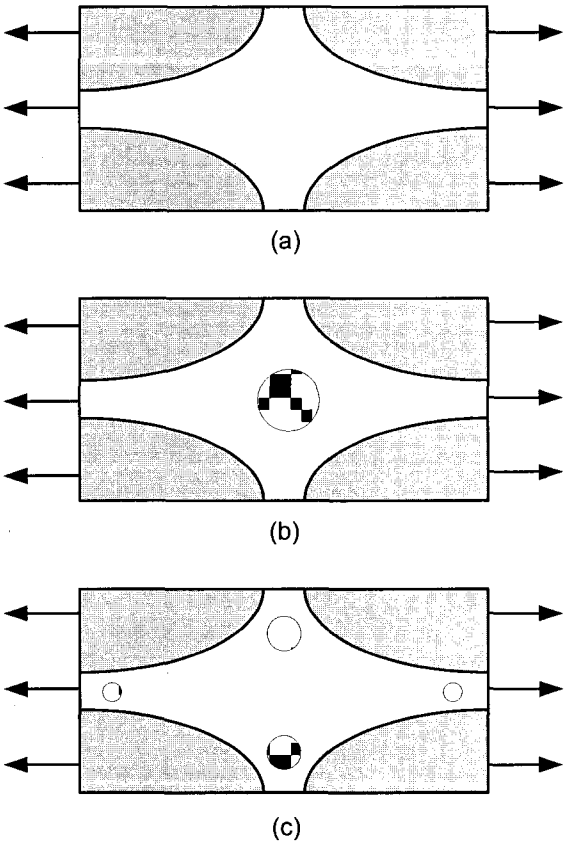

Figure 3-6: Square packing configuration in the repeating unit of tow inside a lamina with (a) no voids, (b) one large center void, and (c) four voids at the gaps. The loading is shown in the z-direction.

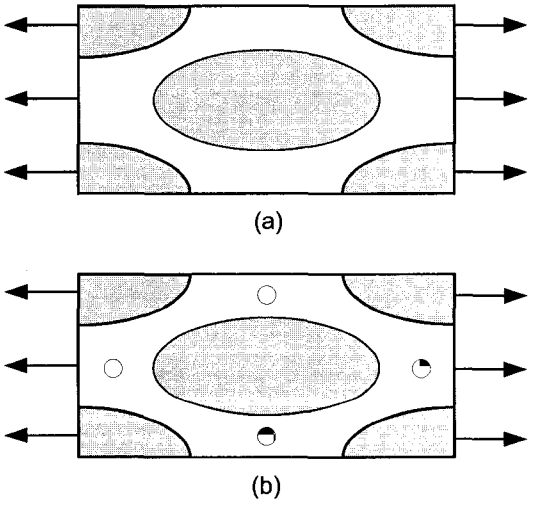

Figure 3-7: Hexagon packing configuration in the repeating unit of tow inside a lamina, (a) no voids and (b) four voids at the gaps.

3.5 Finite Element Mesh & Model

There are two finite element models that are created in ANSYS using APDL code: one of a repeating unit of fibers in a tow and one of a repeating unit of tows in a lamina. Each of the repeating unit geometries was meshed with three-dimensional 10-node tetrahedral structural solid elements, SOLID187. The repeating unit of fibers in a tow, Figure 3-4, was used to calculate the mechanical properties of a tow. The mesh used for this calculation is displayed in Figure 3-8.

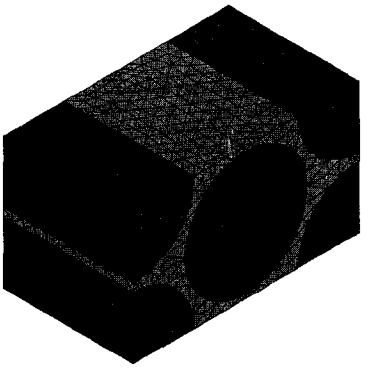

Figure 3-8: Meshed repeating unit of fibers in a tow with hexagonal packing

The tow properties calculated using the model and mesh above are used in the two repeating unit of tows in a lamina finite element models. These models were used to calculate the mechanical properties of the lamina and for the progressive failure model. The mesh of the tow repeating units of tows in a lamina are presented in Figure 3-9.

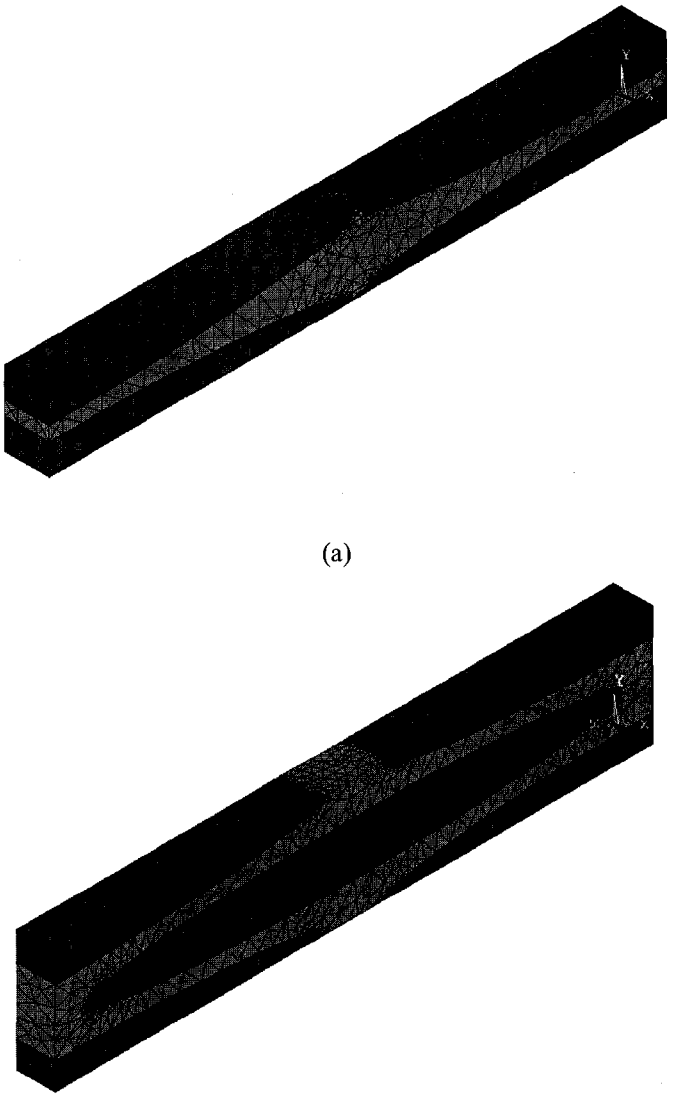

(a)

(b)

Figure 3-9: Meshed repeating units of tows in a lamina with (a) square packing and (b) hexagon packing.

3.6 Analysis Method

3.6.1 Calculation of Mechanical Properties

The mechanical properties, Young's Modulus and Poisson's ratio, of the repeating units were calculated utilizing a iso-strain superposition technique. A unit displacement is applied at one face while the other faces are constrained so that they do not move and

remain planar. The reaction forces are obtained from each face. This process is repeated on each of the other two faces and the results are superposed on each other, Figure 3-10. The *a* and *b* constants are calculated such that two of the faces are stress free while the other face is in uni-axial tension. The mechanical properties are calculated using the simple stress-strain relations.

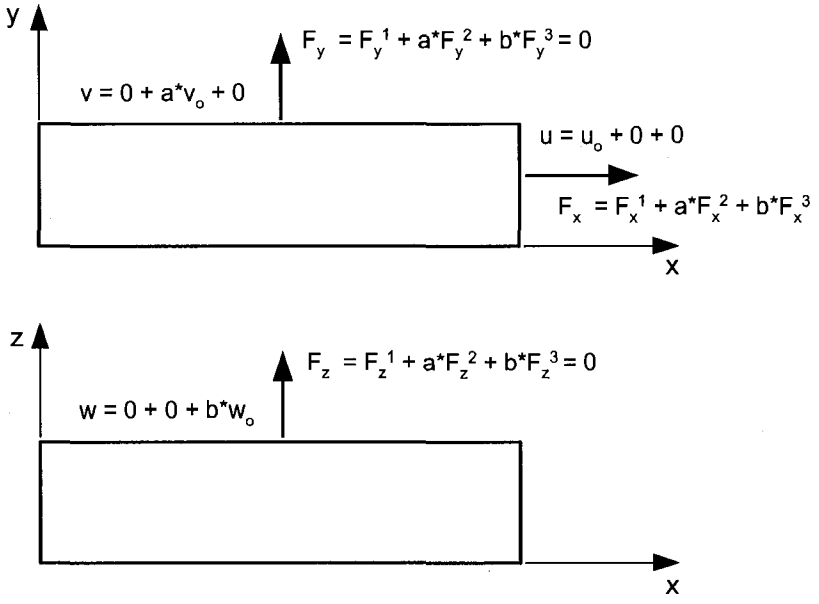

Figure 3-10: Resultant state of mechanical property calculations.

3.6.2 Progressive Failure Model

The objective of the progressive failure model is to determine a correlation between void content, void location, tow packing configuration, and lamina strength by subjecting the repeating unit of tow inside a lamina to an incremental displacement, determined from the strain rate of ASTM D3039. The progressive failure model will be applied to loading transverse to the fibers in the z-direction. The x-direction progressive failure will

not be investigated because the strength in that direction is fiber dominated and the voids have little or no effect.

Figure 3-1 displays the lamina subjected to loading in the z-direction. Boundary conditions for the repeating unit were developed so that the faces perpendicular to the loading (x and y) are stress free. Figure 3-6 and Figure 3-7 display how the loading is applied to each of the repeating units. The incremental displacement is continuously applied until the cross section of the repeating unit fails. At each loading cycle, the reaction force on the face opposite the loading is obtained and the stress in the cross section is calculated. A comparison of the failure stress and failure strain will be made between the various tow packing configurations and void contents.

3.7 Model Parameters

Hercules AS graphite fiber and PMR-15 polyimide matrix were selected as the composite materials for this study. The constituent properties are displayed in Table 3-1.

Table 3-1: Constituent properties of AS graphite fiber and PMR-15 matrix [11].

AS Graphite Fiber		
Longitudinal Young's modulus	E_{1f} (GPa)	213.7
Transverse Young's modulus	E_{2f} (GPa)	13.7
Axial shear modulus	G_{12f} (GPa)	13.7
Transverse shear modulus	G_{23f} (GPa)	6.8
Poisson's ratio	ν_{12f}	0.3
Tensile Strength	σ_{Tf} (MPa)	3033.8
Density	δ_f (g/cm^3)	1.799
PMR-15 Matrix		
Young's modulus	E_m (GPa)	3.2
Shear modulus	G_m (GPa)	1.1
Poisson's ratio	ν_m	0.36
Tensile Strength	σ_{Tm} (MPa)	55.8
Density	δ_m (g/cm^3)	1.313

Some other properties of a common AS graphite/PMR-15 lamina are required for the analysis, Table 3-2, such as the fiber diameter [4], tow and lamina fiber volume ratios, tow flatness ratio and the number of fibers within a tow.

Table 3-2: AS graphite/PMR-15 lamina properties.

Graphite fiber diameter	d_f (μm)	7
Tow fiber volume ratio	$V_{f,t}$	0.80
Lamina fiber volume ratio	V_f	0.50
Number of fibers per tow		3000
Tow flatness ratio (b/a)	fr	0.10

The void sizes used in the generation of the lamina repeating units were based the geometric and finite element model limitations. A maximum void diameter of 50 microns was chosen based on the information from reference [18]. The location chosen for the voids was between the tows. For reference [12] it was determined that the small voids (smaller than the tows) had a larger effect on the performance of the composite than larger voids.

The topics covered in this section are discussed in detail in chapter 4 with the results of the analysis presented in chapter 5.

4 FINITE ELEMENT MODEL

A lamina is a sheet or ply of unidirectional fiber-reinforced composites and multiple layers of lamina are stacked in various angular arrangements to form a multi-directional laminate. The reinforcement can come in the form of individual fiber or bundles of thousands of fiber, called tows. When multi-directional laminates are use in structural applications, accurate predictions of elastic properties such as the Young's and Shear moduli and Poisson's ratios are desirable. To determine the elastic properties of the laminate the elastic properties of the individual lamina must be known. The presence of voids within the matrix of a lamina can have a detrimental effect the elastic properties and thus, the elastic properties of a lamina with voids must be determined. Voids can also affect the failure mode of the lamina, as the voids act as stress risers. It is important to know how and to what extent do the voids affect the properties and strength of the lamina. Finite element modeling can be an effective tool used to predict these properties and evaluate the progressive failure of the lamina. As seen in the previous section much work has been done covering this topic, with the majority focusing on the interlaminar shear strength of a laminate. In addition, most of the research has been completed experimentally with very little utilizing finite element analysis. This focus here is the use of Finite Element Analysis to determine the effect of voids on the elastic properties and strength of a lamina.

4.1 Generation of Finite Element Model

All modeling and analysis were completed in ANSYS 11.0, utilizing the ANSYS Parametric Design Language (APDL). Modeling techniques and mesh generation for the repeating unit of the unidirectional lamina is presented. A finite element model is developed for determination of macroscopic mechanical properties.

4.1.1 Modeling

The geometrical structure of a unidirectional lamina is simple. A lamina (ply) consists of matrix containing tows (bundles of fibers), oriented in one direction. The lamina is an orthotropic material with principal material axes in the direction of the tows, normal to the tows in the plane of the lamina, and normal to the plane of the lamina [6], Figure 4-1 displays the principal axes of a unidirectional lamina. In the model, principal axis 1 coincides with the x-axis, axis 2 with the z-axis, and axis 3 with the y-axis.

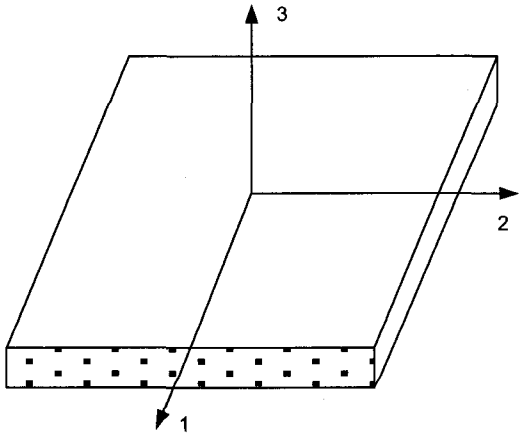

Figure 4-1: Unidirectional lamina and principal coordinate axes.

Repeating Unit of Fibers Inside The Tow

An idealized elliptical shaped tow is utilized for geometric model. The ellipse is comprised of the major radius, *a*, and minor radius, *b*, displayed in Figure 4-2.

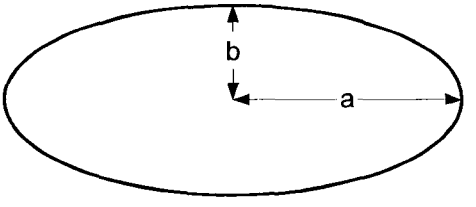

Figure 4-2: Elliptical Tow Cross Section.

A tow is a bundle of fibers with a very high fiber volume fraction, usually between 70 and 80 percent. In order to obtain this high of a fiber volume fraction the fibers are packed in a hexagonal pattern. It is assumed that all of the fibers are of equal size and spacing is held constant. In reality, the diameters of the fibers vary slightly and the proper spacing is not always held true. For this type of cross section, a simple hexagonal pattern and repeating unit can be identified, as shown in Figure 4-3.

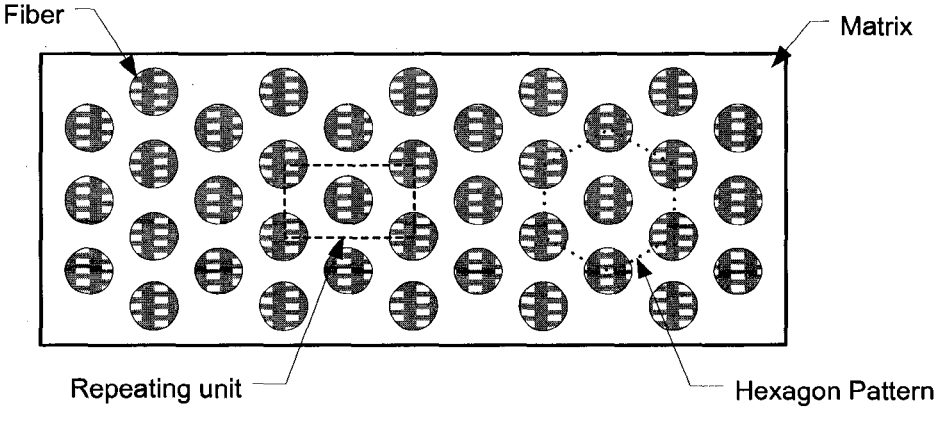

Figure 4-3: A sample of a elliptical tow cross section with a hexagonal packing and repeating unit displayed.

The repeating unit is the simplest model that can be formed to represent the cross section and is very useful for element modeling and analysis. This allows for smaller and an increase number of elements to be used, which will improve the results of the analysis. Figure 4-4 displays the hexagonal unit cell that was used in the model of the tow. In order to model the unit cell its dimensions must be determined. Triangle *kmn* is an equilateral triangle with leg length *c*. The unit cell is rectangular with side lengths, *c* and w_u, fiber radius, r_f, and tow fiber volume fraction, $V_{f,t}$.

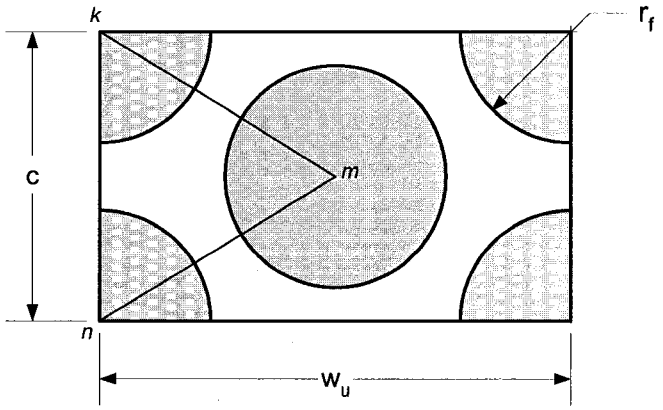

Figure 4-4: Hexagonal (repeating) unit cell.

The fiber radius and tow fiber volume fraction are known quantities, while the side lengths are unknown. The fiber volume fraction is defined as:

$$V_{f,t} = \frac{A_{fiber}}{A_u} = \frac{2\pi r_f^2}{cw_u} \tag{4.1}$$

where A_{fiber} is the fiber area and A_u is the total unit cell area. From triangle *kmn* the width, w_u, is calculated and the height, *c*, is calculated using equation 4.1:

$$w_u = \sqrt{3}c$$
$$c = \left(\frac{2\pi r_f^2}{\sqrt{3} V_{ft}} \right)^{1/2} \tag{4.2}$$

The length of the model was determined to not have an effect on the analysis results and was chosen at a length to ease the amount of computer resources required to run the analysis.

Lamina Repeating Unit Model

The dimensions, a and b, of the elliptical tow, see Figure 4-2, are unknown and must be determined. Using the following relations the can be determined.

$$A_{fiber} = \pi r_f^2$$
$$fr = b/a \tag{4.3}$$
$$A_{tow} = \frac{N\pi r_f^2}{V_f} = \pi ab = \pi a^2 (fr)$$

where N is the total number of fibers in a tow, fr is the flatness ratio (aspect ratio) and V_f is the overall fiber volume fraction in the lamina. The following quantities are known: total number of fiber in tow, N, and the aspect ratio. And finally, a and b are determined:

$$a = \left(\frac{A_{tow}}{\pi \times fr} \right)^{1/2}$$
$$b = a \times fr \tag{4.4}$$

The tows within a laminate are distributed uniformly throughout the cross section. The packing is similar to that of a simple cubic; except instead of circular fiber there are elliptical tows, see Figure 4-5.

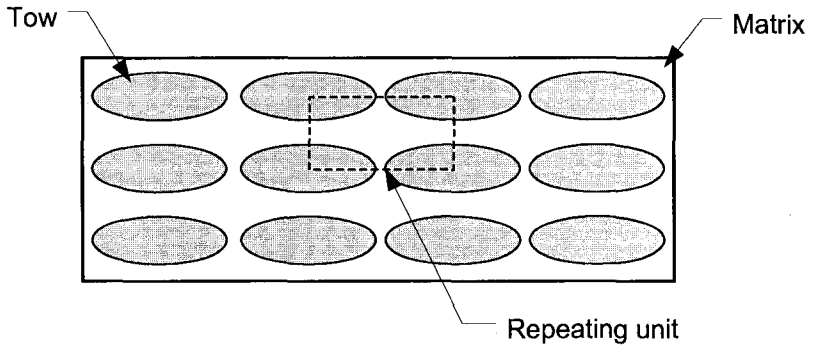

Figure 4-5: The tow distribution within a unidirectional lamina.

The repeating unit of the tow lamina contains a quarter of an elliptical tow at each corner of the rectangular unit. The elliptical shaped tows allow for tighter packing in the lamina, increasing its stiffness and strength. Figure 4-6 displays the repeating unit of a tow-impregnated lamina with height h, width w and gaps g on the top, bottom and side faces.

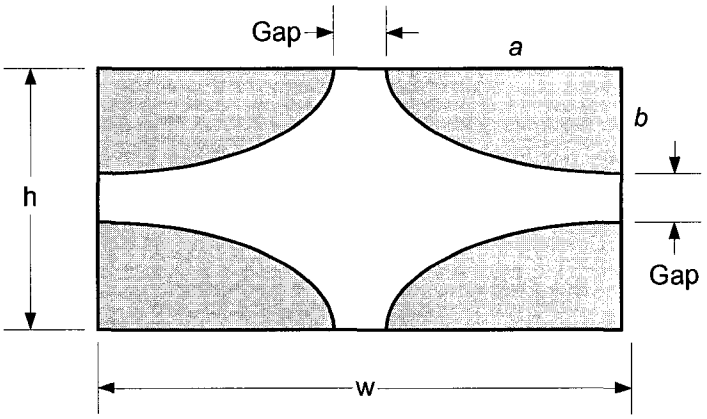

Figure 4-6: Repeating unit of a tow impregnated lamina.

The assumption is that both gaps are of equal length. With a and b already know the dimensions of the repeating unit can be calculated.

$$\begin{aligned} w &= 2a + g \\ h &= 2b + g \\ A_{lam} &= w \times h \times V_f = N \times A_{fiber} \end{aligned} \tag{4.5}$$

where A_{lam} is the area of fibers in within the lamina repeating unit. The equation above can be rearranged into the following quadratic equation:

$$g^2 + 2(a+b)g + \left(4ab - \frac{NA_{fiber}}{V_f}\right) = 0 \tag{4.6}$$

Solving for g using the quadratic formula:

$$g = -(a+b) \pm \left[\left(a+b \right)^2 - \left(4ab - \frac{NA_{fiber}}{V_f} \right) \right]^{1/2} \tag{4.7}$$

The length of the model was determined to not have an effect on the analysis results and was chosen at a length to ease the amount of computer resources required to run the analysis.

4.1.2 Voids

Voids were neglected in the repeating unit of fibers inside a tow. This project is concerned with the voids located around the tows in the lamina. The voids in the lamina are small macro voids, smaller than the tows and located between and around the tows. The number and size of the voids determine the void content of the repeating unit of the tows inside the lamina, it was desired to produce geometries with various void contents with various void locations and geometries where the void locations and sizes are user defined.

Demma and Djordjevice [10] presented in thermoset matrix laminates the voids tend to be spherical in shape. Since, a thermoset matrix was selected for the model, the voids are modeled as spheres.

The void content of the repeating unit of the tows inside the lamina unit with spherical voids is calculated using the equations 4.8.

$$V_{total} = w \times h \times L$$
$$V_{void} = \sum \frac{4}{3} \pi r_v^3 \tag{4.8}$$
$$V_{content} = \frac{V_{void}}{V_{total}} \times 100$$

where V_{total} is the total volume of the repeating unit, V_{void} is the total volume of the voids, r_v is the void radius, and $V_{content}$ is the void volume fraction.

4.1.3 Mesh Generation

The element choice for the model's mesh is SOLID187, a three-dimensional 10-node tetrahedral structural solid, with each of the 10 nodes having three degrees of freedom: translations in the nodal x, y, and z directions. SOLID187 has a quadratic displacement behavior and is well suited to modeling irregular meshes. It is also good for curved boundaries, such as around the voids and fibers. The geometry, node locations, and coordinate system are shown in Figure 4-7.

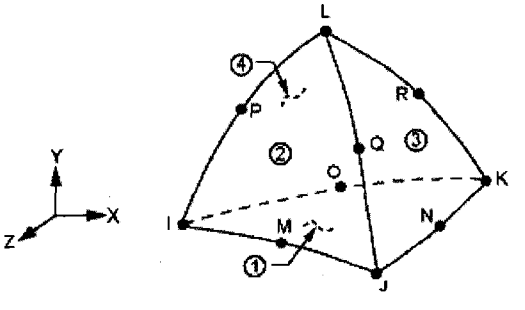

Figure 4-7: SOLID187 geometry, node locations, and the coordinate system [20].

The size of the mesh was determined using the SMRTSIZE command. This command allows ANSYS to automatically determine the size of each element based on the geometry. The smallest element size was used for the mesh, in most cases the finer the mesh the better the results. To avoid element errors (i.e. tetrahedrons with straightened edges, inverted Jacobian determinant, and small interior angles) the tetrahedron element improvement option, MOPT, was utilized. The improvement occurs through the use of face swapping and node smoothing techniques. Finally, the geometry was meshed using the free mesh command.

4.1.4 Tow Geometry Program

A program was developed utilizing the ANSYS Parametric Design Language to create the tow repeating unit geometry, *Tow_repeating_unit.txt* is located in Appendix. ANSYS Parametric Design Language (APDL) is a scripting language that can be used to automate common tasks or build the solid model in terms of parameters. The list of commands can be written as a macro in a text file and imported in ANSYS or each individual command can be entered into the dialog box.

The inputs to the program are the fiber radius, height of unit cell, width of unit cell, length, and material properties. The dimensions of the tow repeating unit are calculated in a spreadsheet using the equations discussed above and the material properties for the individual fibers and matrix were obtained from Bowles and Frimpong [11]. From these parameters the void-free repeating unit geometry is produced by first creating the rectangular matrix and then the circular fibers. The matrix volume that is overlapped by the cylindrical fiber is subtracted and the remaining volumes are glued together. Finally

the volumes are meshed with the SOLID187 elements producing the tow repeating unit, Figure 4-8.

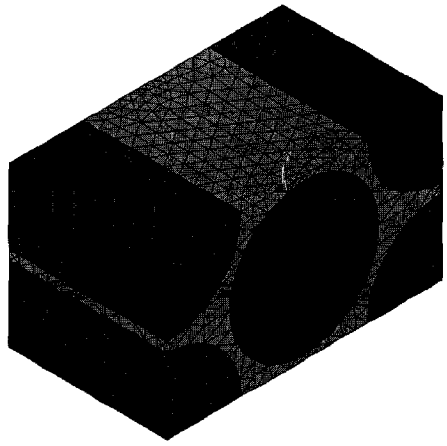

Figure 4-8: Meshed tow repeating unit with hexagonal packing.

4.1.5 Lamina Geometry Programs

Four programs were developed to create four different lamina repeating unit geometries. The first three created a cubic type cross section with varying void contents and the fourth program created a hexagonal cross section. All four programs are located in the Appendix.

Random Void Generation

This program, *Lamina_Geometry_Random.txt*, is capable of creating a void free lamina or a lamina with random void content. The inputs to the program are the tow major and minor radii, tow aspect ratio, lamina repeating unit height, width, length, and mechanical properties. The mechanical properties of the lamina were calculated using the tow repeating unit program and input into this program. From these parameters the

repeating unit geometry is produced by first creating the rectangular matrix and then the elliptical tows. The elliptical volume is not a readily available command in ANSYS; some manipulation of a cylinder was necessary to achieve the appropriate shape. Utilizing the volume scale command (VLSCAL) and the tow aspect ratio, the cylinder was flattened into an elliptical volume. The matrix volume that is overlapped by the elliptical tows is subtracted and the remaining volumes are glued together.

At this point a decision must be made, "Do you want to create voids?" If the answer is "No" the program continues on and meshes the volume. If the answer is "Yes" the program continues to the void creation loop. Five random numbers are generated in the program; a random integer to represent the number of voids, a number between zero and the maximum void radius to represent the radius of one void, and the x, y, and z locations of the void. The x, y and z locations are limited so that the voids are only created within the matrix. To create a void the program generates a spherical volume and that volume is subtracted from the matrix, leaving a "void" of material. The program continues to loop through until the correct number of voids is created. Following the completion of the geometry, the geometry is meshed. The output of the program in addition to the meshed geometry is the number of voids created, the total volume of the voids, and the void content of the geometry.

User-defined Void Locations

The other two programs create the void free lamina repeating unit geometry in the exact same method as the random program. The difference is that instead of randomly generated voids, the user determines the locations of the voids. Program

Lamina_Geometry_center.txt creates one large void in the exact center of the model. Program *Lamina_Geometry_gap.txt* creates four voids, all at the mid-plane in the x direction, two large voids near the top and bottom gaps and two small voids at the side gaps.

Hexagonal Tow Packing

Another tow packing configuration can be model to determine the mode of failure due to transverse tensile loading. The tows are orientated in a hexagonal pattern similar to the arrangement of fibers within a tow. This program also contains the ability for the user to create voids at specified locations.

4.1.6 Computer Information

This section contains the computer specifications used for the analysis, model sizes, and approximate length of computation time. A computer with the following specifications was used for the ANSYS analysis:

Dell Inspiron E1505 Laptop

Intel CPU T2300 @ 1.66 GHz

1.0 GB of RAM

The table below contains the number of nodes, number of elements, and approximate analysis times for each of the repeating unit (RU) models.

Table 4-1: Repeating unit model sizes and approximate analysis times.

Model Type	# of Nodes	# of Elements	Analysis Time (min.)
Tow RU	24,805	16,777	30
Square Lamina RU - No Voids	14,220	8,417	25
Square Lamina RU - Center Void	22,796	14,419	40
Square Lamina RU - Gap Voids	31,506	19,659	50
Hexagon Lamina RU - No Voids	29,318	17,716	45
Hexagon Lamina RU - Gap Voids	60,463	39,363	75

4.2Determination of Elastic Properties

This chapter describes in detail the methodology used to formulate the tests and calculate the effective Young's moduli, Poisson's ratios, and shear modulus of the tow repeating unit and the lamina repeating unit. The sections below detail how the elastic properties of the tow repeating unit is calculated, the elastic properties of the lamina repeating unit are calculated in the exact same method. The only difference is the change of the following nomenclature: $L_u = L$, $w_u = w$, and $c = h$. An APDL program was developed for the computation of the elastic properties, Young's Moduli and Poisson's ratios, and the shear moduli.

4.2.1 For Effective Young's Moduli and Poisson's Ratios

To obtain the mechanical properties for the fiber-reinforced composite unit cell, three iso-strain boundary conditions were superimposed. The objective of the iso-strain boundary conditions is to achieve a state of deformation where all faces remain planar and normal to each other. Only one face, along with its opposite face, has a net force and the remaining surfaces have a net zero force [21]. These conditions create a uniaxial

loading case. Poisson's ratio can be determined by the ratio of lateral strain to axial strain and Young's modulus can be determined by the ratio of axial stress to axial strain.

Boundary Conditions

The three iso-strain cases are described in detail below. The nomenclature for the faces of the finite element model is shown in Figure 4-9.

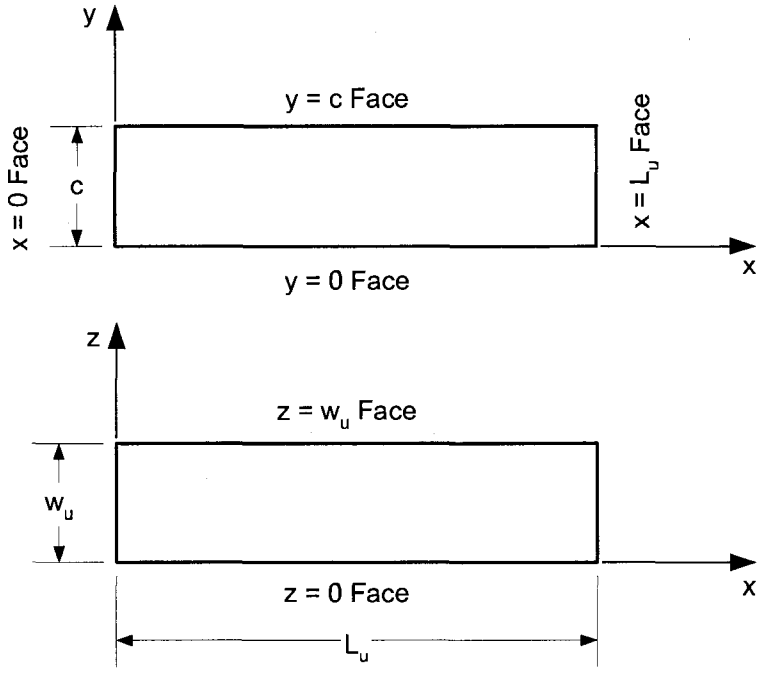

Figure 4-9: Nomenclature for faces of the Finite Element Model.

Case I: uniaxial tension in x-direction, see Figure 4-10.

Constraints:

On x = 0 face: $u = 0$ and on x = L_u face: $u = u_o$.

On y = 0 and y = c faces: $v = 0$.

On z = 0 and z = w_u faces: $w = 0$.

From these constraints, the following reaction forces result.

F_x^1 on either x = 0 or x = L_u face.

F_y^1 on either y = 0 or y = c face.

F_z^1 on either z = 0 or z = w_u face.

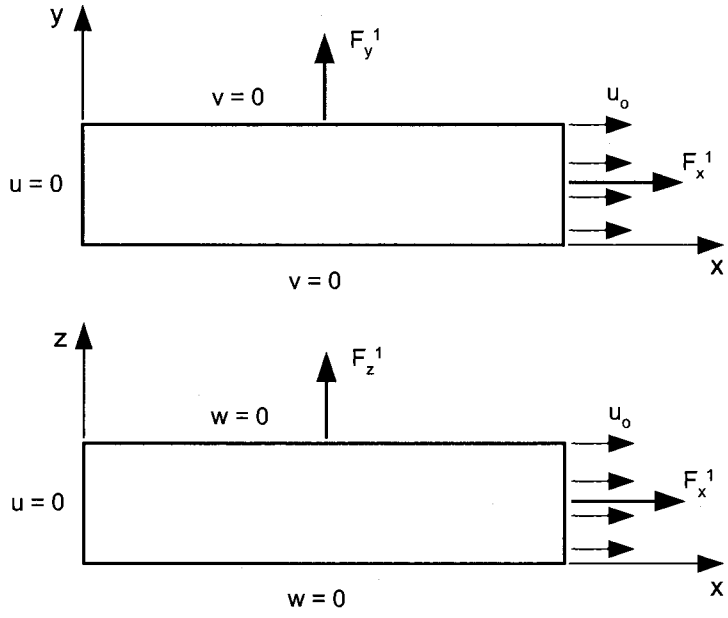

Figure 4-10: Nomenclature for loading Case 1

Case II: uniaxial tension in y-direction, Figure 4-11.

Constraints:

On x = 0 and x = L_u faces: $u = 0$.

On y = 0 face: $v = 0$ and on y = c face: $v = v_o$.

On z = 0 and z = w_u faces: $w = 0$.

From these constraints, the following reaction forces result.

F_x^2 on either x = 0 or x = L_u face.

F_y^2 on either y = 0 or y = c face.

F_z^2 on either z = 0 or z = w_u face.

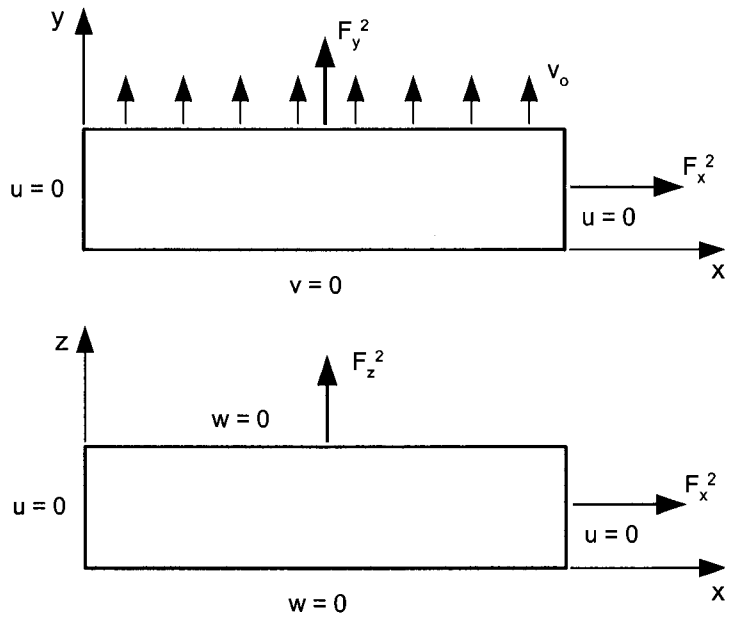

Figure 4-11: Nomenclature for loading Case 2

Case III: uniaxial tension in z-direction, Figure 4-12.

Constraints:

On x = 0 and x = L_u faces: $u = 0$.

On y = 0 and y = c faces: $v = 0$.

On z = 0 face: $w = 0$ and on z = w_u face: $w = w_o$.

From these restraints following reaction forces result.

F_x^3 on either $x = 0$ or $x = L_u$ face.

F_y^3 on either $y = 0$ or $y = c$ face.

F_z^3 on either $z = 0$ or $z = w_u$ face.

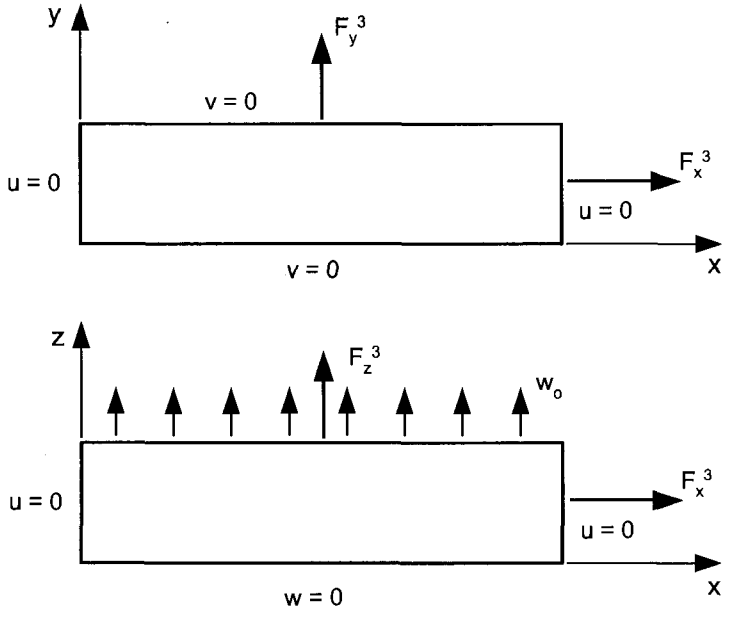

Figure 4-12: Nomenclature for loading Case 3

Computation of Elastic Properties

As stated above, the three iso-strain boundary condition cases were superimposed using two undetermined variables, *a* and *b*. The resultant state of deformation is

Resultant state = (State of Case I) + *a* * (State of Case II) + *b* * (State of Case III)

The resultant displacements in the x, y and z directions are, Figure 4-13:

$$\begin{aligned} u &= u_0 + 0 + 0 \\ v &= 0 + a \cdot v_0 + 0 \\ w &= 0 + 0 + b \cdot w_0 \end{aligned} \tag{4.9}$$

Hence, the three average strains of the unit cell are

$$\begin{aligned} \varepsilon_x &= \frac{u_0}{L_u} \\ \varepsilon_y &= \frac{a \cdot v_0}{c} \\ \varepsilon_z &= \frac{b \cdot w_0}{w_u} \end{aligned} \tag{4.10}$$

and the resultant forces in the x, y, z directions are displayed below and in Figure 4-13:

$$\begin{aligned} F_x &= F_x^1 + a \cdot F_x^2 + b \cdot F_x^3 \\ F_y &= F_y^1 + a \cdot F_y^2 + b \cdot F_y^3 \\ F_z &= F_z^1 + a \cdot F_z^2 + b \cdot F_z^3 \end{aligned} \tag{4.11}$$

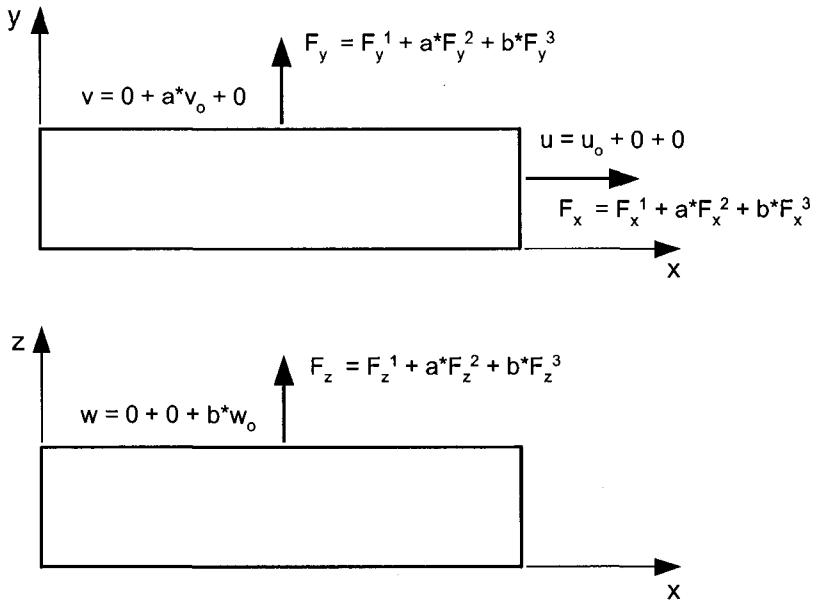

Figure 4-13: Resultant forces and displacements

Computation of E_x, ν_{xy}, ν_{xz}

To determine mechanical properties above, the resultant superposition and choice of constants *a* and *b* are such that the resultant forces on all y and z faces are zero but are non-zero on the x faces; $F_y = 0$, $F_z = 0$, and $F_x \neq 0$. Thus, the stress in each direction is defined as:

$$\begin{aligned} \sigma_x &= \frac{F_x}{w_u c} \\ \sigma_y &= 0 \\ \sigma_z &= 0 \end{aligned} \tag{4.12}$$

Therefore, it is a uniaxial loading case in the x-direction. Consequentially, the following relations can be written.

$$
\begin{aligned}
\nu_{xy} &= -\frac{\varepsilon_y}{\varepsilon_x} = -\frac{a \cdot v_o / c}{u_o / L_u} = -a\frac{v_o L_u}{u_o c} \\
\nu_{xz} &= -\frac{\varepsilon_z}{\varepsilon_x} = -\frac{b \cdot w_o / w_u}{u_o / L_u} = -b\frac{w_o L_u}{u_o w_u} \\
\mathrm{E_x} &= \frac{\sigma_x}{\varepsilon_x} = \frac{\mathrm{F_x} / (w_u c)}{\mathrm{u_o} / L_u} = \frac{L_u}{u_o w_u c}\left(F_x^1 + a \cdot \mathrm{F_x^2} + b \cdot \mathrm{F_x^3}\right)
\end{aligned}
\tag{4.13}
$$

From the case definition and Equation 4.11, the following relation can be achieved

$$
\begin{aligned}
F_y &= F_y^1 + a \cdot F_y^2 + b \cdot F_y^3 = 0 \\
F_z &= F_z^1 + a \cdot F_z^2 + b \cdot F_z^3 = 0
\end{aligned}
\tag{4.14}
$$

Constants *a* and *b* are determined from solving the following simultaneous linear equations, which are obtained by rearranging Equation 4.14.

$$
\begin{aligned}
a \cdot (F_y^2) + b \cdot (F_y^3) &= -F_y^1 \\
a \cdot (F_z^2) + b \cdot (F_z^3) &= -F_z^1
\end{aligned}
\tag{4.15}
$$

Thus,

$$
\begin{aligned}
a_x &= -\frac{F_y^3 \cdot F_z^1 - F_y^1 \cdot F_z^3}{F_y^3 \cdot F_z^2 - F_y^2 \cdot F_z^3} \\
b_x &= \frac{F_y^2 \cdot F_z^1 - F_y^1 \cdot F_z^2}{F_y^3 \cdot F_z^2 - F_y^2 \cdot F_z^3}
\end{aligned}
\tag{4.16}
$$

Hence, E_x , ν_{xy} and ν_{xz} are calculated by substituting *a* and *b* in Equation 4.13.

Computation of E_y, ν_{yx}, ν_{yz}

To determine mechanical properties above, the resultant superposition and choice of constants *a* and *b* are such that the resultant forces on all x and z faces are zero but are non-zero on the y face; $F_x = 0$, $F_z = 0$, and $F_y \neq 0$. Thus, the stress in each direction is defined as:

$$\begin{aligned} \sigma_x &= 0 \\ \sigma_y &= \frac{F_y}{w_u L_u} \\ \sigma_z &= 0 \end{aligned} \tag{4.17}$$

Therefore, it is a uniaxial loading case in the y-direction. Consequentially, the following relations can be written.

$$\begin{aligned} \nu_{yx} &= -\frac{\varepsilon_x}{\varepsilon_y} = -\frac{u_o / L_u}{a \cdot v_o / c} = -\frac{u_o c}{a \cdot v_o L_u} \\ \nu_{yz} &= -\frac{\varepsilon_z}{\varepsilon_y} = -\frac{b \cdot w_o / w_u}{a \cdot v_o / c} = -\frac{b \cdot w_o c}{a \cdot v_o w_u} \\ E_y &= \frac{\sigma_y}{\varepsilon_y} = \frac{F_y / (w_u \cdot L)}{a \cdot v_o / c} = \frac{c}{a \cdot v_o L_u w_u} \left(F_y^1 + a \cdot F_y^2 + b \cdot F_y^3 \right) \end{aligned} \tag{4.18}$$

From the case definition and Equation (4.11), the following relation can be achieved

$$\begin{aligned} F_x &= F_x^1 + a \cdot F_x^2 + b \cdot F_x^3 = 0 \\ F_z &= F_z^1 + a \cdot F_z^2 + b \cdot F_z^3 = 0 \end{aligned} \tag{4.19}$$

and constants a and b are determined from solving the following simultaneous linear equations, which are obtained by rearranging Equation (4.19).

$$\begin{aligned} a \cdot (F_x^2) + b \cdot (F_x^3) &= -F_x^1 \\ a \cdot (F_z^2) + b \cdot (F_z^3) &= -F_z^1 \end{aligned} \tag{4.20}$$

Thus,

$$\begin{aligned} a_y &= -\frac{F_x^3 \cdot F_z^1 - F_x^1 \cdot F_z^3}{F_x^3 \cdot F_z^2 - F_x^2 \cdot F_z^3} \\ b_y &= \frac{F_x^2 \cdot F_z^1 - F_x^1 \cdot F_z^2}{F_x^3 \cdot F_z^2 - F_x^2 \cdot F_z^3} \end{aligned} \tag{4.21}$$

Hence, E_y , ν_{yx} and ν_{yz} are calculated by substituting a and b in Equation 4.18.

Computation of E_z, ν_{zy}, ν_{zx}

To determine mechanical properties above, the resultant superposition and choice of constants a and b are such that the resultant forces on all x and y faces are zero but are non-zero on the z face; $F_x = 0$, $F_y = 0$, and $F_z \neq 0$. Thus, the stress in each direction is defined as:

$$\begin{aligned} \sigma_x &= 0 \\ \sigma_y &= 0 \\ \sigma_z &= \frac{F_z}{c \cdot L_u} \end{aligned} \tag{4.22}$$

Therefore, it is a uniaxial loading case in the z-direction. Consequentially, the following relations can be written.

$$\nu_{zx} = -\frac{\varepsilon_x}{\varepsilon_z} = -\frac{u_o / L_u}{b \cdot w_o / w_u} = -\frac{u_o w_u}{b \cdot w_o L_u}$$
$$\nu_{zy} = -\frac{\varepsilon_y}{\varepsilon_z} = -\frac{a \cdot v_o / c}{b \cdot w_o / w_u} = -\frac{a \cdot v_o w_u}{b \cdot w_o c} \qquad (4.23)$$
$$\mathrm{E}_z = \frac{\sigma_z}{\varepsilon_z} = \frac{\mathrm{F}_z / (c \cdot L)}{\mathrm{b} \cdot \mathrm{w}_o / w_u} = \frac{w_u}{b \cdot w_o L_u c}\left(\mathrm{F}_z^1 + a \cdot \mathrm{F}_z^2 + b \cdot \mathrm{F}_z^3\right)$$

From the case definition and Equation (4.11), the following relation can be achieved

$$F_x = F_x^1 + a \cdot F_x^2 + b \cdot F_x^3 = 0$$
$$F_y = F_y^1 + a \cdot F_y^2 + b \cdot F_y^3 = 0 \qquad (4.24)$$

and constants a and b are determined from solving the following simultaneous linear equations, which are obtained by rearranging Equation 4.24.

$$a \cdot (F_x^2) + b \cdot (F_x^3) = -F_x^1$$
$$a \cdot (F_y^2) + b \cdot (F_y^3) = -F_y^1 \qquad (4.25)$$

Thus,

$$a_z = -\frac{F_x^3 \cdot F_y^1 - F_x^1 \cdot F_y^3}{F_x^3 \cdot F_y^2 - F_x^2 \cdot F_y^3}$$
$$b_z = \frac{F_x^2 \cdot F_y^1 - F_x^1 \cdot F_y^2}{F_x^3 \cdot F_y^2 - F_x^2 \cdot F_y^3} \tag{4.26}$$

Hence, E_z, ν_{zy}, and ν_{zx} are calculated by substituting a_z and b_z in Equation 4.23.

Elastic Properties Program

Two APDL programs, Appendix, were developed to apply the iso-strain boundary conditions to the tow repeating unit and the lamina repeating unit for each of the three cases. The inputs into the program are the unit displacements for each of the three cases. The program progresses through each of the three cases independently, removing the previous cases boundary conditions before applying the new boundary conditions. The output is the reaction forces for each of the three cases. The reaction forces from the program were imported into a spreadsheet where the *a* and *b* constants and elastic properties were calculated using the method discussed above.

4.2.2 For Effective Shear Moduli

To obtain the effective shear moduli, three more boundary conditions are applied to the faces of the model remain planar to its opposite face. The shear modulus can be determined by the ratio of shear stress to shear strain.

Boundary Conditions

Refer to Chapter 3 for the model geometry. The boundary conditions for the three cases are described in detail below.

Case G_{xy}:

The boundary conditions for the computation of G_{xy} are below, see Figure 4-14.

On y = 0 face: u = 0 and v = 0

On y = c face: $u = u_o$ and v = 0

On x = 0 and x = L_u faces: $u = u_o*(y/c)$ and v = 0

On z = o and z = w_u faces: w = 0

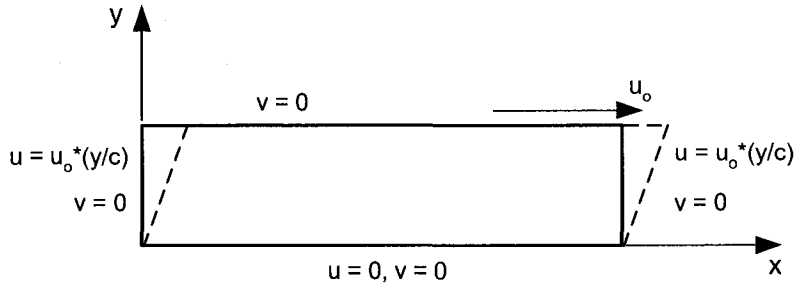

Figure 4-14: Boundary conditions for case G_{xy}

From these constraints, the following reaction forces result.

F_x^U and F_y^U on y = c face

F_x^R and F_y^R on x = L_u face

F_x^B and F_y^B on y = 0 face

F_x^L and F_y^L on x = 0 face

Case G_{xz}:

The boundary conditions for the computation of G_{xz} are below, see Figure 4-15.

On z = 0 face: u = 0 and w = 0

On $z = w_u$ face: $u = u_o$ and w = 0

On x = 0 and $x = L_u$ faces: $u = u_o*(z/w_u)$ and v = 0

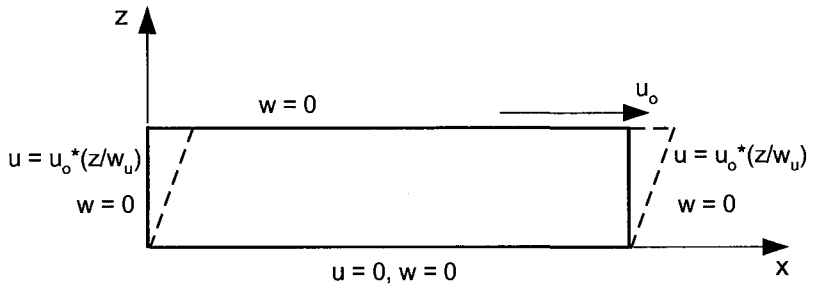

Figure 4-15: Boundary conditions for case G_{xz}

From these constraints the following reaction forces result.

F_x^U and F_z^U on $z = w_u$ face

F_x^R and F_z^R on $x = L_u$ face

F_x^B and F_z^B on z = 0 face

F_x^L and F_z^L on x = 0 face

Case G_{zy}:

The boundary conditions for the computation of G_{zy} are below, see Figure 4-16.

On y = 0 face: v = 0 and w = 0

On y = c face: v = 0 and $w = w_o$

On z = 0 and z = w_u faces: v = 0 and w = w_o*(y/c)

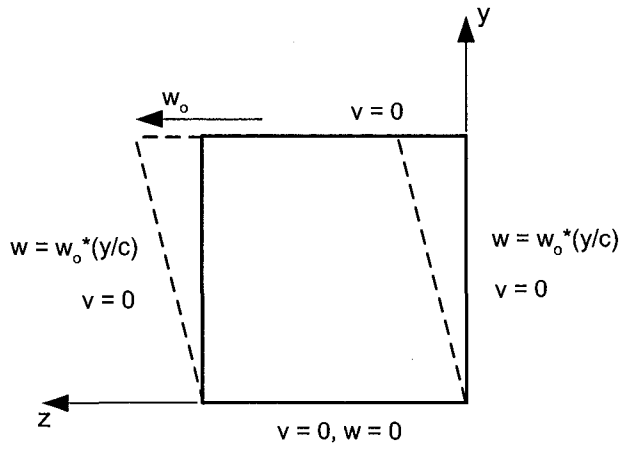

Figure 4-16: Boundary conditions for case G_{zy}

From these constraints the following reaction forces result.

F_y^U and F_z^U on y = c face

F_y^R and F_z^R on z = w_u face

F_y^B and F_z^B on y = 0 face

F_y^L and F_z^L on z = 0 face

Computation of Shear Properties

Computation of G_{xy}

Refer to the reaction forces discussed above and see Figure 4-17.

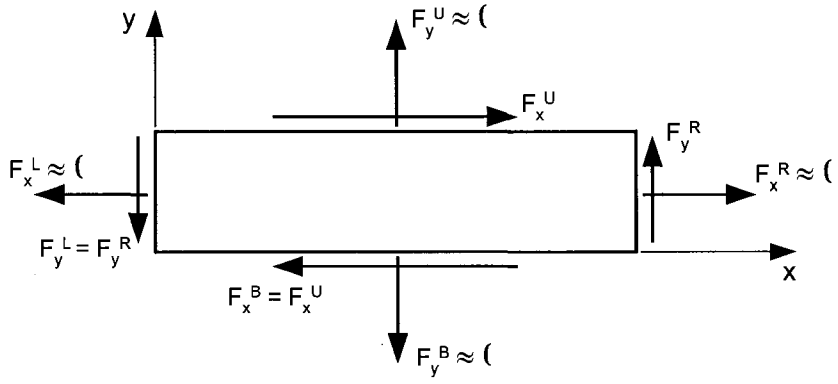

Figure 4-17: Reaction forces for the case to obtain G_{xy}

It was observed from the results in ANSYS that F_y^U was insignificant when compared to F_x^U on the y = c face (F_x^U was on the order of ten thousand times greater than F_y^U). Therefore, there was only a shear force on this face. Similarly, it was observed that F_x^R was insignificant when compared to F_y^R on the $x = L_u$ face. Therefore, there was only a shear force on this face. It was also observed that $F_y^L = F_y^R$, $F_x^U = F_x^B$, and $F_x^L = F_y^B \approx 0$. Hence, calculating the average shear stress on $x = L_u$ face and y = c face and utilizing the small angle theorem to calculate the shear strain:

$$\tau_{xy} = \frac{V}{A} = \frac{1}{2}\left[\frac{F_x^U}{w_u L_u} + \frac{F_y^R}{w_u c}\right]$$

$$\gamma_{xy} = \frac{u_o}{c} \qquad (4.27)$$

$$G_{xy} = \frac{\tau_{xy}}{\gamma_{xy}} = \frac{c}{2u_o w_u}\left[\frac{F_x^U}{L_u} + \frac{F_y^R}{c}\right]$$

Computation of G_{xz}

G_{xz} is calculated similarly to G_{xy}. Refer to the reaction forces discussed above and see Figure 4-18.

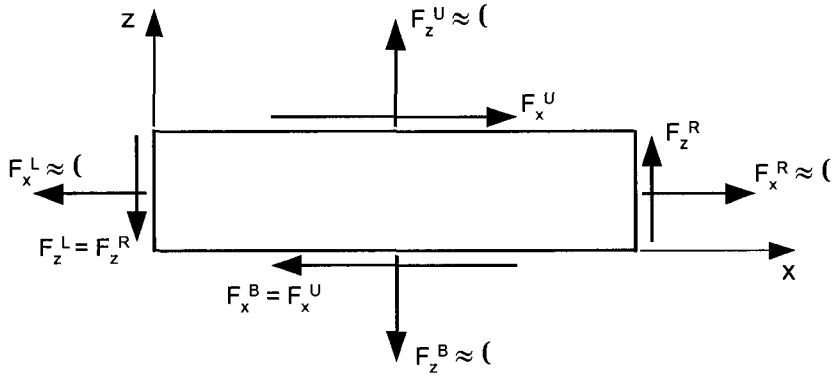

Figure 4-18: Reaction forces for the case to obtain G_{xz}

It was observed from the results in ANSYS that F_z^U was insignificant when compared to F_x^U on the z = d face (F_x^U was on the order of ten thousand times greater than F_z^U). Therefore, there was only a shear force on this face. Similarly, it was observed that F_x^R was insignificant when compared to F_z^R on the $x = L_u$ face. Therefore, there was only a shear force on this face. It was also observed that $F_z^L = F_z^R$, $F_x^U = F_x^B$, and $F_x^L = F_z^B \approx 0$. Hence, calculating the average shear stress on $x = L_u$ face and $z = w_u$ face and utilizing the small angle theorem to calculate the shear strain:

$$\tau_{xz} = \frac{V}{A} = \frac{1}{2}\left[\frac{F_x^U}{c \cdot L_u} + \frac{F_z^R}{w_c c}\right]$$

$$\gamma_{xz} = \frac{u_o}{w_u} \qquad (4.28)$$

$$G_{xz} = \frac{\tau_{xz}}{\gamma_{xz}} = \frac{w_u}{2u_o c}\left[\frac{F_x^U}{L_u} + \frac{F_z^R}{w_u}\right]$$

Computation of G_{yz}

Refer to the reaction forces discussed above and see Figure 4-19.

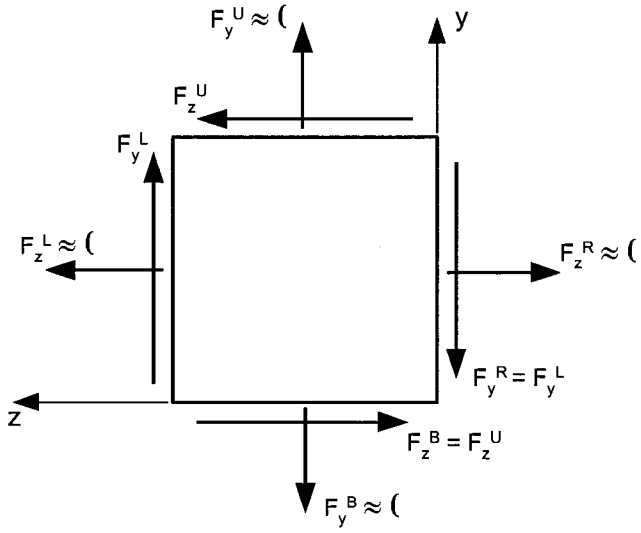

Figure 4-19: Reaction forces for the case to obtain G_{yz}

It was observed from the results in ANSYS that F_y^U was insignificant when compared to F_z^U on the y = d face (F_z^U was approximately on the order of ten thousand times greater than F_y^U). Therefore, there was only a shear force on this face. Similarly, it was observed that F_z^L was insignificant when compared to F_y^L on the z = w_u face.

Therefore, there was only a shear force on this face. It was also observed that $F_z^U \approx F_y^L$, $F_y^L = F_y^R$, $F_z^U = F_z^B$, and $F_z^L = F_y^B \approx 0$. Hence, calculating the average shear stress on y = c face and z = w_u face and utilizing the small angle theorem to calculate the shear strain:

$$\tau_{yz} = \frac{V}{A} = \frac{1}{2L_u}\left[\frac{F_z^U}{w_u} + \frac{F_y^L}{c}\right]$$
$$\gamma_{yz} = \frac{w_o}{c} \qquad (4.29)$$
$$G_{yz} = \frac{\tau_{yz}}{\gamma_{yz}} = \frac{c}{2w_o L_u}\left[\frac{F_z^U}{w_u} + \frac{F_y^L}{c}\right]$$

Shear Modulus Program

The shear modulus program, located in Appendix A, works in a very similar manner as the elastic properties program. The program was only utilized to calculate the shear moduli of the tow repeating unit. The inputs into the program are the unit displacements for each of the three cases. The boundary conditions are then applied to the geometry and the reaction forces are exported for each of the three cases. The program progresses through each of the three cases independently; removing the previous cases boundary conditions before applying the new boundary conditions. The reaction forces for the two faces of interest for each case were imported into a spreadsheet where the three shear moduli properties are calculated. The three tow shear moduli properties are then used as inputs for the Lamina geometry creation program.

Shear Modulus Comments

The shear modulus property results will not be found in the results section of this report. It was discovered that the shear modulus is dependent upon the length of the finite element model, where as the length does not affect the Young's modulus and Poisson's ratio results. Since, the progressive failure model is a tensile test the shear modulus properties of the materials will not factor in to the results. Much time and effort was put into the development of the shear modulus program, especially the application of the boundary conditions. Further investigation is required to determine how and why the length of the model affects the results.

4.3 Progressive Failure Model

The objective of the progressive failure model is to determine a correlation between void content, void location, tow packing configuration, and lamina strength by subjecting the lamina repeating unit to a incremental displacement. The progressive failure model will be applied to loading transverse to the fibers in the y-direction and the z-direction. The x-direction progressive failure will not be investigated because the strength in that direction is fiber dominated and the voids have little or no effect.

4.3.1 Methodology

The ASTM Standard Test Method for Tensile Properties of Polymer Matrix Composites Materials (D3039) was utilized as the model for the progressive failure model. ASTM International is an international standards organization that develops and

publishes voluntary consensus technical standards for a wide range of materials, products, systems, and services. ASTM D3039 is widely used and has been found to perform better than others with varying widths such as ASTM Test Method for Tensile Properties of Plastics (D638-91) [22]. The test method is designed to produce tensile property data for material specifications, research and development, quality assurance, and structural design and analysis [23]. ASTM D3039 utilizes a straight-sided coupon with bonded tabs with the following dimensions: 25 mm wide, 250 mm long, 2-3 mm thick, and 12° tapered tabs with a gage length of 180 mm [24]. The tensile test can be performed using a universal testing machine or an Instron mechanical testing machine at a constant cross-speed of approximately 0.5 mm per minute, at room temperature.

Incremental Displacement

The ASTM D3039 tensile test was applied to the lamina repeating unit. Since, the repeating unit is much smaller than the actual test specimen, the applied strain rate must be scaled down. The ASTM D3039 testing strain, ε_{test} is defined below as well as the repeating unit applied displacements.

$$\begin{aligned} \varepsilon_{test} &= \frac{\Delta L_t}{L_t} = \frac{0.5\,mm/\min}{180mm} \\ \delta_{rate\_y} &= \varepsilon_{test} \times h \\ \delta_{rate\_z} &= \varepsilon_{test} \times w \end{aligned} \tag{4.30}$$

Where δ_{rate_y} is the incremental displacement along the y-axis and δ_{rate_z} is the incremental displacement along the z-axis. These displacements are applied to the geometry in increments and the reaction loads at the face opposite the incremental

displacement are recorded. The stress in the matrix is calculated by dividing the reaction force by the cross sectional area of the repeating unit.

Boundary Conditions

The repeating unit of fiber/tow in a lamina is one very small section from the center of the lamina. Boundary conditions must be applied so that the repeating unit acts as if it is really at that location within the lamina.

Considering the case of failure in the z-direction, the boundary conditions on the x and y faces are such that the reaction forces obtained from these faces are zero, hence the x and y faces are stress free. Figure 4-20 displays the boundary conditions for this case.

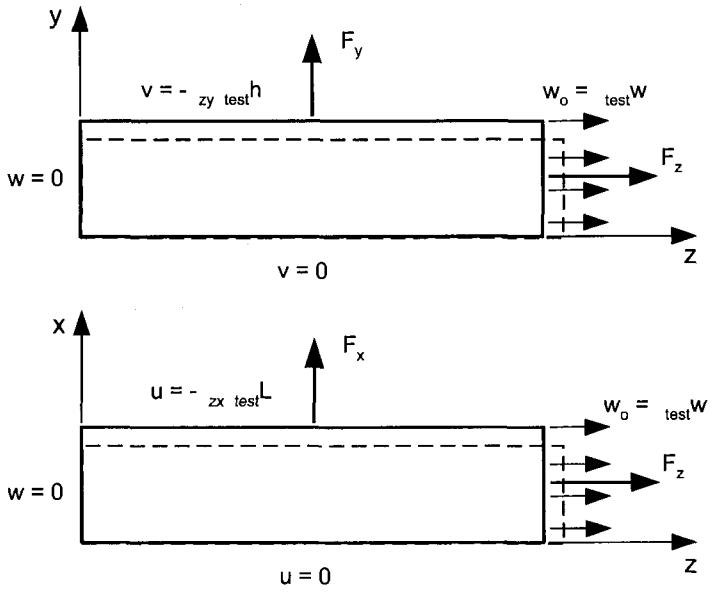

Figure 4-20: Boundary conditions for the progressive failure of a repeating unit in the z-direction.

The constraints applied to the x and y faces to ensure the faces are stress free are as follows:

$$x_{o,z} = -\nu_{zx}\varepsilon_{test}L$$
$$y_{o,z} = -\nu_{zy}\varepsilon_{test}h \tag{4.31}$$

The boundary conditions applied to each face in the analysis are:

On y = 0 face: $v = 0$

On y = h face: $v = y_{o,z}$

On x = 0 face: $u = 0$

On x = L face: $u = x_{o,z}$

On z = 0 face: $w = 0$

On z = w face: $w = w_o$

The constraints were applied during each cycle to force the geometry to contract at the proper rate, so that the faces are stress free.

4.3.2 Progressive Failure Program

The progressive failure APDL programs, *Z_PROGRESSIVE_FAILURE.txt* and *Y_PROGRESSIVE_FAILURE.txt*, are used to model the micro-crack propagation within the lamina do to the presence of voids. Two separate programs were generated for the y-direction progressive failure and the z-direction progressive failure.

The inputs to the program are the testing strain, the incremental displacement and the directional Poisson's ratios used to determine the boundary conditions. The boundary conditions and incremental displacement are applied to the geometry and the von Mises stress is calculated for each matrix element and placed in an element table (ETABLE).

The stress values are also written (INISTATE) to file to be used later. The element table is sorted (ESORT) in descending order and the element with the highest stress is selected. The element stress is compared to the matrix material yield strength. If the element stress is less than the yield strength, the program loops back toward the beginning of the program. The nodal coordinates are updated (UPGEOM) to the displaced locations and the stress values are input (INISTATE) as initial stress for the next iteration. At this point the boundary conditions and incremental displacement are reapplied and the loop continues. If the element stress is greater than the matrix yield strength, the stiffness (Young's Modulus) of the element is reduced by 10^{-3}. By doing this, the element acts as if it is not there, hence a failed element. The color of a failed element changes from green to red for visual inspection purposes. Now the stress value of the next element in the element table is examined and compared to the yield strength. If this element also fails the process is repeated until an element does not fail. When this occurs, the matrix is visually inspected to determine if the failed element propagated throughout the entire cross section. If the cross section completely failed the process is over. However, if the cross section is still intact the program continues until the lamina fails.

The outputs of the program are the sum of the reaction force in the direction of the loading at each iteration, the number of iterations and the number of failed elements. The reaction force is used to calculate the amount of stress in the cross section. The program can be found in the Appendix and Figure 4-21 displays the logic flow chart of the program.

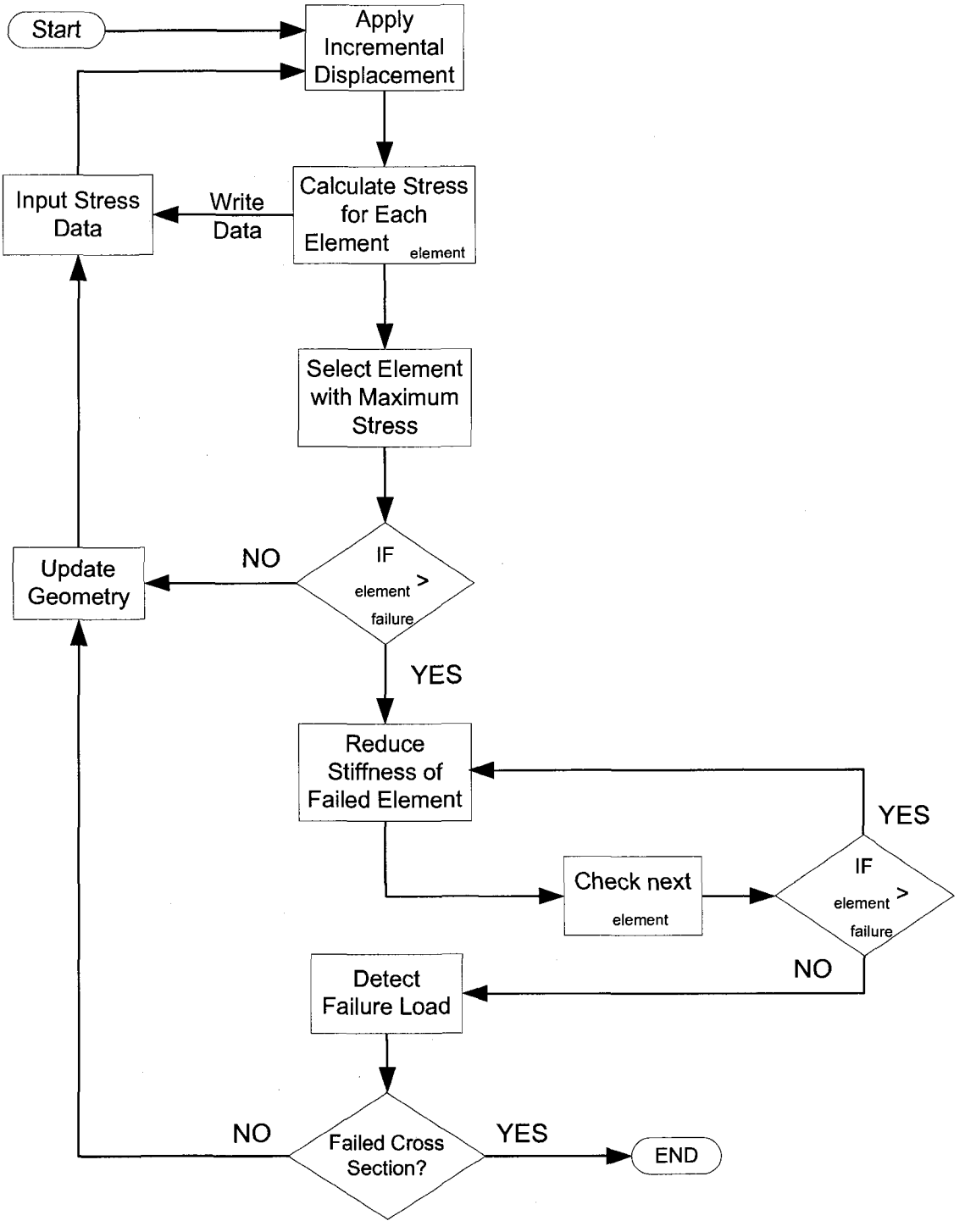

Figure 4-21: Progressive failure program logic flow chart.

5 RESULTS AND DISCUSSION

To determine the effectiveness of the analysis, the elastic properties predicted using Finite element analysis are compared with those of predicted by the rule of mixtures for both the repeating unit of fibers in a tow and the repeating unit for fibers/tows in a lamina.

Finite element analysis is one type of numerical method. As with all numerical methods the results are approximate. For this reason, it is required to have convergence data. Usually in finite element analysis, the higher the number of elements in the model improves the accuracy of the results. In the present work, a convergence study was not completed due to insufficient hard disk space. In finite element analysis, the convergence of displacements is achieved much earlier than convergence of stresses. This is because the stresses are obtained by differentiating the calculated displacements. In the current work, the mechanical properties are obtained from reaction forces and displacements; the results do not involve stresses. Hence, even without the convergence study, the results are assumed accurate.

5.1 Material Selection, Properties and Dimensions

The fiber-reinforced polymer composite material selected for use in this study is Hercules AS graphite fiber/PMR-15 matrix. The graphite fiber is made entirely of carbon and is soft and brittle. Graphite is also very lightweight and has an extremely high tensile strength. Its high strength-to-weight ration is what makes graphite an attractive material for use in a fiber-reinforced composite. Some of the major uses of graphite-reinforced

polymers is in the shaft of golf clubs, fishing poles, and bicycle frames. PMR-15 is a high temperature polyimide developed in the mid-1970's at the NASA Lewis Research Center. PMR-15 offers the combination of ease of processing, low cost, and good stability and performance at high temperatures [25]. The individual material properties for the fiber and matrix are given in Table 5-1.

Table 5-1: Fiber and Matrix Material Properties [11].

AS graphite fiber		
Longitudinal Young's modulus	E_{1f} (GPa)	213.7
Transverse Young's modulus	E_{2f} (GPa)	13.7
Axial shear modulus	G_{12f} (GPa)	13.7
Transverse shear modulus	G_{23f} (GPa)	6.8
Poisson's ratio	ν_{12f}	0.3
Tensile Strength	σ_{Tf} (MPa)	3033.8
PMR-15 matrix		
Young's modulus	E_m (GPa)	3.2
Shear modulus	G_m (GPa)	1.1
Poisson's ratio	ν_m	0.36
Tensile Strength	σ_{Tm} (MPa)	55.8

Some other properties of a common AS graphite/PMR-15 lamina are required for the analysis, such as the fiber diameter [26], fiber volume ratio and matrix volume ratio, Table 5-2.

Table 5-2: AS graphite/PMR-15 tow and lamina properties.

Graphite fiber diameter	d_f (μm)	7
Tow fiber volume ratio	$V_{f,t}$	0.8
Lamina fiber volume ratio	V_f	0.5
Number of fibers per tow		3000
Tow flatness ratio (b/a)	fr	0.1

The dimensions used for the model of the repeating unit of fibers inside a tow are displayed in Table 5-3.

Table 5-3: Dimensions of repeating unit of fibers inside a tow.

Height	c (μm)	7.45
Width	w_u (μm)	12.91
Length	L_u (μm)	7.45

The dimensions used in the model of the repeating unit of tows in a lamina with square tow packing are presented in Table 5-4.

Table 5-4: Dimensions of the square packed repeating unit of tows in a lamina.

Major radius of tow	a (μm)	678
Minor radius of tow	b (μm)	68
Gap	g (μm)	31
Width	w (μm)	1387
Height	h (μm)	167
Length	L (μm)	100

The dimensions used in the model of the repeating unit of tows in a lamina with hexagon tow packing are presented in Table 5-5.

Table 5-5: Dimensions of the hexagon packed repeating unit of tows in a lamina.

Major radius of tow	a (μm)	678
Minor radius of tow	b (μm)	68
Gap	g (μm)	168
Width	w (μm)	1523
Height	h (μm)	303
Length	L (μm)	100

For the square packed repeating unit of tows in a lamina with a center void, the void diameter is 60 micron. The gap void repeating unit has the following gap sizes, a 40 micron diameter for the two vertical voids and a 15 micron diameter for the two horizontal voids.

For the hexagon packed repeating unit of tows in a lamina with gap voids, all four voids have a 40 micron diameter.

The overall AS graphite/PMR-15 lamina properties can be predicted using the rule of mixtures [6]. The longitudinal Young's modulus, E_1, and the transverse Young's modulus, E_2/E_3, is given by:

$$E_1 = V_f E_{1f} + V_m E_m$$
$$E_2 / E_3 = \frac{E_{2f} E_m}{V_f E_m + V_m E_{2f}} \tag{5.1}$$

In our case in-plane transverse Young's modulus, E2, and out-of-plane transverse Young's modulus, E3, are equal because the cross section is a square. The major (longitudinal) Poisson's ratio, ν_{12}, is given by the following relation:

$$\nu_{12} = V_f \nu_{12f} + V_m \nu_m \tag{5.2}$$

The in-plane (longitudinal) shear modulus, G_{12}, is given by the following relationship:

$$G_{12} = \frac{G_{12f} G_m}{V_f G_m + V_m G_{12f}} \tag{5.3}$$

The rule of mixtures prediction of mechanical properties are displayed and compared to the finite element calculated properties in section 5.2.

5.2 Comparison of Mechanical Properties

The mechanical properties of the repeating unit of fibers inside a tow and the repeating unit of tow inside the lamina were calculated using the method discussed in Chapter 3 and are compared to the mechanical properties calculated by the rule of mixtures. These properties are utilized in the subsequent Progressive Failure Analysis.

5.2.1 Repeating Unit of Fibers inside a Tow

Table 5-6 displays the comparison of the Finite element model mechanical properties with the rule of mixtures properties with a fiber volume ratio in the tow of 80%. There is good agreement between the axial Young's Moduli and the Poisson's ratios in the xy and xz planes. The differences between the transverse mechanical properties is most likely due to the fact that, the rule of mixtures assume a plane of isotropy at the cross section, when in reality the transverse Young's moduli should have different values as seen in the Finite element results.

Table 5-6: Comparison of mechanical properties of the repeating unit of fibers inside a tow using rule of mixtures and Finite Element Analysis, $V_{f,t} = 80\%$.

Property	Rule of Mixtures	FEA
E_x (GPa)	171.60	168.47
E_y (GPa)	8.27	9.68
E_z (GPa)	8.27	9.58
ν_{xy}	0.312	0.311
ν_{xz}	0.312	0.311
ν_{yx}	0.015	0.018
ν_{yz}	N/A	0.373
ν_{zx}	0.015	0.018
ν_{zy}	N/A	0.372

5.2.2 Repeating Unit of Fibers/Tows inside a Lamina

The results displayed in Table 5-7 show the comparison of the Finite element model mechanical properties with the rule of mixtures properties of the square packed repeating unit of tows inside a lamina with a fiber volume ratio in the lamina of 50%. Much like the results in the previous section, there is good agreement between the axial Young's Moduli and the Poisson's ratios in the xy and xz planes for the rule of mixtures result and the results of the model with no voids. The assumptions of the rule of mixtures method may be the reason for the differences in values. The mechanical properties of the center void model and gap void model are close agreement to those of the model with no voids. This is presumably due to the very low void content of the two models. Figure 5-1 presents the three square packed repeating unit of tows in a lamina models.

Table 5-7: Comparison of the mechanical properties of the square packed repeating unit of fibers/tows inside a lamina using rule of mixture and finite element analysis, $V_f = 50\%$.

Property	Rule of Mixtures	No Voids	Center Void	Gap Voids
$V_{content}$ (%)	-	-	0.49	0.30
E_x (GPa)	106.49	99.05	99.03	98.83
E_y (GPa)	5.48	6.12	6.08	6.09
E_z (GPa)	5.48	6.66	6.58	6.44
ν_{xy}	0.312	0.333	0.332	0.332
ν_{xz}	0.312	0.323	0.322	0.322
ν_{yx}	0.017	0.021	0.021	0.021
ν_{yz}	N/A	0.404	0.399	0.404
ν_{zx}	0.017	0.022	0.022	0.022
ν_{zy}	N/A	0.430	0.422	0.425

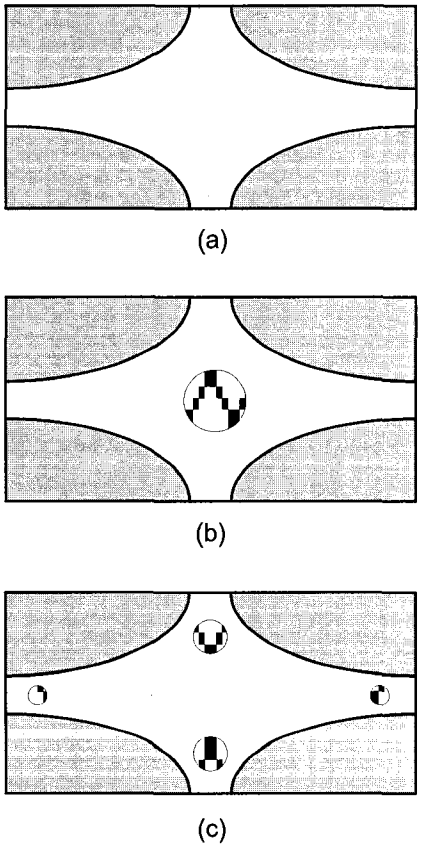

Figure 5-1: Models of the square packed repeating unit of tows in a lamina with (a) no voids, (b) a center void, and (c) gap voids.

The mechanical properties displayed in Table 5-8 are for the hexagon packed repeating unit of tows inside lamina compared to the rule of mixtures results. The values of the mechanical properties of the hexagon model with no voids and the hexagon model with gap voids are extremely close to each other, most likely due to the low void content of the gap voids model. Figure 5-2 presents the two hexagon packed repeating unit of tows in a lamina models.

Table 5-8: Comparison of the mechanical properties of the hexagon packed repeating unit of tows inside a lamina using rule of mixture and finite element analysis, $V_f = 50\%$.

Property	Rule of Mixtures	No Voids	Gap Voids
$V_{content}$ (%)	-	-	0.11
E_x (GPa)	106.49	102.62	102.61
E_y (GPa)	5.48	6.08	6.04
E_z (GPa)	5.48	6.69	6.61
ν_{xy}	0.312	0.334	0.334
ν_{xz}	0.312	0.322	0.322
ν_{yx}	0.017	0.021	0.021
ν_{yz}	N/A	0.404	0.404
ν_{zx}	0.017	0.022	0.022
ν_{zy}	N/A	0.439	0.439

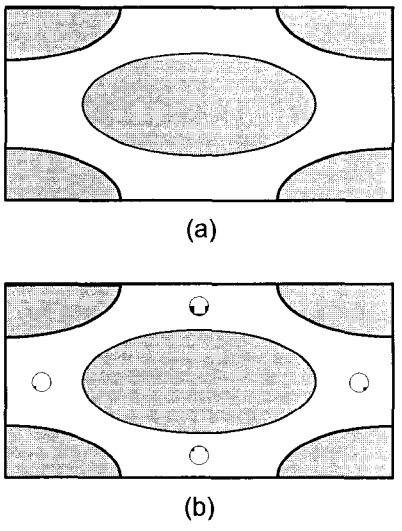

Figure 5-2: Models of the hexagon packed repeating unit of tows in a lamina with (a) no voids and (b) gap voids.

5.2.3 Number of Samples to Be Analyzed

A practical issue that arises in the examination of the difference in mechanical properties is determining the number of samples that should be analyzed. The statistical variation of the mechanical properties due to the presence of voids is the reason for this issue. As the sample size increases, we expect the accuracy of the data to improve. Conversely, increasing the sample size occupies valuable time and resources. The goal is to find a balance between accuracy and computation time [27].

For analysis purposes, it is assumed that the mechanical property values of a fiber-reinforced composite repeating unit are normally distributed about the true value, T_e, for each property. We want to determine the required sample size so that we are 95 percent confident that the true value of each mechanical property lies within ±5 percent of its observed average value.

The sample standard deviation, s, is defined as

$$s = \sqrt{\frac{\sum(x - \bar{x})^2}{n-1}} \tag{5.4}$$

where x is the individual values of the mechanical properties, $\bar{x}$ is the sample mean, and n is the sample size. Since, the initial sample size is less than approximately 30 samples, the sample values are distributed according to the student t rather than the normal distribution [27]. The confidence interval statement for the student t is:

$$\Pr\left(T_e \_ lies \_ within \_ \bar{x} \pm t_{a/2}\frac{s}{\sqrt{n}}\right) = (1-\alpha) \tag{5.5}$$

The objective is to find the value of sample size n that will satisfy the specification of α and interval size for the values of the sample mean, $\bar{x}$, and standard deviation, s, that have been determined from the data collected from ANSYS.

The required sample size to meet the specified confidence interval and interval size can be calculated using

$$n = \left(\frac{t_{a/2}s}{k\bar{x}}\right)^2 \tag{5.6}$$

where k is a proportion that specifies the interval size and $t_{\alpha/2}$ can be found from the student t distribution chart in Appendix B.

The largest number of measurements made for one of the configurations, square packing, was four and the values lacked a large amount of spread. The confidence interval selected for the analysis is 95% and the desired interval size is 5%. The defined values required for the student t-distribution test are in Table 5-9.

Table 5-9: The values required for the student t-distribution test.

Confidence Interval =	0.95
alpha =	0.05
alpha/2 =	0.025
dof =	3
k =	0.05

The values in Table 5-9 were used to determine the $t_{a/2}$ value from the table in Appendix B, $t_{a/2} = 3.182$. The statistical results of the mechanical properties of the square packed repeating unit of tows inside a lamina are in Table 5-10.

Table 5-10: Statistical analysis of the mechanical properties of the square packed repeating unit of tows inside a lamina.

Property	Mean	Std. Dev.	$t_{a/2}$	n
E_x (GPa)	98.99	0.11	3.182	0
E_y (GPa)	6.10	0.02	3.182	0
E_z (GPa)	6.58	0.10	3.182	1
ν_{xy}	0.33	0.00	3.182	0
ν_{xz}	0.32	0.00	3.182	0
ν_{yx}	0.02	0.00	3.182	0
ν_{yz}	0.40	0.00	3.182	0
ν_{zx}	0.02	0.00	3.182	0
ν_{zy}	0.43	0.00	3.182	0

It can be seen from the n results in Table 5-10 that no additional measurements are need to achieve the desired confidence interval and interval size. This test would be better if more varied results were available, such as geometries with a higher variability of void content. The raw mechanical property data can be seen in Appendix C.

5.3 Progressive Failure Analysis Results

The progressive failure model was applied to five different lamina geometries in the z-direction to determine the effect of tow packing configuration, void size and void location. The five different model various are: the square packing model without voids, sqare model with one large center void, a square model with one void at each of the gaps between the tows, the hexagon packing model with no voids, and the hexagon model with voids at each of the gaps, Figure 5-1 and Figure 5-2.

The constraints and loading, Appendix C, are applied to the appropriate faces as discussed in section 4.3, the z face reaction forces are output into a text file by ANSYS. The tensile stress in the lamina cross section is calculated, by dividing the reaction force by the cross section area. As a method of validation the measured tensile stress is compared to the initial stiffness of the geometry at each iteration prior to the first element failure. The initial stiffness is calculated using:

$$\sigma_{initial\_stiffness} = E_z \varepsilon_{test} \tag{5.7}$$

where E_z is the transverse (z-axis) Young's Modulus and ε_{test} is the applied strain.

5.3.1 Square Tow Packing Configuration

The results of the progressive failure analysis for the square tow packing configuration are plotted below in Figure 5-3. All three cases closely follow the initial stiffness stress, the full results can be seen in Appendix C.

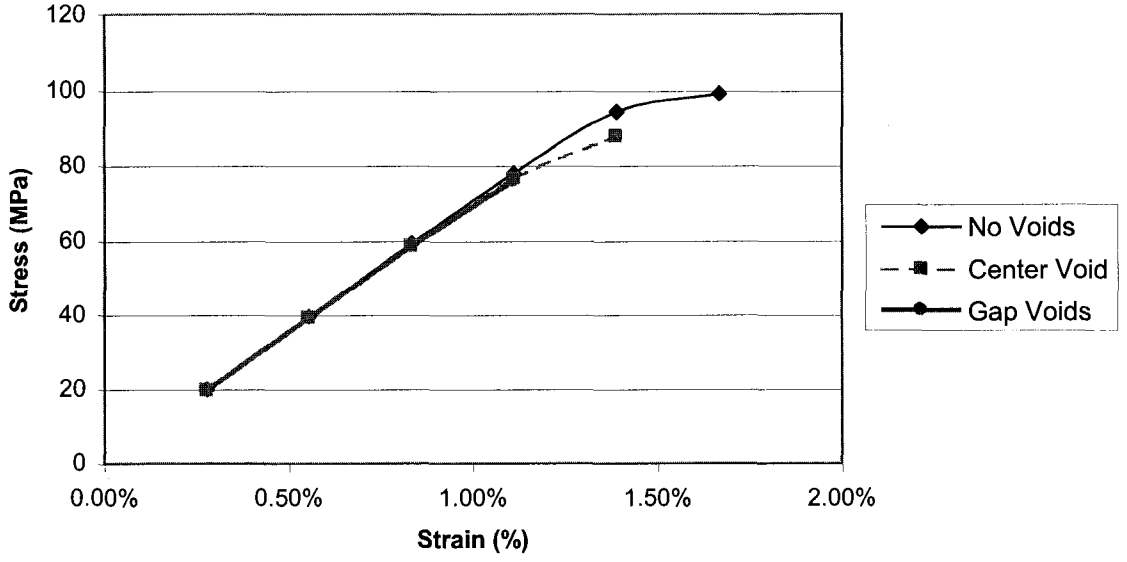

Figure 5-3: Comparison of the Progressive Failure of Three Square Packing Configurations with Different Void Content.

It can be seen from the graph that when the geometry nears failure the stress-strain curve begins to flatten out. As the elements in the finite element model begin to fail it takes less of a force to continue the deformations. The void-free model fails at a load of approximately 99 MPa after six iterations, while the center void model fails at a load of 88 MPa after five iterations. Lastly, the gap void model fails at a load of 76 MPa after only four iterations. The failure results are displayed in Table 5-11. These results so that

voids closer to the gaps, even though smaller in size, decrease the strength of the lamina more than a larger void in the center of the cross section.

Table 5-11: The failure results for the square packed repeating unit of tow in a lamina.

	Square – No Voids	Square – Center Voids	Square – Gap Voids
Strain at Failure	1.7 %	1.4 %	1.1 %
Stress at Failure	99 MPa	88 MPa	76 MPa

The screenshots from ANSYS in Figure 5-4 show an example of failure progression for the square packed repeating unit of tows inside the lamina with a center void. The pictures display the tows in gray, however the mesh is not shown, the void can be seen in the center of the matrix and the failed elements are represented in red. As a side note, the front plane of the geometry is transparent allowing the ability to see the interior void. That is the reason why the tow meshes do not match. All three of the repeating unit geometries follow the same path to failure. The crack, failed elements, begins at the top and bottom gaps and progresses until they meet in the center of the geometry, at this point the lamina has completely failed. These results are a little different from what was expected. From the previous research, one would expect that the failed elements would begin around the void. However, the gaps are very small compared to the rest of the geometry and a large change in area occurs at each gap, resulting in a stress concentration.

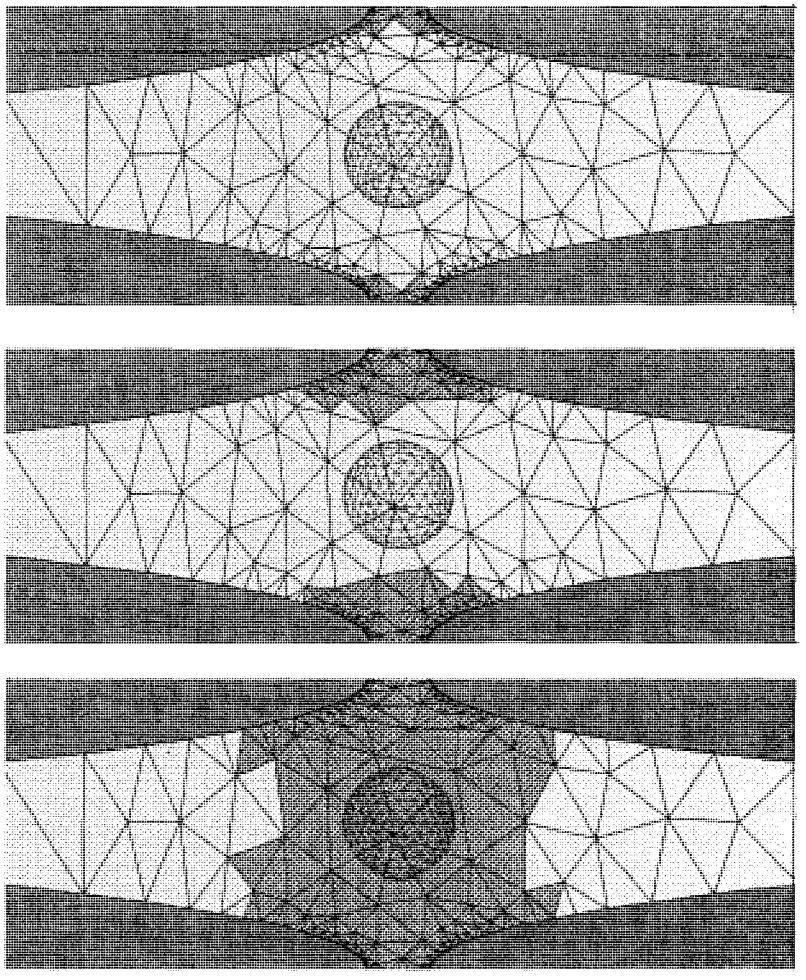

Figure 5-4: Screenshots from ANSYS of the progressive failure of the square packed repeating unit of tows inside a lamina with a center void. The fibers are in gray and the mesh is not shown.

5.3.2 Hexagon Tow Packing Configuration

The results of the progressive failure analysis for the hexagon tow packing configuration are plotted below in . Both cases closely follow the initial stiffness stress, the full results can be seen in Appendix C.

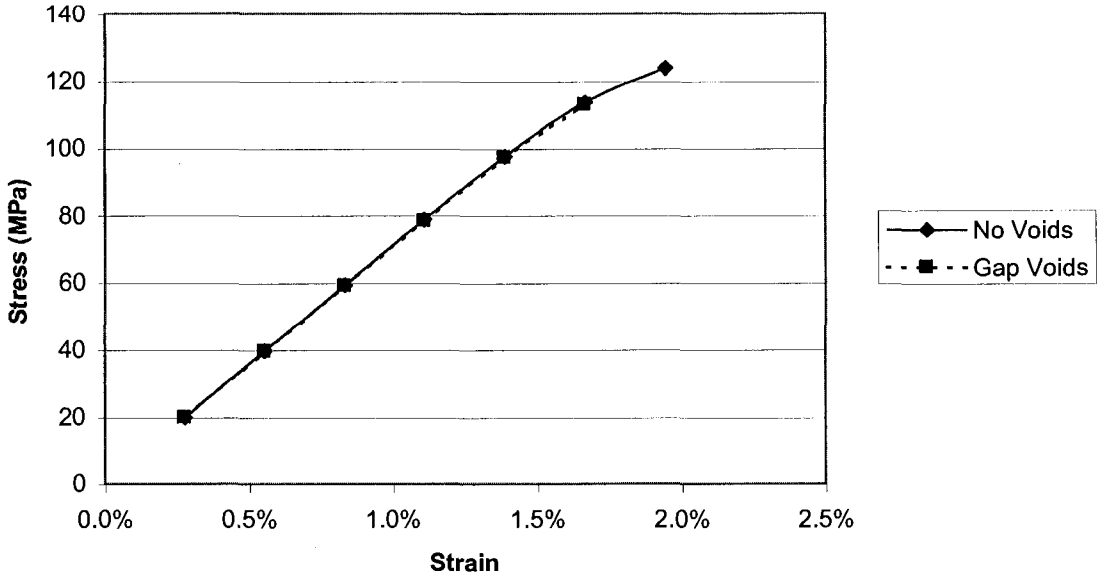

Figure 5-5: Comparison of the Progressive Failure of the Two Hexagon Packing Configurations with Different Void Content.

Both repeating units closely follow the same path, telling us that the gap voids in the lamina geometry do not affect the stiffness of the repeating unit. The void do affect is the strength of the lamina. The repeating unit with gap voids fails at an applied strain of 1.7% and a stress of 113 MPa, while the repeating unit with no voids fails at an applied strain of 1.9% and a stress of 124 MPa. These values can be seen in Table 5-12.

Table 5-12: The failure results for the square packed repeating unit of tow in a lamina.

	Hexagon – No Voids	**Hexagon – Gap Voids**
Strain at Failure	1.9%	1.7%
Stress at Failure	124 MPa	113 MPa

The screenshots from ANSYS in Figure 5-6 show an example of failure progression for the square packed repeating unit of tows inside the lamina with a center void. The pictures display the tows in gray with the elements, the matrix is light blue and the failed elements are represented in red. From Figure 5-6, you can see how the failed elements follow the outside of the center tow until they converge, thus the complete failure of the lamina.

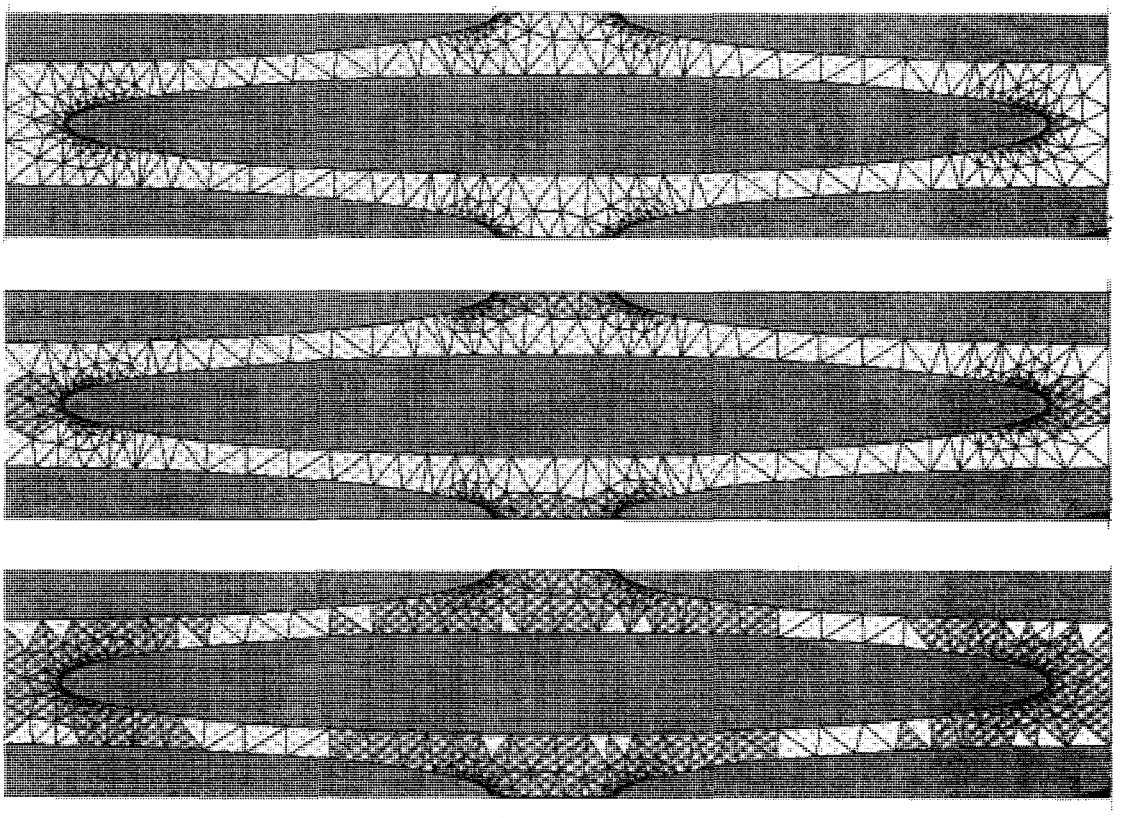

Figure 5-6: Screenshots from ANSYS of the progressive failure of the hexagon packed repeating unit of tows inside a lamina with a no voids. The tows are shown in gray, without mesh.

5.3.3 Comparison of Different Tow Packing Configurations

A method to determine the affect of the tow packing configuration on the strength of a lamina can be seen in a comparison of the square packed repeating unit and the hexagon repeating unit. The two geometries with no voids are compared, as well as the two with gap voids.

Figure 5-7 displays the square packed repeating unit and the hexagon repeating unit with no voids. Initially the stiffnesses of the two are equal but after the strain of 1.1% is applied the square packed repeating unit begins to fail while the hexagon packed repeating unit continues at a fairly linear rate.

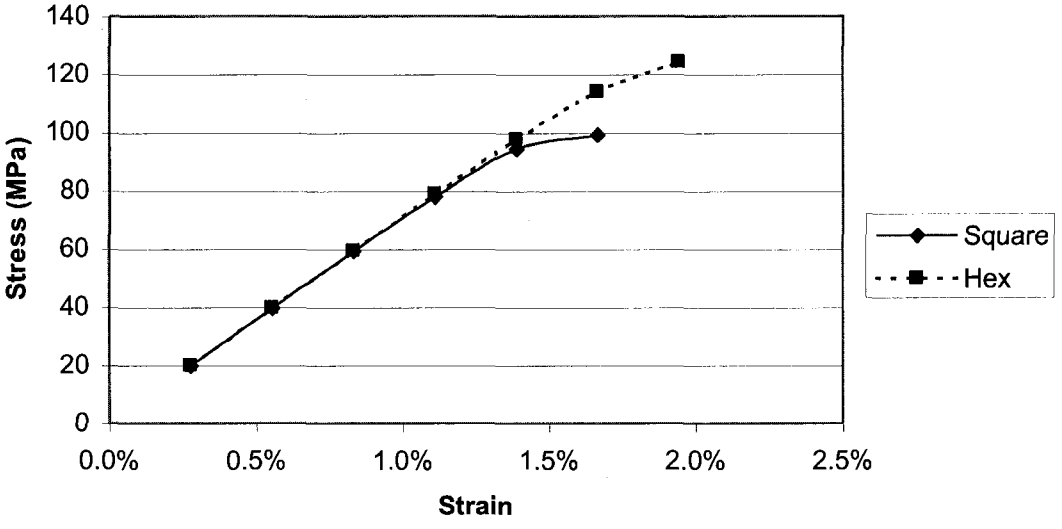

Figure 5-7: Comparison of Square and Hexagon Tow Packing Configurations with No Voids.

The failure strain and stress are displayed in Table 5-13. These results show that the arrangement of tows inside the lamina has a great affect on the transverse strength of the

lamina. The ultimate transverse tensile strength of the hexagon tow configuration is approximately 25 percent greater than the square tow configuration.

Table 5-13: The failure results for the square packed and hexagon packed repeating units of tow in a lamina with no voids.

	Square – No Voids	Hexagon – No Voids
Strain at Failure	1.7%	1.9%
Stress at Failure	99 MPa	124 MPa

Figure 5-8 presents square packed repeating unit and the hexagon repeating unit with gap voids. Initially the stiffness of the two are similar but after the strain of 0.6% is applied the square packed repeating unit begins to fail while the hexagon packed repeating unit continues at a fairly linear rate until it begins to fail at a strain of 0.8%.

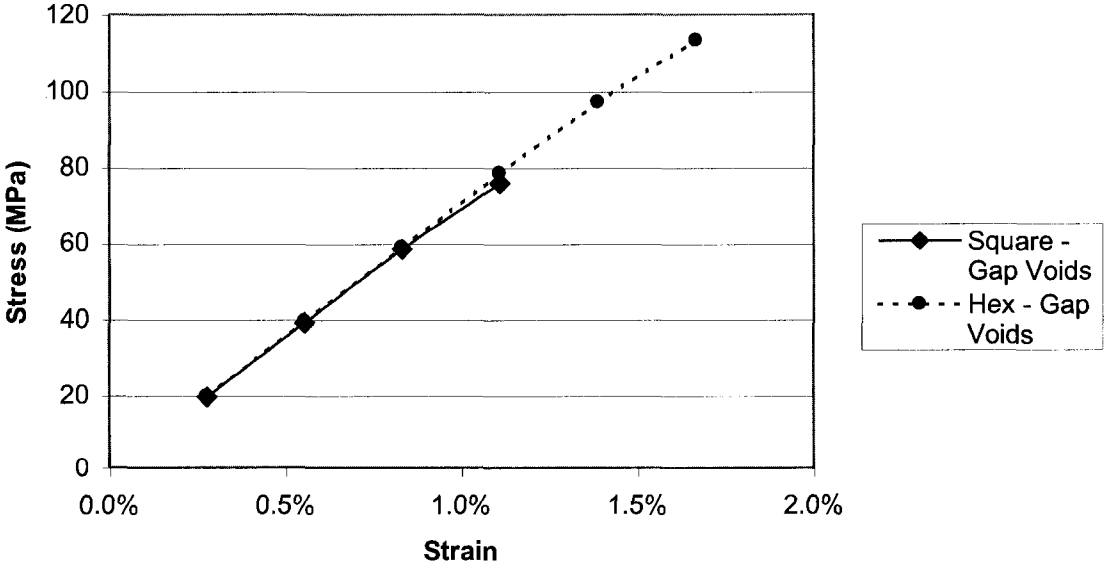

Figure 5-8: Comparison of Square and Hexagon Tow Packing Configurations with Gap Voids.

The failure strain and stress are displayed in Table 5-14. These results confirm the previous results that the arrangement of tows inside the lamina has a great affect on the transverse strength of the lamina. The ultimate transverse tensile strength of the hexagon tow configuration with gap voids is approximately 49 percent greater than the square tow configuration.

Table 5-14: The failure results for the square packed and hexagon packed repeating units of tow in a lamina with gap voids.

	Square – Gap Voids	**Hexagon – Gap Voids**
Strain at Failure	1.1%	1.7%
Stress at Failure	76 MPa	113 MPa

The hexagon packing of tows creates a stronger lamina. Refer to Figures 1 & 2, in order for the crack to propagate through the square packed repeating unit there is no resistance. However, for the hexagon packed repeating unit with a tow in the center, the crack must propagate around the tow before the cross section completely fails.

5.3.4 Comparison of Graphite and Glass Fibers

A comparison is made between graphite and glass fibers to determine if there is a correlation between the transverse stiffness of the fibers and the strength of the lamina. The mechanical properties of the glass fibers are displayed in Table 5-15.

Table 5-15: Glass fiber mechanical properties and strength [28].

Glass Fiber		
Longitudinal Young's modulus	E_{1f} (GPa)	71
Transverse Young's modulus	E_{2f} (GPa)	71
Axial shear modulus	G_{12f} (GPa)	30
Transverse shear modulus	G_{23f} (GPa)	10
Poisson's ratio	ν_{21}	0.22
Tensile Strength	σ_{Tf} (MPa)	3500
Density	δ_f (g/cm^3)	2.45

The repeating unit of tow in a lamina with hexagon tow packing and no voids was used for the analysis. The exact same repeating unit dimensions, fiber diameter, number of fibers in a tow, tow fiber volume fraction (0.8), lamina fiber volume fraction (0.5), and matrix material (PMR-15) were used to calculate the mechanical properties of glass fibers in a lamina. The mechanical properties of glass fibers in a tow and lamina are displayed in Table 5-16.

Table 5-16: Tow and Lamina mechanical properties with glass fibers.

Property	Fibers in a Tow	Tows in a Lamina
$V_{f,t}/V_f$ (%)	0.8	0.5
E_x (GPa)	56.4	35.2
E_y (GPa)	22.3	5.5
E_z (GPa)	22.1	8.0
ν_{xy}	0.24	0.30
ν_{xz}	0.24	0.26
ν_{yx}	0.10	0.08
ν_{yz}	0.34	0.29
ν_{zx}	0.10	0.09
ν_{zy}	0.34	0.41

Comparing the mechanical properties of the lamina with glass fibers and the lamina with graphite fibers, it can be seen that the glass fibers have a higher transverse Young's Modulus (z-axis) and a higher Poisson's ratio (zx plane). The results of the comparison of laminae with glass fibers and graphite fibers can be seen in Figure 5-9.

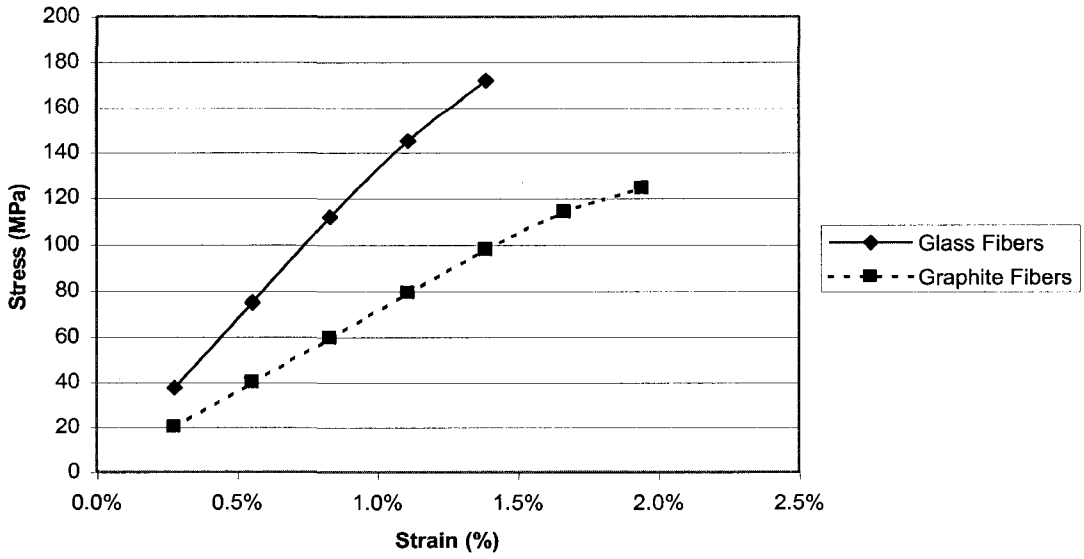

Figure 5-9: Comparison of glass fiber and graphite fiber lamina with hexagon tow packing configurations and no voids.

Both materials clearly have different stiffness, with the glass fibers being higher. The lamina with glass fibers failed at a transverse tensile stress of 172 MPa and a strain of 1.4%. The lamina with graphite fibers failed at a stress of 124 MPa and a strain of 1.9%, these results are displayed in Table 5-17. The higher stiffness of the lamina with glass fibers allowed the lamina to take on a higher load but a lower elongation was allowed. The lamina with graphite fibers may have failed at a lower strength however, the lamina was able to deform more before failure. These results show that the transverse stiffness

of the fiber tows in the lamina affect the transverse strength of the lamina. A small increase in the stiffness value can significantly increase the transverse lamina strength.

Table 5-17: The failure results for the hexagon packed repeating units of tow in a lamina with glass fibers and graphite fibers with no voids.

	Hexagon – Glass Fibers	**Hexagon – Graphite Fibers**
Strain at Failure	1.4%	1.9%
Stress at Failure	172 MPa	124 MPa

6 CONCLUSIONS & FUTURE WORK

6.1 Conclusions

Void formation in composites is an unfortunate side effect of some manufacturing processes. There have been many previous investigations into the effect that voids have on the mechanical properties and strength of composites. Most of these investigations were of the physical testing variety. There have also been some studies on the progressive failure of composites, though they were of laminates and the progressive failure was of each ply. The progressive failure model looked at the laminate macroscopically and did not take void effects or fiber orientation into account.

This project investigated the mechanical properties and strength of fiber tows in a polymer matrix lamina. Two different tow packing configurations were studied. Finite element analysis was utilized to calculate the mechanical properties of the lamina repeating units and used as inputs into the progressive failure model. The progressive failure model applied incremental displacements transverse to the fiber direction and monitored element failure until the lamina was completely failed.

The location of the voids and the tow packing configuration inside a tow has a significant effect on the failure progression of a lamina. It can be concluded from the results in chapter 5 that void content and distribution has a major negative effect on the transverse axial strength of a fiber-reinforced composite. Fewer loading cycles and a lower applied force is required to cause a lamina with voids to fail. In addition, the hexagon packing of tows within a lamina without voids has an ultimate transverse tensile strength approximately 25 percent greater than the square packed tows within a lamina.

Moreover, the hexagon packing of tows within a lamina with gap voids has an ultimate transverse tensile strength approximately 49 percent greater than the square packed tows within a lamina with gap voids.

Another observation was made regarding the effects of tow transverse stiffness on the strength of the lamina. A lamina with glass tows with a higher transverse stiffness can positively affect the strength of the lamina. However, the failure strain of this material was much lower than the failure strain of the lamina with graphite tows.

6.2 Future Work

The most logical next step to this project would be physical testing. A polymer fiber/tow reinforced composite lamina should be obtained and all the important dimensions measured: fiber diameter, fiber volume ratio in tow, number of fibers in the tow, tow major and minor radius, tow flatness ratio, overall fiber ratio in the lamina, the tow configuration in the lamina, and the void content. All these values could be used in the APDL programs developed during this project. The actual and finite element lamina should tested using the same method (i.e. loading rate and orientation) and the results should be compared to check the validity of the finite element progressive failure model.

There are some modifications that could be made that do not involve physical testing. Develop a method to recalculate the Young's Modulus and Poisson's ratios of the model after each iteration in the progressive failure model. When the elements begin to fail, the mechanical properties of the lamina begin to change. The stiffness of the material decreases; consequently, it requires a lower force to create the same displacement.

There are also changes that could be made to how the geometry is created. Make modifications to the repeating unit of tows within a lamina to account for different gap sizes. This could possibly change the origin of crack initiation. Investigate the effect of higher void contents. Model voids in the tows as well as around the tows. The interphase between the fibers/tows and the matrix could be model. The interphase is an important area of a composite, where void formation often occurs and other defects.

The variations that could be implemented into this analysis are virtually endless. However, the best option for the continuation of this work to compare the finite element results to experimental results.

7 REFERENCES

1. Mallick, P.K., "Composites Engineering Handbook", Marcel Dekker Inc., 1997
2. Schwartz, Mel M. Composite Materials, Volume I: Properties, Non-Destructive Testing, and Repair. Upper Saddle River, N.J.: Prentice Hall PTR, 1996.
3. Colling, David A. and Thomas Vasilos. Industrial Materials: Polymers, Ceramics, and Composites. Volume 2. Englewood Cliffs, New Jersey: Prentice-Hall, 1995.
4. Schwartz, Mel M. Composite Materials, Volume I: Properties, Non-Destructive Testing, and Repair. Upper Saddle River, N.J. : Prentice Hall PTR, 1996.
5. ASM International. ASM Handbook: Composites. Volume 21. Materials Park, Ohio: ASM International, 2001.
6. Daniel, Isaac M. and Ori Ishai. Engineering Mechanics of Composite Materials. New York, New York: Oxford University Press, 1994.
7. Harper, B. D., G. H. Staab, and R. S. Chen. "A Note on the Effects of Voids Upon the Hygral and Mechanical Properties of AS4/3502 Graphite/Epoxy." Journal of Composite Materials 21 (1987): 280-289.
8. Guo, Zhan-Sheng, et al. (2006). "Critical Void Content for Thermoset Composite Laminates," Journal of Composite Materials, Vol. 00, No. 00, pp 1-16.
9. Farahmand, Bahram. Boeing Technical Fellow. Fracture Mechanics of Metals, Composites, Welds, and Bolted Joints. New York: Springer, 2000.
10. Demma, A. and Djordjevic, B.B. "Effects of porosity on the Mechanical Strength and Ultrasonic Attenuation of CF-Peek fibre Placed Composites." 15th World Conference on Nondestructive Testing, October 2000. 18 February 2008. <http://www.ndt.net/article/wcndt00/papers/idn018/idn018.htm>.
11. Bowles, Kenneth J. and Stephen Frimpong. (1992). "Void Effects on the Interlaminar Shear Strength of Unidirectional Graphite-Fiber-Reinforced Composites," Journal of Composite Materials, Vol. 26, No. 10, pp 1487-1509.
12. Wu, Yinan, Rajiv Shivpuri, and L. James Lee. "Effect of Macro and Micro Voids on Elastic Properties of Polymer Composites." Journal of Reinforced Plastics and Composites 17 (1998): 1391-1402.
13. Black, Sara. "Tooling roundup: New materials, new methods". September 2004. High Performance Composites. 31 January 2008. <http://www.compositesworld.com/hpc/issues/2004/September/559>.
14. Mason, Karen Fisher. "Carbon/glass hybrids used in composite wind turbine rotor blade design". April 2004. Composites Technology. 31 January 2008. <http://www.compositesworld.com/ct/issues/2004/April/431/2>.
15. Konev, S. F., A. S. Konev, and D. R. Baitimirov. "Method of Measuring the Modulus of Elasticity of Carbon Tow." Fibre Chemistry 39 (2007): 76-78.
16. Binetruy, C., B. Hilaire, and J. Pabiot. "Tow Impregnation Model and Void Formation Mechanisms During RTM." Journal of Composite Materials 32 (1998): 223-245.
17. He, Jianmei, Martin Y.m. Chiang, Donald L. Hunston, and Charles C. Han. "Application of the V-Notch Shear Test for Unidirectional Hybrid Composites." Journal of Composite Materials 36 (2002): 2653-2666.

18. Hamidi, Youssef K., Levent Aktas, and M. Cengiz Altan. "Effect of Packing on Void Morphology in Resin Transfer Molded E-Glass/Epoxy Composites." Polymer Composites 26 (2005): 614-627.
19. Pal, P., and S. K. Bhattacharyya. "Progressive Failure Analysis of Cross-Ply Laminated Composite Plates by Finite Element Method." Journal of Reinforced Plastics and Composites 26 (2007): 465-477.
20. "SOLID187." Release 11.0 Documentation for ANSYS.
21. Pramod Chaphalkar and Ajit D. Kelkar, "Three Dimensional Finite Element Analysis of Twill Woven Composite Laminates", AIAA-2000-1765, SDM 52, April 2000.
22. Chatterjee, S. N., Yen, C.-F., and Oplinger, D. W., "On the Determination of Tensile and Compressive Strengths of Unidirectional Fiber Composites," *Composite Materials: Fatigue and Fracture (Sixth Volume)*, ASTM STP 1285, E.A. Armanios, Ed., American Society for Testing and Materials 1997, pp. 203-224.
23. ASTM Standard D3039/D3039M-07, "Standard Test Method for Tensile Properties of Polymer Matrix Composite Materials," ASTM International, West Conshohocken, PA, <http://www.astm.org>.
24. Paiva, Jane Maria Faulstich de, Mayer, Sérgio and Rezende, Mirabel Cerqueira. "Comparison of tensile strength of different carbon fabric reinforced epoxy composites." *Mat. Res.* [online]. 2006, vol. 9, no. 1, pp. 83-90. 9 Apr. 2008 <http://www.scielo.br/scielo.php?script=sci_arttext&pid=S1516-14392006000100016&lng=en&nrm=iso>.
25. Chuang, Kathy. "DMBZ Polyimides Provide an Alternative to PMR-15 for High-Temperature Applications." Apr. 1996. NASA. 1 Apr. 2008 <http://www.grc.nasa.gov/WWW/RT/RT1995/5000/5150c.htm>.
26. Cavette, Chris. "Carbon Fiber." How Products are Made :: Volume 4. 8 Apr. 2008 <http://www.madehow.com/Volume-4/Carbon-Fiber.html>.
27. Groover, Mikell P. Work Systems and the Methods, Measurement, and Management of Work. Upper Saddle River, New Jersey: Pearson Prentice Hall, 2007.
28. "Mechanical Properties Data." 23 Apr. 2008 <http://www.mse.mtu.edu/~drjohn/my4150/compositesdesign/props.html>.
29. Stat Manual: Page 3. <http://rvgs.k12.va.us/statman/Table-B.jpg>.

APPENDIX A: APDL PROGRAMS

The following chapter contains all of the APDL programs used to create the finite element models, calculate mechanical properties and perform the progressive failure analysis. To use the following APDL programs, simply cut and paste the code into a text (.txt) file and input the file into ANSYS.

Repeating Unit of Fibers within a Tow

```
!Tow_Repeating_Unit.txt
!By: Michael Maletta
!Created on:  01/10/2008

! This program creates the tow repeating unit geometry with a hexagonal packing.
! A void free model is created but with a few modifications voids could be
! introduced to the geometry.

/CLEAR,START
/FILNAM,unit_cell,1
/PREP7
! Values calculated in packing-calculations Excel file
*SET,fiberR,3.5          ! Fiber radius, um
*SET,PI,ACOS(-1)         ! Define the constant Pi, calculated to machine accuracy
*SET,c,7.4530            ! Height of unit cell, um, y-axis
*SET,wu,12.9090              ! Width of unit cell, um, z-axis
*SET,Lu,c                ! Length of test specimen, um
                         ! Tow Fiber volume fraction is 80%

ET,1,SOLID187            ! Define element type

MPTEMP,,,,,,,,
MPTEMP,1,0
UIMP,1,EX,EY,EZ,3.2e-3,3.2e-3,3.2e-3     ! Matrix material properties(N/um^2), PMR-15 polymer
UIMP,1,PRXY,PRYZ,PRXZ,0.36,0.36,0.36
UIMP,1,GXY,GYZ,GXZ,1.1e-3,1.1e-3,1.1e-3          ! N/um^2
UIMP,2,EX,EY,EZ,0.2137,13.7e-3,13.7e-3           ! Fiber material properties(N/um^2), AS graphite
UIMP,2,PRXY,PRYZ,PRXZ,0.3,,
UIMP,2,GXY,GYZ,GXZ,13.7e-3,6.8e-3,13.7e-3        ! N/um^2

! Create geometry
WPROTA,,,-90.000000              ! Rotate WP - x-axis is fiber direction
BLOCK,0,wu,0,c,0,-Lu             ! Create block - matrix (V1)
CYL4,0,0,fiberR,0, ,90,-Lu       ! Create partial cylinder - lower left (V2)
CYL4,wu,0,fiberR,90, ,180,-Lu    ! Create partial cylinder - lower right (V3)
```

```
CYL4,wu,c,fiberR,180, ,270,-Lu          ! Create partial cylinder - upper right (V4)
CYL4,0,c,fiberR,270, ,360,-Lu       ! Create partial cylinder - upper left (V5)
CYL4,0.5*wu,0.5*c,fiberR,0, ,360,-Lu  ! Create full cylinder - center (V6)

VSBV, 1, 2,,,KEEP          ! Subtract V2 from V1 generating a new volume (V7)
VSBV, 7, 3,,,KEEP          ! Subtract V3 from V7 generating a new volume (V1)
VSBV, 1, 4,,,KEEP          ! Subtract V4 from V1 generating a new volume (V7)
VSBV, 7, 5,,,KEEP          ! Subtract V5 from V7 generating a new volume (V1)
VSBV, 1, 6,,,KEEP          ! Subtract V6 from V1 generating a new volume (V7)
VGLUE,ALL                  ! Glue matrix and fibers

WPCSYS,,0             ! Return working plane back to origin

! Change material of fiber volumes
VSEL,S, , ,    2       ! Select fiber 1 (V2)
VSEL,A, , ,    3       ! Select fiber 2 (V3)
VSEL,A, , ,    4           ! Select fiber 3 (V4)
VSEL,A, , ,    5       ! Select fiber 4 (V5)
VSEL,A, , ,    6       ! Select fiber 5 (V6)
VATT,2,,1,0
ALLSEL
!*
/PNUM,KP,0
/PNUM,LINE,0
/PNUM,AREA,0
/PNUM,VOLU,0
/PNUM,NODE,0
/PNUM,TABN,0
/PNUM,SVAL,0
/NUMBER,1
!*
/PNUM,MAT,1
/REPLOT
!*

! Mesh geometry
SMRTSIZE,2                 ! Select size of mesh
!MOPT,TIMP,DEFAULT      ! Allows ANSYS to choose the appropriate mesher to use
MOPT,TIMP,3                ! Level 3 tetrahedra element improvement
MSHKEY,0
MSHAPE,1,3d
VMESH,ALL                  ! Volume mesh
NUMMRG,ALL                 ! Merge all duplicate nodes
```

Lamina Geometry with Random Voids

```
! Lamina_geometry_random.txt
! By: Michael Maletta
! Created on: 4/12/08
!
! This program creates a rectangular lamina repeating unit geometry with four quarter
! elliptical tows at the corners. The model can be created without voids are will
! a random distribution of a random number of voids.

/CLEAR,START
/FILNAM,lamina_testing,1
/PREP7
*SET,major,678          ! Tow major radius (a), um
*SET,minor,68           ! Tow minor radius (b), um
*SET,PI,ACOS(-1)        ! Define the constant Pi, calculated to machine accuracy
*SET,w,1387             ! Width of repeating unit, um - z-axis
*SET,h,167              ! Heigh of repeating unit, um - y-axis
*SET,L,100              ! Length of repeating unit, um
*SET,ratio,minor/major      ! Aspect ratio of tow
*SET,V_total,w*h*L      ! Define total geometry volume, um^2
*SET,maxvoidR,25        ! Define maximum void radius, um

ET,1,SOLID187           ! Define element type

MPTEMP,,,,,,,,
MPTEMP,1,0
UIMP,1,EX,EY,EZ,3.2e-3,3.2e-3,3.2e-3          ! Matrix material properties(N/um^2), PMR-15 polymer
UIMP,1,PRXY,PRYZ,PRXZ,0.36,0.36,0.36
UIMP,1,GXY,GYZ,GXZ,1.1e-3,1.1e-3,1.1e-3      ! N/um^2
UIMP,2,EX,EY,EZ,168.47e-3,9.68e-3,9.58e-3    ! Tow material properties(N/um^2), AS graphite
UIMP,2,PRXY,PRYZ,PRXZ,0.31,0.37,0.31
UIMP,2,GXY,GYZ,GXZ,2.52e-3,2.16e-3,2.52e-3          ! N/um^2

! Create geometry
WPROTA,,,-90.000000         ! Rotate WP - x-axis is fiber direction
BLOCK,0,w,0,h,0,-L          ! Create block - matrix (V1)
CYL4,0,0,major,0, ,90,-L    ! Create partial cylinder - lower left (V2)
VLSCAL,2, , ,1,ratio,1, ,1,1  ! Scale cylinder to create ellipse - scales y
CYL4,w,0,major,90, ,180,-L  ! Create partial cylinder - lower right (V3)
VLSCAL,3, , ,1,ratio,1, ,1,1  ! Scale cylinder to create ellipse - scales y
CYL4,w,h,major,180, ,270,-L ! Create partial cylinder - upper right (V4)
CLOCAL,11,0,w,h,0
VLSCAL,4, , ,1,ratio,1, ,1,1  ! Scale cylinder to create ellipse - scales y
CSYS,0
CYL4,0,h,major,270, ,360,-L ! Create partial cylinder - upper left (V5)
CLOCAL,12,0,0,h,0
VLSCAL,5, , ,1,ratio,1, ,1,1  ! Scale cylinder to create ellipse - scales y
CSYS,0
VSBV, 1, 2,,,KEEP       ! Subtract V2 from V1 generating a new volume (V6)
VSBV, 6, 3,,,KEEP       ! Subtract V3 from V6 generating a new volume (V1)
VSBV, 1, 4,,,KEEP       ! Subtract V4 from V1 generating a new volume (V6)
VSBV, 6, 5,,,KEEP       ! Subtract V5 from V6 generating a new volume (V1)
VGLUE,ALL               ! Glue matrix and fibers
```

```
WPCSYS,,0           ! Return working plane back to origin

! Introduce the first void
*SET,Volume_void,0          ! Define total void volume

*ASK,bypass,"Do you want to create voids? (1=yes, 2=no)",1      ! Void creation bypass
*IF,bypass,EQ,2,:END_2

:START_1                                ! Start of initial loop
 *SET,voidX,RAND(0,L)                   ! Void location along length (x-axis)
 *SET,voidZ,RAND(.49*w,.51*w)           ! Void location along width (z-axis)
 *SET,voidY,RAND(.12*h,.88*h)           ! Void location along height (y-axis)
 *SET,voidR,RAND(0,maxvoidR)            ! Generate void (sphere) radius

 WPOFFS,voidX,voidY,voidZ           ! Move working plane to void location
 SPHERE,voidR                       ! Create void (V6)
 VSBV, 1, 6                         ! Subtract void from matrix generating V7
 *SET,V_void,(4/3)*PI*(voidR)**3    ! Calculate individual void volume
 Volume_void = Volume_void + V_void ! Total void volume
 WPCSYS,,0                          ! Return working plane back to origin

:END_1              ! End of initial loop


! Introduce the remaining voids into the matrix
/OUTPUT,V0ID_OUT,TXT,,APPEND
!*SET,void_num,NINT(RAND(1,30))     ! Generate a random number of voids, force to integer
*SET,void_num,35                    ! Force number of voids to certain value
/OUTPUT
*SET,count,0            ! Define count

:START_2                ! Beginning of second loop
 WPCSYS,,0              ! Return working plane back to origin
 *SET,voidX2,RAND(0,L)          ! Void location along length (x-axis)
 *SET,voidZ2,RAND(.38*w,.62*w)          ! Void location along width (z-axis)
 *SET,voidY2,RAND(.38*h,.62*h)          ! Void location along height (y-axis)
 *SET,voidR2,RAND(0,maxvoidR)       ! Generate void (sphere) radius

 count = count + 1                  ! Increase count with each loop
 WPOFFS,voidX2,voidY2,voidZ2        ! Move working plane to void location
 SPHERE,voidR2              ! Create void
 *SET,ACTION,(-1)**count
 *IF,ACTION,EQ,-1,THEN
  VSBV, 7, 1                        ! Subtract sphere from matrix volume
 *ELSEIF,ACTION,EQ,1,THEN
  VSBV, 6, 1
 *ENDIF

 *SET,V_void2,(4/3)*PI*(voidR2)**3      ! Calculate individual void volume, mm^3
 Volume_void = Volume_void + V_void2    ! Total void volume, mm^3

 *IF,count,LT,void_num,:START_2

WPCSYS,,0           ! Return working plane back to origin
```

```
/OUTPUT,V0ID_OUT,TXT,,APPEND          ! Redirect output to file
*SET,NumberVoid,count                 ! Check number of voids created
Volume_void = Volume_void
*SET,Void_content,(Volume_void/V_total)*100          ! CALCULATE VOID CONTENT
/OUTPUT                               ! Return output to output window

:END_2                  ! End of second loop

! Change material of fiber volumes
VSEL,S, , ,    2        ! Select fiber 1 (V2)
VSEL,A, , ,    3        ! Select fiber 2 (V3)
VSEL,A, , ,    4            ! Select fiber 3 (V4)
VSEL,A, , ,    5        ! Select fiber 4 (V5)
VATT,2,,1,0
ALLSEL,ALL
!*
/PNUM,KP,0
/PNUM,LINE,0
/PNUM,AREA,0
/PNUM,VOLU,0
/PNUM,NODE,0
/PNUM,TABN,0
/PNUM,SVAL,0
/NUMBER,1
!*
/PNUM,MAT,1
/REPLOT
!*

! Mesh geometry
SMRTSIZE,1              ! Select size of mesh
!MOPT,TIMP,DEFAULT      ! Allows ANSYS to choose the appropriate mesher to use
MOPT,TIMP,4             ! Level 4 tetrahedra element improvement
MSHKEY,0
MSHAPE,1,3d
VMESH,ALL               ! Volume mesh
NUMMRG,ALL              ! Merge all duplicate nodes
```

Lamina Geometry with Center Void

```
! Lamina_geometry_center.txt
! By: Michael Maletta
! Created on: 4/12/08
!
! This program creates a rectangular lamina repeating unit geometry with four quarter
! elliptical tows at the corners. One void is created at each of the center of the model.

/CLEAR,START
/FILNAM,lamina_center,1
/PREP7
*SET,major,678          ! Tow major radius (a), um
*SET,minor,68           ! Tow minor radius (b), um
*SET,PI,ACOS(-1)        ! Define the constant Pi, calculated to machine accuracy
*SET,w,1387             ! Width of repeating unit, um - z-axis
*SET,h,167          ! Heigh of repeating unit, um - y-axis
*SET,L,100          ! Length of repeating unit, um
*SET,ratio,minor/major      ! Aspect ratio of tow
*SET,V_total,w*h*L      ! Define total geometry volume, um^2
*SET,maxvoidR,30        ! Define maximum void radius, um

ET,1,SOLID187           ! Define element type

MPTEMP,,,,,,,,
MPTEMP,1,0
UIMP,1,EX,EY,EZ,3.2e-3,3.2e-3,3.2e-3     ! Matrix material properties(N/um^2), PMR-15 polymer
UIMP,1,PRXY,PRYZ,PRXZ,0.36,0.36,0.36
UIMP,1,GXY,GYZ,GXZ,1.1e-3,1.1e-3,1.1e-3    ! N/um^2
UIMP,2,EX,EY,EZ,168.47e-3,9.68e-3,9.58e-3    ! Tow material properties(N/um^2), AS graphite
UIMP,2,PRXY,PRYZ,PRXZ,0.311,0.373,0.311
UIMP,2,GXY,GYZ,GXZ,1.30e-3,3.34e-3,11.30e-3    ! N/um^2

! Create geometry
WPROTA,,,-90.000000         ! Rotate WP - x-axis is fiber direction
BLOCK,0,w,0,h,0,-L          ! Create block - matrix (V1)
CYL4,0,0,major,0, ,90,-L    ! Create partial cylinder - lower left (V2)
VLSCAL,2, , ,1,ratio,1, ,1,1    ! Scale cylinder to create ellipse - scales y
CYL4,w,0,major,90, ,180,-L  ! Create partial cylinder - lower right (V3)
VLSCAL,3, , ,1,ratio,1, ,1,1    ! Scale cylinder to create ellipse - scales y
CYL4,w,h,major,180, ,270,-L ! Create partial cylinder - upper right (V4)
CLOCAL,11,0,w,h,0
VLSCAL,4, , ,1,ratio,1, ,1,1    ! Scale cylinder to create ellipse - scales y
CSYS,0
CYL4,0,h,major,270, ,360,-L ! Create partial cylinder - upper left (V5)
CLOCAL,12,0,0,h,0
VLSCAL,5, , ,1,ratio,1, ,1,1    ! Scale cylinder to create ellipse - scales y
CSYS,0
VSBV, 1, 2,,,KEEP       ! Subtract V2 from V1 generating a new volume (V6)
VSBV, 6, 3,,,KEEP       ! Subtract V3 from V6 generating a new volume (V1)
VSBV, 1, 4,,,KEEP       ! Subtract V4 from V1 generating a new volume (V6)
VSBV, 6, 5,,,KEEP       ! Subtract V5 from V6 generating a new volume (V1)
VGLUE,ALL               ! Glue matrix and fibers
```

```
WPCSYS,,0           ! Return working plane back to origin

! Introduce the first void in center
*SET,Volume_void,0          ! Define total void volume

*SET,voidX,0.5*L            ! Void location along length (x-axis)
*SET,voidZ,0.5*w            ! Void location along width (z-axis)
*SET,voidY,0.5*h            ! Void location along height (y-axis)
*SET,voidR,maxvoidR             ! Generate void (sphere) radius

WPOFFS,voidX,voidY,voidZ        ! Move working plane to void location
SPHERE,voidR                        ! Create void (V6)
VSBV, 1, 6                          ! Subtract void from matrix generating V7
*SET,V_void,(4/3)*PI*(voidR)**3     ! Calculate individual void volume
Volume_void = Volume_void + V_void      ! Total void volume
WPCSYS,,0                           ! Return working plane back to origin


/OUTPUT,V0ID_OUT_center,TXT,,APPEND         ! Redirect output to file
Volume_void = Volume_void
*SET,Void_content,(Volume_void/V_total)*100 ! CALCULATE VOID CONTENT
/OUTPUT                             ! Return output to output window


! Change material of fiber volumes
VSEL,S, , ,     2           ! Select fiber 1 (V2)
VSEL,A, , ,     3           ! Select fiber 2 (V3)
VSEL,A, , ,     4               ! Select fiber 3 (V4)
VSEL,A, , ,     5           ! Select fiber 4 (V5)
VATT,2,,1,0
ALLSEL,ALL
!*
/PNUM,KP,0
/PNUM,LINE,0
/PNUM,AREA,0
/PNUM,VOLU,0
/PNUM,NODE,0
/PNUM,TABN,0
/PNUM,SVAL,0
/NUMBER,1
!*
/PNUM,MAT,1
/REPLOT
!*

! Mesh geometry
SMRTSIZE,1              ! Select size of mesh
!MOPT,TIMP,DEFAULT      ! Allows ANSYS to choose the appropriate mesher to use
MOPT,TIMP,4             ! Level 4 tetrahedra element improvement
MSHKEY,0
MSHAPE,1,3d
VMESH,ALL               ! Volume mesh
NUMMRG,ALL              ! Merge all duplicate nodes
```

Lamina Geometry with Voids at Gaps

```
! Lamina_geometry_edge.txt
! By: Michael Maletta
! Created on: 4/12/08
!
! This program creates a rectangular lamina repeating unit geometry with four quarter
! elliptical tows at the corners. Four voids are created at each of the edge gaps.

/CLEAR,START
/FILNAM,lamina_edge,1
/PREP7
*SET,major,678          ! Tow major radius (a), um
*SET,minor,68           ! Tow minor radius (b), um
*SET,PI,ACOS(-1)        ! Define the constant Pi, calculated to machine accuracy
*SET,w,1387             ! Width of repeating unit, um - z-axis
*SET,h,167          ! Heigh of repeating unit, um - y-axis
*SET,L,100          ! Length of repeating unit, um
*SET,ratio,minor/major      ! Aspect ratio of tow
*SET,V_total,w*h*L      ! Define total geometry volume, um^2
*SET,maxvoidR,20        ! Define maximum void radius, um

ET,1,SOLID187           ! Define element type

MPTEMP,,,,,,,,
MPTEMP,1,0
UIMP,1,EX,EY,EZ,3.2e-3,3.2e-3,3.2e-3     ! Matrix material properties(N/um^2), PMR-15 polymer
UIMP,1,PRXY,PRYZ,PRXZ,0.36,0.36,0.36
UIMP,1,GXY,GYZ,GXZ,1.1e-3,1.1e-3,1.1e-3    ! N/um^2
UIMP,2,EX,EY,EZ,168.47e-3,9.68e-3,9.58e-3    ! Tow material properties(N/um^2), AS graphite
UIMP,2,PRXY,PRYZ,PRXZ,0.311,0.373,0.311
UIMP,2,GXY,GYZ,GXZ,1.30e-3,3.34e-3,11.30e-3        ! N/um^2

! Create geometry
WPROTA,,,-90.000000         ! Rotate WP - x-axis is fiber direction
BLOCK,0,w,0,h,0,-L      ! Create block - matrix (V1)
CYL4,0,0,major,0, ,90,-L  ! Create partial cylinder - lower left (V2)
VLSCAL,2, , ,1,ratio,1, ,1,1    ! Scale cylinder to create ellipse - scales y
CYL4,w,0,major,90, ,180,-L   ! Create partial cylinder - lower right (V3)
VLSCAL,3, , ,1,ratio,1, ,1,1    ! Scale cylinder to create ellipse - scales y
CYL4,w,h,major,180, ,270,-L  ! Create partial cylinder - upper right (V4)
CLOCAL,11,0,w,h,0
VLSCAL,4, , ,1,ratio,1, ,1,1    ! Scale cylinder to create ellipse - scales y
CSYS,0
CYL4,0,h,major,270, ,360,-L   ! Create partial cylinder - upper left (V5)
CLOCAL,12,0,0,h,0
VLSCAL,5, , ,1,ratio,1, ,1,1    ! Scale cylinder to create ellipse - scales y
CSYS,0
VSBV, 1, 2,,,KEEP       ! Subtract V2 from V1 generating a new volume (V6)
VSBV, 6, 3,,,KEEP       ! Subtract V3 from V6 generating a new volume (V1)
VSBV, 1, 4,,,KEEP       ! Subtract V4 from V1 generating a new volume (V6)
VSBV, 6, 5,,,KEEP       ! Subtract V5 from V6 generating a new volume (V1)
VGLUE,ALL               ! Glue matrix and fibers
```

```
WPCSYS,,0           ! Return working plane back to origin

! Introduce the first void - top
*SET,Volume_void,0      ! Define total void volume

*SET,voidX,0.5*L        ! Void location along length (x-axis), all voids here
*SET,voidZ1,0.5*w       ! Void location along width (z-axis)
*SET,voidY1,0.8*h       ! Void location along height (y-axis)
*SET,voidR1,maxvoidR        ! Generate void (sphere) radius

WPOFFS,voidX,voidY1,voidZ1          ! Move working plane to void location
SPHERE,voidR1               ! Create void (V6)
VSBV, 1, 6              ! Subtract void from matrix generating (V7)
*SET,V_void,(4/3)*PI*(voidR1)**3            ! Calculate individual void volume
Volume_void = Volume_void + V_void! Total void volume
WPCSYS,,0               ! Return working plane back to origin

! Introduce second void - bottom
*SET,voidZ2,0.5*w           ! Void location along width (z-axis)
*SET,voidY2,0.20*h          ! Void location along height (y-axis)
*SET,voidR2,maxvoidR            ! Generate void (sphere) radius

WPOFFS,voidX,voidY2,voidZ2          ! Move working plane to void location
SPHERE,voidR2               ! Create void (V1)
VSBV, 7, 1              ! Subtract sphere from matrix generating (V6)
*SET,V_void2,(4/3)*PI*(voidR2)**3   ! Calculate individual void volume, mm^3
Volume_void = Volume_void + V_void2     ! Total void volume, mm^3
WPCSYS,,0               ! Return working plane back to origin

! Introduce third void - right
*SET,voidZ3,0.05*w          ! Void location along width (z-axis)
*SET,voidY3,0.5*h           ! Void location along height (y-axis)
*SET,voidR3,7.5             ! Generate void (sphere) radius

WPOFFS,voidX,voidY3,voidZ3          ! Move working plane to void location
SPHERE,voidR3               ! Create void (V1)
VSBV, 6, 1              ! Subtract sphere from matrix generating (V7)
*SET,V_void3,(4/3)*PI*(voidR3)**3   ! Calculate individual void volume, mm^3
Volume_void = Volume_void + V_void3     ! Total void volume, mm^3
WPCSYS,,0               ! Return working plane back to origin

! Introduce forth void - left
*SET,voidZ4,0.95*w          ! Void location along width (z-axis)
*SET,voidY4,0.5*h           ! Void location along height (y-axis)
*SET,voidR4,7.5             ! Generate void (sphere) radius

WPOFFS,voidX,voidY4,voidZ4          ! Move working plane to void location
SPHERE,voidR4               ! Create void (V1)
VSBV, 7, 1              ! Subtract sphere from matrix generating (V6)
*SET,V_void4,(4/3)*PI*(voidR4)**3   ! Calculate individual void volume, mm^3
Volume_void = Volume_void + V_void4     ! Total void volume, mm^3
WPCSYS,,0               ! Return working plane back to origin


/OUTPUT,V0ID_OUT_edge,TXT,,APPEND               ! Redirect output to file
Volume_void = Volume_void
```

```
*SET,Void_content,(Volume_void/V_total)*100 ! CALCULATE VOID CONTENT
/OUTPUT                          ! Return output to output window


! Change material of fiber volumes
VSEL,S, , ,     2          ! Select fiber 1 (V2)
VSEL,A, , ,     3          ! Select fiber 2 (V3)
VSEL,A, , ,     4              ! Select fiber 3 (V4)
VSEL,A, , ,     5          ! Select fiber 4 (V5)
VATT,2,,1,0
ALLSEL,ALL
!*
/PNUM,KP,0
/PNUM,LINE,0
/PNUM,AREA,0
/PNUM,VOLU,0
/PNUM,NODE,0
/PNUM,TABN,0
/PNUM,SVAL,0
/NUMBER,1
!*
/PNUM,MAT,1
/REPLOT
!*

! Mesh geometry
SMRTSIZE,1              ! Select size of mesh
!MOPT,TIMP,DEFAULT      ! Allows ANSYS to choose the appropriate mesher to use
MOPT,TIMP,4             ! Level 4 tetrahedra element improvement
MSHKEY,0
MSHAPE,1,3d
VMESH,ALL               ! Volume mesh
NUMMRG,ALL              ! Merge all duplicate nodes
```

Lamina Geometry with Hexagon Packing

```
! Lamina_geometry_hexagon.txt
! By: Michael Maletta
! Created on: 4/12/08
!
! This program creates a rectangular lamina repeating unit geometry with four quarter
! elliptical tows at the corners and one full elliptical tow at the center. The packing
! of the repeating unit is hexagonal. Four voids are created at each of the edge gaps.

/CLEAR,START
/FILNAM,lamina_hex,1
/PREP7
*SET,major,678          ! Tow major radius (a), um
*SET,minor,68           ! Tow minor radius (b), um
*SET,PI,ACOS(-1)        ! Define the constant Pi, calculated to machine accuracy
*SET,w,1523             ! Width of repeating unit, um - z-axis
*SET,h,303          ! Heigh of repeating unit, um - y-axis
*SET,L,100          ! Length of repeating unit, um
*SET,ratio,minor/major      ! Aspect ratio of tow
*SET,V_total,w*h*L      ! Define total geometry volume, um^2
*SET,maxvoidR,20        ! Define maximum void radius, um

ET,1,SOLID187           ! Define element type

MPTEMP,,,,,,,,
MPTEMP,1,0
UIMP,1,EX,EY,EZ,3.2e-3,3.2e-3,3.2e-3    ! Matrix material properties(N/um^2), PMR-15 polymer
UIMP,1,PRXY,PRYZ,PRXZ,0.36,0.36,0.36
UIMP,1,GXY,GYZ,GXZ,1.1e-3,1.1e-3,1.1e-3   ! N/um^2
UIMP,2,EX,EY,EZ,168.47e-3,9.68e-3,9.58e-3   ! Tow material properties(N/um^2), AS graphite
UIMP,2,PRXY,PRYZ,PRXZ,0.311,0.373,0.311
UIMP,2,GXY,GYZ,GXZ,1.30e-3,3.34e-3,11.30e-3       ! N/um^2

! Create geometry
WPROTA,,,-90.000000         ! Rotate WP - x-axis is fiber direction
BLOCK,0,w,0,h,0,-L      ! Create block - matrix (V1)
CYL4,0,0,major,0, ,90,-L  ! Create partial cylinder - lower left (V2)
VLSCAL,2, , ,1,ratio,1, ,1,1    ! Scale cylinder to create ellipse - scales y
CYL4,w,0,major,90, ,180,-L   ! Create partial cylinder - lower right (V3)
VLSCAL,3, , ,1,ratio,1, ,1,1    ! Scale cylinder to create ellipse - scales y
CYL4,w,h,major,180, ,270,-L  ! Create partial cylinder - upper right (V4)
CLOCAL,11,0,0,h,w
VLSCAL,4, , ,1,ratio,1, ,1,1    ! Scale cylinder to create ellipse - scales y
CSYS,0
CYL4,0,h,major,270, ,360,-L   ! Create partial cylinder - upper left (V5)
CLOCAL,12,0,0,h,0
VLSCAL,5, , ,1,ratio,1, ,1,1    ! Scale cylinder to create ellipse - scales y
CSYS,0
CYL4,0.5*w,0.5*h,major,0,,360,-L ! Create full cylinder - center (V6)
CLOCAL,13,0,0,0.5*h,0.5*w
VLSCAL,6, , ,1,ratio,1, ,1,1    ! Scale cylinder to create ellipse - scales y
CSYS,0
WPCSYS,,0           ! Return working plane back to origin
```

```
VSBV, 1, 2,,,KEEP       ! Subtract V2 from V1 generating a new volume (V7)
VSBV, 7, 3,,,KEEP       ! Subtract V3 from V7 generating a new volume (V1)
VSBV, 1, 4,,,KEEP       ! Subtract V4 from V1 generating a new volume (V7)
VSBV, 7, 5,,,KEEP       ! Subtract V5 from V7 generating a new volume (V1)
VSBV, 1, 6,,,KEEP       ! Subtract V6 from V1 generating a new volume (V7)
VGLUE,ALL               ! Glue matrix and tow


*ASK,bypass,"Do you want to create voids? (1=yes, 2=no)",1 ! Void creation bypass
*IF,bypass,EQ,2,:END_2

! Introduce the first void - top
*SET,Volume_void,0      ! Define total void volume

*SET,voidX,0.5*L        ! Void location along length (x-axis), all voids here
*SET,voidZ1,0.5*w       ! Void location along width (z-axis)
*SET,voidY1,0.85*h      ! Void location along height (y-axis)
*SET,voidR1,maxvoidR        ! Generate void (sphere) radius

WPOFFS,voidX,voidY1,voidZ1          ! Move working plane to void location
SPHERE,voidR1               ! Create void (V1)
VSBV, 7, 1              ! Subtract void from matrix generating (V7)
*SET,V_void,(4/3)*PI*(voidR1)**3            ! Calculate individual void volume
Volume_void = Volume_void + V_void! Total void volume
WPCSYS,,0               ! Return working plane back to origin

! Introduce second void - bottom
*SET,voidZ2,0.5*w           ! Void location along width (z-axis)
*SET,voidY2,0.15*h          ! Void location along height (y-axis)
*SET,voidR2,maxvoidR            ! Generate void (sphere) radius

WPOFFS,voidX,voidY2,voidZ2          ! Move working plane to void location
SPHERE,voidR2               ! Create void (V1)
VSBV, 8, 1              ! Subtract sphere from matrix generating (V6)
*SET,V_void2,(4/3)*PI*(voidR2)**3   ! Calculate individual void volume, mm^3
Volume_void = Volume_void + V_void2     ! Total void volume, mm^3
WPCSYS,,0               ! Return working plane back to origin

! Introduce third void - right
*SET,voidZ3,0.025*w             ! Void location along width (z-axis)
*SET,voidY3,0.5*h           ! Void location along height (y-axis)
*SET,voidR3,10              ! Generate void (sphere) radius

WPOFFS,voidX,voidY3,voidZ3          ! Move working plane to void location
SPHERE,voidR3               ! Create void (V1)
VSBV, 7, 1              ! Subtract sphere from matrix generating (V7)
*SET,V_void3,(4/3)*PI*(voidR3)**3   ! Calculate individual void volume, mm^3
Volume_void = Volume_void + V_void3     ! Total void volume, mm^3
WPCSYS,,0               ! Return working plane back to origin

! Introduce forth void - left
*SET,voidZ4,0.975*w             ! Void location along width (z-axis)
*SET,voidY4,0.5*h           ! Void location along height (y-axis)
*SET,voidR4,10              ! Generate void (sphere) radius
```

```
WPOFFS,voidX,voidY4,voidZ4          ! Move working plane to void location
SPHERE,voidR4                ! Create void (V1)
VSBV, 8, 1                   ! Subtract sphere from matrix generating (V6)
*SET,V_void4,(4/3)*PI*(voidR4)**3   ! Calculate individual void volume, mm^3
Volume_void = Volume_void + V_void4     ! Total void volume, mm^3
WPCSYS,,0                    ! Return working plane back to origin


/OUTPUT,V0ID_OUT_hex,TXT,,APPEND          ! Redirect output to file
Volume_void = Volume_void
*SET,Void_content,(Volume_void/V_total)*100 ! CALCULATE VOID CONTENT
/OUTPUT

:END_2                       ! Return output to output window


! Change material of fiber volumes
VSEL,S, , ,     2            ! Select fiber 1 (V2)
VSEL,A, , ,     3            ! Select fiber 2 (V3)
VSEL,A, , ,     4                ! Select fiber 3 (V4)
VSEL,A, , ,     5            ! Select fiber 4 (V5)
VSEL,A, , ,     6            ! Select fiber 5 (V6)
VATT,2,,1,0
ALLSEL,ALL
!*
/PNUM,KP,0
/PNUM,LINE,0
/PNUM,AREA,0
/PNUM,VOLU,0
/PNUM,NODE,0
/PNUM,TABN,0
/PNUM,SVAL,0
/NUMBER,1
!*
/PNUM,MAT,1
/REPLOT
!*

! Mesh geometry
SMRTSIZE,2                   ! Select size of mesh
!MOPT,TIMP,DEFAULT       ! Allows ANSYS to choose the appropriate mesher to use
MOPT,TIMP,5                  ! Level 5 tetrahedra element improvement
MSHKEY,0
MSHAPE,1,3d
VMESH,ALL                    ! Volume mesh
NUMMRG,ALL                   ! Merge all duplicate nodes
```

Progressive Failure with Loading along Z-axis

```
! Z_PROGRESSIVE_FAILURE.txt
! March 31, 2008
! By: Michael Maletta

! This program performs a progressive failure analysis on the laminal geometry. A
! incremental displacement is applied in the z-direction and the elemental stress
! is calculated and compared to the matrix yield strength.

! NOTE: A FILE NAMED FAILURE_Z.IST MUST BE PRESENT IN THE WORKING DIRECTORY.
! This is were the initial stress values are written.

!*
FINISH
/FILNAM,FAILURE_Z,1        ! Set file name

! ASTM D3039 tensile strength test is run at a speed of 0.5 mm/min (500 um/min)
! The specimen size is 180(gage L) x 25(w) x 2(t) mm

*SET,test_strain,500/180E3          ! Define strain rate (um/step) - defined as the
*SET,rate_z,w*test_strain       ! ASTM D3039 rate x ratio of model and gauge length

*ASK,vzx,"What is the value of vzx?",0.022
*ASK,vzy,"What is the value of vzy?",0.429

/UIS,MSGPOP,3              ! Turn off warning messages
/NERR,20,10000,

/PREP7
UIMP,3,EX,EY,EZ,3.2e-6,3.2e-6,3.2e-6      ! Define material model 3, N/um^2
UIMP,3,PRXY,PRYZ,PRXZ,0.36,0.36,0.36
NSEL,S,LOC,Y,h,10000
CM,y_face,node                  ! Call this group of nodes 'y_face'
ALLSEL,ALL
NSEL,S,LOC,X,L,10000
CM,x_face,node
ALLSEL,ALL
NSEL,S,LOC,Z,w,10000
CM,z_face,node
ALLSEL,ALL
COUNT = 0
COUNT2 = 0

:START_Z
ALLSEL,ALL
NSEL,S,LOC,Y,0                  ! Constrain nodes at y = 0, x=0, z=0
D,ALL,UY,0
NSEL,S,LOC,X,0
D,ALL,UX,0
NSEL,S,LOC,Z,0
D,ALL,UZ,0
ALLSEL,ALL
CMSEL,S,z_face                  ! Add unit displacement at z = w
```

```
D,ALL,UZ,rate_z
ALLSEL,ALL
CMSEL,S,x_face
D,ALL,UX,-vzx*test_strain*L      ! boundary condition for x face
ALLSEL,ALL
CMSEL,S,y_face
D,ALL,UY,-vzy*test_strain*h      ! boundary condition for y face
ALLSEL,ALL
FINISH

/SOLU                ! Enter Solution processor
ANTYPE,0
INISTATE,READ,FAILURE_Z,IST,,0 ! Reads initial stress file
!/STATUS,SOLU
INISTATE,WRITE,1,,,,0       ! Write stress values to file, failure_z.ist
SOLVE                ! Solve
FINISH

ESEL,S,MAT,,1            ! Select matrix elements
/TRLCY,ELEM,0.5,ALL      ! Make elements translucent
ALLSEL,ALL

/POST1
*GET,enumber,ELEM,0,COUNT  ! Get number of elements in matrix
COUNT = COUNT + 1

FILE,FAILURE_Z,RST       ! Declare and write to results file
FINISH

*DO,I,1,enumber          ! Loop through all matrix elements
/POST1
ESEL,S,MAT,,1            ! Enter general postprocessor
ETABLE,maxstress,S,EQV       ! Create maximum Von Mises stress element table
ETABLE,REFL              ! REFRESH ELEMENT TABLE
ESORT,ETAB,maxstress,0       ! Sort element table, descending
*GET,e_stress,SORT,0,MAX  ! Get maximum stress from ESORT
*GET,e_num,SORT,0,IMAX       ! Get element number of max stress element
FINISH

/PREP7
*IF,e_stress,LT,55.80e-6,*EXIT    ! Determine if the element stress is greater than or
*IF,e_stress,GE,55.80e-6,THEN    ! equal to the allowable matrix stress(55.8 MPa), N/um^2
 EMODIF,e_num,MAT,3,             ! Change the material type of a element
!  *ASK,color,"Element failed",1   ! Notification of failed element
 COUNT2 = COUNT2 + 1
*ENDIF
ALLSEL,ALL
FINISH
*ENDDO

/POST1
NSEL,S,LOC,Z,0
/OUTPUT,Z_STRESS_VALUE,TXT,,APPEND
PRRSOL,FZ
STEP = COUNT
Failed = COUNT2
```

```
/OUTPUT
ALLSEL,ALL
FINISH

/PREP7
DDELE,ALL,ALL          ! Remove all constraints from geometry
UPGEOM,1,,,FAILURE_Z,RST    ! Update geometry with displaced node locations
                  ! using results file
ESEL,S,MAT,,1
ESEL,A,MAT,,3
EPLOT

*ASK,stop_it,"Do you want to continue? (1=yes, 2=no)",1
*IF,stop_it,EQ,1,THEN
  *GO,:START_Z
```

Progressive Failure with Loading along Y-axis

```
! Y_PROGRESSIVE_FAILURE.txt
! March 31, 2008
! By: Michael Maletta
!*
! This program performs a progressive failure analysis on the laminal geometry. A
! incremental displacement is applied in the y-direction and the elemental stress
! is calculated and compared to the matrix yield strength.

! NOTE: A FILE NAMED FAILURE_Y.IST MUST BE PRESENT IN THE WORKING DIRECTORY.
! This is were the initial stress values are written.

!*
FINISH
/FILNAM,FAILURE_Y,1        ! Set file name
! ASTM D3039 tensile strength test is run at a speed of 0.5 mm/min (500 um/min)
! The specimen size is 180(gage L) x 25(w) x 2(t) mm

*SET,test_strain,500/180E3          ! Define strain rate (um/step) - defined as the
*SET,rate_y,h*test_strain           ! ASTM D3039 rate x ratio of model and gauge length

*ASK,vyx,"What is the value of vyx?",0.020
*ASK,vyz,"What is the value of vyz?",0.356

/UIS,MSGPOP,3              ! Turn off warning messages
/NERR,20,10000,

/PREP7
UIMP,3,EX,EY,EZ,3.2e-6,3.2e-6,3.2e-6      ! Define material model 3, N/um^2
UIMP,3,PRXY,PRYZ,PRXZ,0.36,0.36,0.36
NSEL,S,LOC,Y,h,10000
CM,y_face,node                  ! Call this group of nodes 'y_face'
ALLSEL,ALL
NSEL,S,LOC,X,L,10000
CM,x_face,node
ALLSEL,ALL
NSEL,S,LOC,Z,w,10000
CM,z_face,node
ALLSEL,ALL
COUNT = 0
COUNT2 = 0

:START_Y
ALLSEL,ALL
NSEL,S,LOC,Y,0                  ! Constrain nodes at y = 0, x=0, z=0
D,ALL,UY,0
NSEL,S,LOC,X,0
D,ALL,UX,0
NSEL,S,LOC,Z,0
D,ALL,UZ,0
ALLSEL,ALL
CMSEL,S,y_face                  ! Add unit displacement at y = h
D,ALL,UY,rate_y
```

```
ALLSEL,ALL
CMSEL,S,x_face
D,ALL,UX,-vyx*test_strain*L      ! boundary condition for x face
ALLSEL,ALL
CMSEL,S,z_face
D,ALL,UZ,-vyz*test_strain*w      ! boundary condition for z face
ALLSEL,ALL
FINISH

/SOLU                ! Enter Solution processor
ANTYPE,0
INISTATE,READ,FAILURE_Y,IST,,0 ! Reads initial stress file
!/STATUS,SOLU
INISTATE,WRITE,1,,,,0        ! Write stress values to file, failure_y.ist
SOLVE                ! Solve
FINISH

ESEL,S,MAT,,1            ! Select matrix elements
/TRLCY,ELEM,0.6,ALL        ! Make elements translucent

/POST1
*GET,enumber,ELEM,0,COUNT   ! Get number of elements in matrix
COUNT = COUNT + 1
ALLSEL,ALL

FILE,FAILURE_Y,RST        ! Declare and write to results file
FINISH

*DO,I,1,enumber            ! Loop through all matrix elements
/POST1
ESEL,S,MAT,,1            ! Enter general postprocessor
ETABLE,maxstress,S,EQV          ! Create maximum Von Mises stress element table
ETABLE,REFL              ! REFRESH ELEMENT TABLE
ESORT,ETAB,maxstress,0          ! Sort element table, descending
*GET,e_stress,SORT,0,MAX  ! Get maximum stress from ESORT
*GET,e_num,SORT,0,IMAX        ! Get element number of max stress element
FINISH

/PREP7
*IF,e_stress,LT,55.80e-6,*EXIT    ! Determine if the element stress is greater than or
*IF,e_stress,GE,55.80e-6,THEN    ! equal to the allowable matrix stress(55.8 MPa), N/um^2
  EMODIF,e_num,MAT,3,            ! Change the material type of a element
!  *ASK,color,"Element failed",1   ! Notification of failed element
  COUNT2 = COUNT2 + 1
*ENDIF
ALLSEL,ALL
FINISH
*ENDDO

/POST1
NSEL,S,LOC,Y,0
/OUTPUT,Y_STRESS_VALUE,TXT,,APPEND
FSUM,,
STEP = COUNT              ! Output iteration number
Failed = COUNT2                ! Output number of failed elements
/OUTPUT
```

```
ALLSEL,ALL
FINISH

/PREP7
DDELE,ALL,ALL          ! Remove all constraints from geometry
UPGEOM,1,,,FAILURE_Y,RST    ! Update geometry with displaced node locations
                    ! using results file
ESEL,S,MAT,,1
ESEL,A,MAT,,3
EPLOT

*ASK,stop_it,"Do you want to continue? (1=yes, 2=no)",1
*IF,stop_it,EQ,1,THEN
  *GO,:START_Y
```

Tow Stiffness Calculations

```
! Tow_Stiffness_Calcs.txt
! By: Michael Maletta
! Created on: 4/1/08

! This program is used to help determine the Young's Modulus and Poisson's ratio
! for the tow repeating unit.  The inputs are the unit displacements for the each
! of the three cases and outputs are the reaction forces at each face.

*SET,unit_dx,Lu/10              ! Define x unit displacement, um
*SET,unit_dy,c/10               ! Define y unit displacement, um
*SET,unit_dz,wu/10              ! Define z unit displacement, um

!*
! CASE I - load on x face
!*
/PREP7
NSEL,S,LOC,Y,0                  ! Constrain nodes in the y-direction
NSEL,A,LOC,Y,c,10000
D,ALL, ,0, , , ,UY
ALLSEL,ALL
NSEL,S,LOC,X,0              ! Constrain nodes at x = 0
D,ALL, ,0, , , ,UX
ALLSEL,ALL
NSEL,S,LOC,X,Lu,10000               ! Add unit displacement at x = L
D,ALL, ,unit_dx, , , ,UX
ALLSEL,ALL
NSEL,S,LOC,Z,0              ! Constrain nodes in z-direction
NSEL,A,LOC,Z,wu,10000
D,ALL, ,0, , , ,UZ
ALLSEL,ALL
/REPLOT,RESIZE
FINISH
!*
/SOLU                   ! Solve
ANTYPE,0
!/STATUS,SOLU
SOLVE
FINISH
!*
/POST1                  ! Begin post-processing
NSEL,S,LOC,Y,0
NSEL,A,LOC,X,0
NSEL,A,LOC,Z,0

/OUTPUT,STIFFNESS_TOW,TXT,,APPEND
FSUM,,
/OUTPUT
FINISH

! Prepare geometry for case II
ALLSEL,ALL
/PREP7
```

```
DDELE,ALL,ALL

! CASE II - load on y face
!*
NSEL,S,LOC,X,0          ! Constrain nodes in the x-direction
NSEL,A,LOC,X,Lu,10000
D,ALL, ,0, , , ,UX
ALLSEL,ALL
NSEL,S,LOC,Z,0          ! Constrain nodes in the z-direction
NSEL,A,LOC,Z,wu,10000
D,ALL, ,0, , , ,UZ
ALLSEL,ALL
NSEL,S,LOC,Y,0              ! Constrain nodes at y = 0
D,ALL, ,0, , , ,UY
ALLSEL,ALL
NSEL,S,LOC,Y,c,10000            ! Add unit displacement at y = d
D,ALL, ,unit_dy, , , ,UY
ALLSEL,ALL
/REPLOT,RESIZE
FINISH
!*
/SOLU               ! Solve
ANTYPE,0
!/STATUS,SOLU
SOLVE
FINISH
!*
/POST1              ! Begin post-processing
NSEL,S,LOC,Y,0
NSEL,A,LOC,X,0
NSEL,A,LOC,Z,0

/OUTPUT,STIFFNESS_TOW,TXT,,APPEND
FSUM,,
/OUTPUT

! Prepare geometry for case III
FINISH
/PREP7
ALLSEL,ALL
DDELE,ALL,ALL

! CASE III - load on z face
!*
NSEL,S,LOC,Y,0              ! Constrain nodes in the y-direction
NSEL,A,LOC,Y,c,10000
D,ALL, ,0, , , ,UY
ALLSEL,ALL
NSEL,S,LOC,X,0              ! Constrain nodes in the x-direction
NSEL,A,LOC,X,Lu,10000
D,ALL, ,0, , , ,UX
ALLSEL,ALL
NSEL,S,LOC,Z,0          ! Constrain nodes at z = 0
D,ALL, ,0, , , ,UZ
ALLSEL,ALL
NSEL,S,LOC,Z,wu,10000               ! Add unit displacement at z = d
```

```
D,ALL, ,unit_dz, , , ,UZ
ALLSEL,ALL
/REPLOT,RESIZE
FINISH
!*
/SOLU                   ! Solve
ANTYPE,0
!/STATUS,SOLU
SOLVE
FINISH
!*
/POST1                  ! Begin post-processing
NSEL,S,LOC,Y,0
NSEL,A,LOC,X,0
NSEL,A,LOC,Z,0

/OUTPUT,STIFFNESS_TOW,TXT,,APPEND
FSUM,,
/OUTPUT
FINISH
```

Lamina Stiffness Calculations

```
! Lamina_Stiffness_Calculations.txt
! By: Michael Maletta
! Created on: 4/12/08

! This program is used to help determine the Young's Modulus and Poisson's ratio
! for the lamina repeating unit.  The inputs are the unit displacements for the
! each of the three cases and outputs are the reaction forces at each face.

*SET,unit_dx,L/10              ! Define x unit displacement, um
*SET,unit_dy,h/10              ! Define y unit displacement, um
*SET,unit_dz,w/10              ! Define z unit displacement, um

!*
! CASE I - load on x face
!*
/PREP7
NSEL,S,LOC,Y,0                 ! Constrain nodes in the y-direction
NSEL,A,LOC,Y,h,10000
D,ALL, ,0, , , ,UY
ALLSEL,ALL
NSEL,S,LOC,X,0            ! Constrain nodes at x = 0
D,ALL, ,0, , , ,UX
ALLSEL,ALL
NSEL,S,LOC,X,L,10000        ! Add unit displacement at x = L
D,ALL, ,unit_dx, , , ,UX
ALLSEL,ALL
NSEL,S,LOC,Z,0            ! Constrain nodes in z-direction
NSEL,A,LOC,Z,w,10000
D,ALL, ,0, , , ,UZ
ALLSEL,ALL
/REPLOT,RESIZE
FINISH
!*
/SOLU                  ! Solve
ANTYPE,0
!/STATUS,SOLU
SOLVE
FINISH
!*
/POST1                 ! Begin post-processing
NSEL,S,LOC,Y,0
NSEL,A,LOC,X,0
NSEL,A,LOC,Z,0

/OUTPUT,STIFFNESS_Lamina,TXT,,APPEND
FSUM,,
/OUTPUT
FINISH

! Prepare geometry for Case II
ALLSEL,ALL
/PREP7
```

```
DDELE,ALL,ALL

! CASE II - load on y face
!*
NSEL,S,LOC,X,0          ! Constrain nodes in the x-direction
NSEL,A,LOC,X,L,10000
D,ALL, ,0, , , ,UX
ALLSEL,ALL
NSEL,S,LOC,Z,0          ! Constrain nodes in the z-direction
NSEL,A,LOC,Z,w,10000
D,ALL, ,0, , , ,UZ
ALLSEL,ALL
NSEL,S,LOC,Y,0              ! Constrain nodes at y = 0
D,ALL, ,0, , , ,UY
ALLSEL,ALL
NSEL,S,LOC,Y,h,10000        ! Add unit displacement at y = d
D,ALL, ,unit_dy, , , ,UY
ALLSEL,ALL
/REPLOT,RESIZE
FINISH
!*
/SOLU                   ! Solve
ANTYPE,0
!/STATUS,SOLU
SOLVE
FINISH
!*
/POST1                  ! Begin post-processing
NSEL,S,LOC,Y,0
NSEL,A,LOC,X,0
NSEL,A,LOC,Z,0

/OUTPUT,STIFFNESS_Lamina,TXT,,APPEND
FSUM,,
/OUTPUT
FINISH

! Prepare geometry for case III
/PREP7
ALLSEL,ALL
DDELE,ALL,ALL

! CASE III - load on z face
!*
NSEL,S,LOC,Y,0              ! Constrain nodes in the y-direction
NSEL,A,LOC,Y,h,10000
D,ALL, ,0, , , ,UY
ALLSEL,ALL
NSEL,S,LOC,X,0              ! Constrain nodes in the x-direction
NSEL,A,LOC,X,L,10000
D,ALL, ,0, , , ,UX
ALLSEL,ALL
NSEL,S,LOC,Z,0          ! Constrain nodes at z = 0
D,ALL, ,0, , , ,UZ
ALLSEL,ALL
NSEL,S,LOC,Z,w,10000            ! Add unit displacement at z = d
```

```
D,ALL, ,unit_dz, , , ,UZ
ALLSEL,ALL
/REPLOT,RESIZE
FINISH
!*
/SOLU                   ! Solve
ANTYPE,0
!/STATUS,SOLU
SOLVE
FINISH
!*
/POST1                  ! Begin post-processing
NSEL,S,LOC,Y,0
NSEL,A,LOC,X,0
NSEL,A,LOC,Z,0

/OUTPUT,STIFFNESS_Lamina,TXT,,APPEND
FSUM,,
/OUTPUT
FINISH
```

Tow Shear Moduli Calculations

```
! Tow_Shear_Modulus.txt
! Created on:  February 11, 2008
! By:  Michael Maletta
!*
!*
/OUTPUT,SHEAR_OUTPUT,TXT,,APPEND
*SET,shear_xy,c/10              ! Define shear unit displacement in x-dir, um
*SET,shear_zy,c/10              ! Define shear unit displacement in z-dir, um
*SET,shear_xz,wu/10             ! Define shear unit displacement in x-dir, um
/OUTPUT

! CASE Gxy (G13) - Front view of specimen
!*
/PREP7
NSEL,S,LOC,Y,0                  ! Constrain nodes at y = 0
D,ALL,UY,0
D,ALL,UX,0
ALLSEL,ALL
NSEL,S,LOC,Y,d,100              ! Constrain nodes at y = d
D,ALL,UY,0
D,ALL,UX,shear_xy
ALLSEL, ALL
NSEL,S,LOC,Z,0              ! Constrain nodes in the z-direction
NSEL,A,LOC,Z,wu,10000
D,ALL,UZ,0
ALLSEL,ALL

! Define x-displacements on the x=Lu face, u = u0*(y/d)
NSEL,S,LOC,X,Lu,10000
*GET,NUM1,NODE,0,COUNT              ! Get number of nodes
*GET,MIN1,NODE,0,NUM,MIN        ! Get minimum node #
CURNOD = MIN1                   ! Initialize current node #
*DO,I,1,NUM1
*GET,YLOC,NODE,CURNOD,LOC,Y     ! Get y-location of node
D,CURNOD,UX,(YLOC/c)*shear_xy       ! Define x-displacement
D,CURNOD,UY,0                   ! Define y-displacement
CURNOD = NDNEXT(CURNOD)             ! Update current node #
*ENDDO

ALLSEL,ALL

! Define x-displacements on the x=0 face, u = u0*(y/d)
NSEL,S,LOC,X,0
*GET,NUM2,NODE,0,COUNT              ! Get number of nodes
*GET,MIN2,NODE,0,NUM,MIN        ! Get minimum node #
CURNOD2 = MIN2                  ! Initialize current node #
*DO,J,1,NUM2
*GET,YLOC2,NODE,CURNOD2,LOC,Y       ! Get y-location of node
D,CURNOD2,UX,(YLOC2/c)*shear_xy         ! Define x-displacement
D,CURNOD2,UY,0                  ! Define y-displacement
CURNOD2 = NDNEXT(CURNOD2)       ! Update current node #
*ENDDO
```

```
ALLSEL,ALL
FINISH
!*
/SOLU                   ! Solve
ANTYPE,0
!/STATUS,SOLU
SOLVE
FINISH
!*
/POST1                  ! Begin post-processing
NSEL,S,LOC,Y,c,10000
/OUTPUT,SHEAR_OUTPUT,TXT,,APPEND
FSUM,,                  ! Need sum in x-direction
/OUTPUT
ALLSEL,ALL

NSEL,S,LOC,X,Lu,10000
/OUTPUT,SHEAR_OUTPUT,TXT,,APPEND
FSUM,,                  ! Need sum in y-direction
/OUTPUT
ALLSEL,ALL
FINISH

! CASE Gzy (G23) - cross section of specimen
!*
! Prepare geometry
/PREP7
DDELE,ALL,ALL
!
! Apply Constraints
NSEL,S,LOC,Y,0                  ! Constrain nodes at y = 0
D,ALL,UY,0
D,ALL,UZ,0
ALLSEL,ALL
NSEL,S,LOC,Y,c,10000            ! Constrain nodes at y = d
D,ALL,UY,0
D,ALL,UZ,shear_zy
ALLSEL, ALL
NSEL,S,LOC,X,0                  ! Constrain nodes in the x-direction
NSEL,A,LOC,X,Lu,10000
D,ALL,UX,0
ALLSEL,ALL

! Define z-displacements on the z=wu face, w = w0*(y/d)
NSEL,S,LOC,Z,wu,10000
*GET,NUM1,NODE,0,COUNT          ! Get number of nodes
*GET,MIN1,NODE,0,NUM,MIN        ! Get minimum node #
CURNOD = MIN1                   ! Initialize current node #
*DO,I,1,NUM1
*GET,YLOC,NODE,CURNOD,LOC,Y     ! Get y-location of node
D,CURNOD,UZ,(YLOC/c)*shear_zy   ! Define z-displacement
D,CURNOD,UY,0                   ! Define y-displacement
CURNOD = NDNEXT(CURNOD)         ! Update current node #
*ENDDO
```

```
ALLSEL,ALL

! Define z-displacements on the z=0 face, w = w0*(y/d)
NSEL,S,LOC,Z,0
*GET,NUM2,NODE,0,COUNT              ! Get number of nodes
*GET,MIN2,NODE,0,NUM,MIN            ! Get minimum node #
CURNOD2 = MIN2                      ! Initialize current node #
*DO,J,1,NUM2
*GET,YLOC2,NODE,CURNOD2,LOC,Y       ! Get y-location of node
D,CURNOD2,UZ,(YLOC2/c)*shear_zy     ! Define z-displacement
D,CURNOD2,UY,0                      ! Define y-displacement
CURNOD2 = NDNEXT(CURNOD2)           ! Update current node #
*ENDDO

ALLSEL,ALL
FINISH
!*
/SOLU                           ! Solve
ANTYPE,0
!/STATUS,SOLU
SOLVE
FINISH
!*
/POST1                          ! Begin post-processing
NSEL,S,LOC,Y,c,10000
/OUTPUT,SHEAR_OUTPUT,TXT,,APPEND
FSUM,,                          ! Need sum in z-direction
/OUTPUT
ALLSEL,ALL

NSEL,S,LOC,Z,wu,10000
/OUTPUT,SHEAR_OUTPUT,TXT,,APPEND
FSUM,,                          ! Need sum in y-direction
/OUTPUT
ALLSEL,ALL
FINISH

! Prepare geometry for case Gxz
/PREP7
ALLSEL,ALL
DDELE,ALL,ALL
!
! CASE Gxz (G12) - top face of specimen
!*
!
NSEL,S,LOC,Z,0                  ! Constrain nodes at z = 0
D,ALL,UX,0
D,ALL,UZ,0
ALLSEL,ALL
NSEL,S,LOC,Z,wu,10000           ! Constrain nodes at z = d
D,ALL,UZ,0
D,ALL,UX,shear_xz
ALLSEL, ALL
NSEL,S,LOC,Y,0                  ! Constrain nodes in the y-direction
NSEL,A,LOC,Y,c,10000
D,ALL,UY,0
```

```
ALLSEL,ALL

! Define x-displacements on the x=Lu face, u = u0*(z/d)
NSEL,S,LOC,X,Lu,10000
*GET,NUM1,NODE,0,COUNT              ! Get number of nodes
*GET,MIN1,NODE,0,NUM,MIN            ! Get minimum node #
CURNOD = MIN1                       ! Initialize current node #
*DO,I,1,NUM1
*GET,ZLOC,NODE,CURNOD,LOC,Z         ! Get z-location of node
D,CURNOD,UX,(ZLOC/wu)*shear_xz      ! Define x-displacement
D,CURNOD,UZ,0                       ! Define z-displacement
CURNOD = NDNEXT(CURNOD)             ! Update current node #
*ENDDO

ALLSEL,ALL

! Define x-displacements on the x=0 face, u = u0*(z/d)
NSEL,S,LOC,X,0
*GET,NUM2,NODE,0,COUNT              ! Get number of nodes
*GET,MIN2,NODE,0,NUM,MIN            ! Get minimum node #
CURNOD2 = MIN2                      ! Initialize current node #
*DO,J,1,NUM2
*GET,ZLOC2,NODE,CURNOD2,LOC,Z       ! Get z-location of node
D,CURNOD2,UX,(ZLOC2/wu)*shear_xz    ! Define x-displacement
D,CURNOD2,UZ,0                      ! Define z-displacement
CURNOD2 = NDNEXT(CURNOD2)           ! Update current node #
*ENDDO

ALLSEL,ALL
FINISH
!*
/SOLU                   ! Solve
ANTYPE,0
!/STATUS,SOLU
SOLVE
FINISH
!*
/POST1                  ! Begin post-processing
NSEL,S,LOC,Z,wu,10000
/OUTPUT,SHEAR_OUTPUT,TXT,,APPEND
FSUM,,                  ! Need sum in x-direction
/OUTPUT
ALLSEL,ALL

NSEL,S,LOC,X,Lu,10000
/OUTPUT,SHEAR_OUTPUT,TXT,,APPEND
FSUM,,                  ! Need sum in Z-direction
/OUTPUT
ALLSEL,ALL
FINISH
```

APPENDIX B: t-DISTRIBUTION TABLE [29]

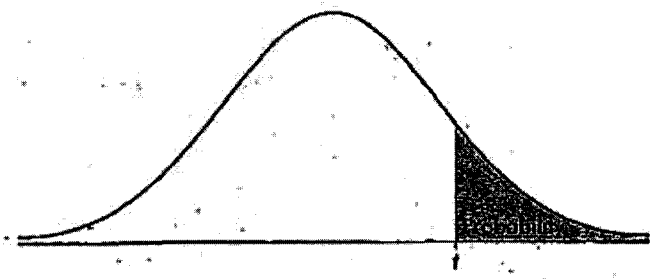

TABLE B: t-DISTRIBUTION CRITICAL VALUES

	Tail probability p											
df	.25	.20	.15	.10	.05	.025	.02	.01	.005	.0025	.001	.0005
1	1.000	1.376	1.963	3.078	6.314	12.71	15.89	31.82	63.66	127.3	318.3	636.6
2	.816	1.061	1.386	1.886	2.920	4.303	4.849	6.965	9.925	14.09	22.33	31.60
3	.765	.978	1.250	1.638	2.353	3.182	3.482	4.541	5.841	7.453	10.21	12.92
4	.741	.941	1.190	1.533	2.132	2.776	2.999	3.747	4.604	5.598	7.173	8.610
5	.727	.920	1.156	1.476	2.015	2.571	2.757	3.365	4.032	4.773	5.893	6.869
6	.718	.906	1.134	1.440	1.943	2.447	2.612	3.143	3.707	4.317	5.208	5.959
7	.711	.896	1.119	1.415	1.895	2.365	2.517	2.998	3.499	4.029	4.785	5.408
8	.706	.889	1.108	1.397	1.860	2.306	2.449	2.896	3.355	3.833	4.501	5.041
9	.703	.883	1.100	1.383	1.833	2.262	2.398	2.821	3.250	3.690	4.297	4.781
10	.700	.879	1.093	1.372	1.812	2.228	2.359	2.764	3.169	3.581	4.144	4.587
11	.697	.876	1.088	1.363	1.796	2.201	2.328	2.718	3.106	3.497	4.025	4.437
12	.695	.873	1.083	1.356	1.782	2.179	2.303	2.681	3.055	3.428	3.930	4.318
13	.694	.870	1.079	1.350	1.771	2.160	2.282	2.650	3.012	3.372	3.852	4.221
14	.692	.868	1.076	1.345	1.761	2.145	2.264	2.624	2.977	3.326	3.787	4.140
15	.691	.866	1.074	1.341	1.753	2.131	2.249	2.602	2.947	3.286	3.733	4.073
16	.690	.865	1.071	1.337	1.746	2.120	2.235	2.583	2.921	3.252	3.686	4.015
17	.689	.863	1.069	1.333	1.740	2.110	2.224	2.567	2.898	3.222	3.646	3.965
18	.688	.862	1.067	1.330	1.734	2.101	2.214	2.552	2.878	3.197	3.611	3.922
19	.688	.861	1.066	1.328	1.729	2.093	2.205	2.539	2.861	3.174	3.579	3.883
20	.687	.860	1.064	1.325	1.725	2.086	2.197	2.528	2.845	3.153	3.552	3.850
21	.686	.859	1.063	1.323	1.721	2.080	2.189	2.518	2.831	3.135	3.527	3.819
22	.686	.858	1.061	1.321	1.717	2.074	2.183	2.508	2.819	3.119	3.505	3.792
23	.685	.858	1.060	1.319	1.714	2.069	2.177	2.500	2.807	3.104	3.485	3.768
24	.685	.857	1.059	1.318	1.711	2.064	2.172	2.492	2.797	3.091	3.467	3.745
25	.684	.856	1.058	1.316	1.708	2.060	2.167	2.485	2.787	3.078	3.450	3.725
26	.684	.856	1.058	1.315	1.706	2.056	2.162	2.479	2.779	3.067	3.435	3.707
27	.684	.855	1.057	1.314	1.703	2.052	2.158	2.473	2.771	3.057	3.421	3.690
28	.683	.855	1.056	1.313	1.701	2.048	2.154	2.467	2.763	3.047	3.408	3.674
29	.683	.854	1.055	1.311	1.699	2.045	2.150	2.462	2.756	3.038	3.396	3.659
30	.683	.854	1.055	1.310	1.697	2.042	2.147	2.457	2.750	3.030	3.385	3.646
40	.681	.851	1.050	1.303	1.684	2.021	2.123	2.423	2.704	2.971	3.307	3.551
50	.679	.849	1.047	1.299	1.676	2.009	2.109	2.403	2.678	2.937	3.261	3.496
60	.679	.848	1.045	1.296	1.671	2.000	2.099	2.390	2.660	2.915	3.232	3.460
80	.678	.846	1.043	1.292	1.664	1.990	2.088	2.374	2.639	2.887	3.195	3.416
100	.677	.845	1.042	1.290	1.660	1.984	2.081	2.364	2.626	2.871	3.174	3.390
1000	.675	.842	1.037	1.282	1.646	1.962	2.056	2.330	2.581	2.813	3.098	3.300
∞	.674	.841	1.036	1.282	1.645	1.960	2.054	2.326	2.576	2.807	3.091	3.291
	50%	60%	70%	80%	90%	95%	96%	98%	99%	99.5%	99.8%	99.9%
	Confidence level C											

APPENDIX C: MISCALENEOUS DATA

Table C-1: Square packed repeating unit of tows inside a lamina mechanical properties.

Void Content %	E_x (GPa)	E_y (GPa)	E_z (GPa)	ν_{xy}	ν_{xz}	ν_{yx}	ν_{yz}	ν_{zx}	ν_{zy}
0.00	99.05	6.12	6.66	0.333	0.323	0.021	0.404	0.022	0.430
0.49	99.03	6.08	6.58	0.332	0.322	0.021	0.399	0.022	0.422
0.30	98.83	6.09	6.44	0.332	0.322	0.021	0.404	0.022	0.425
0.00	99.05	6.12	6.65	0.332	0.323	0.021	0.403	0.022	0.429

Table C-2: Hexagon packed repeating unit of tows inside a lamina mechanical properties.

Void Content %	E_x (GPa)	E_y (GPa)	E_z (GPa)	ν_{xy}	ν_{xz}	ν_{yx}	ν_{yz}	ν_{zx}	ν_{zy}
0.00	102.62	6.08	6.69	0.334	0.322	0.021	0.404	0.022	0.439
0.11	102.61	6.04	6.61	0.334	0.322	0.021	0.404	0.022	0.439

Table C-3: The mechanical properties and constraints used for the three square packing configuration progressive failure analyses.

Run	**Void Content (%)**	**Mechanical Properties**			**Constraints**		
		E_z (GPa)	ν_{zx}	ν_{zy}	δ_{rate_z} (m)	$x_{o,z}$ (m)	$y_{o,z}$ (m)
No Voids	0.00	6.66	0.022	0.430	3.85E-06	-6.11E-09	-1.99E-07
Center Void	0.49	6.58	0.022	0.422	3.85E-06	-6.02E-09	-1.95E-07
Gap Voids	0.30	6.44	0.022	0.425	3.85E-06	-6.04E-09	-1.97E-07

Table C-4: The mechanical properties and constraints used for the two hexagon packing configuration progressive failure analyses.

Run	**Void Content (%)**	**Mechanical Properties**			**Constraints**		
		E_z (GPa)	ν_{zx}	ν_{zy}	δ_{rate_z} (m)	$x_{o,z}$ (m)	$y_{o,z}$ (m)
No Voids	0.00	6.69	0.022	0.439	4.23E-06	-9.02E-09	-3.70E-07
Gap Voids	0.11	6.61	0.022	0.439	4.23E-06	-8.98E-09	-3.69E-07

Table C-5: The progressive failure results for the square packed tow repeating unit, ***first failed element.***

	Square - No Voids			Square - Center Voids			Square - Gap Voids		
Applied ε_z	**F_z (N)**	σ_z (MPa)	Initial stiffness (MPa)	**F_z (N)**	σ_z (MPa)	Initial stiffness (MPa)	**F_z (N)**	σ_z (MPa)	Initial stiffness (MPa)
0.003	0.330	19.84	18.49	0.326	19.60	18.27	0.327	19.62	17.90
0.006	0.659	39.55	36.97	0.651	39.07	36.54	***0.652***	***39.12***	35.80
0.008	***0.985***	***59.15***	55.46	***0.973***	***58.42***	54.81	0.974	58.46	53.70
0.011	1.296	77.81	73.95	1.271	76.33	73.07	1.264	75.91	71.59
0.014	1.569	94.22	92.44	1.460	87.64	91.34			
0.017	1.650	99.07	110.92						

Table C-6: The progressive failure results for the hexagon packed tow repeating unit, ***first failed element.***

	Hexagon - No Voids			Hexagon - Gap Voids		
Applied ε_z	**F_z (N)**	σ_z (MPa)	Initial stiffness (MPa)	**F_z (N)**	σ_z (MPa)	Initial stiffness (MPa)
0.003	0.904	19.87	18.58	0.600	19.79	18.58
0.006	1.802	39.62	37.16	1.197	39.46	37.16
0.008	2.695	59.25	55.74	***1.789***	***59.02***	55.74
0.011	***3.582***	***78.76***	74.32	2.378	78.44	74.32
0.014	4.435	97.52	92.90	2.943	97.07	92.90
0.017	5.174	113.76	111.48	3.432	113.18	111.48
0.019	5.635	123.90	130.06			